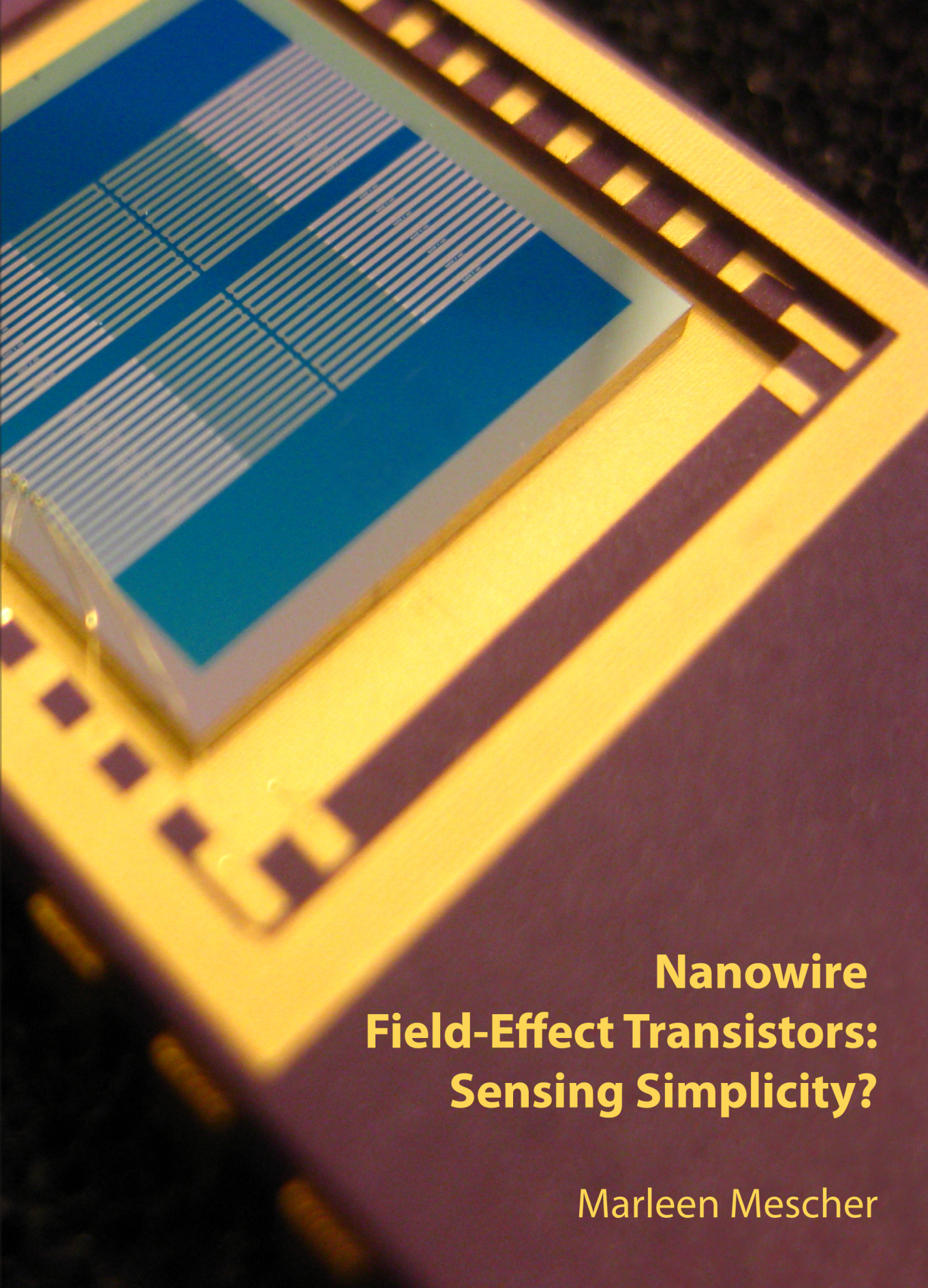

Nanowire Field-Effect Transistors: Sensing Simplicity?

Marleen Mescher

NANOWIRE FIELD-EFFECT TRANSISTORS: SENSING SIMPLICITY?

Proefschrift

ter verkrijging van de graad van doctor
aan de Technische Universiteit Delft,
op gezag van de Rector Magnificus prof. ir. K. C. A. M. Luyben,
voorzitter van het College voor Promoties,
in het openbaar te verdedigen op maandag 14 april 2014 om 15:00 uur

door

Marleen MESCHER

Master of Science
in Chemical Sciences
geboren te Eindhoven

Dit proefschrift is goedgekeurd door de promotor:

Prof. dr. E. J. R. Sudhölter

Copromotor: Dr. ir. L. C. P. M. de Smet

Samenstelling promotiecommissie:

Rector Magnificus,	voorzitter
Prof. dr. E. J. R. Sudhölter,	Technische Universiteit Delft, promotor
Dr. ir. L. C. P. M. de Smet,	Technische Universiteit Delft, copromotor
Prof. dr. S. Ingebrandt,	University of Applied Sciences Kaiserslautern
Prof. dr. M. A. Reed,	Yale University
Prof. dr. R. Dekker,	Technische Universiteit Delft
Prof. dr. L. D. A. Siebeles,	Technische Universiteit Delft
Dr. ir. J. H. Klootwijk,	Philips Research, adviseur
Prof. dr. S. J. Picken,	Technische Universiteit Delft, reservelid

Printed by: Ipskamp Drukkers B.V., Enschede

Front: Chip with NW-FETs

This research was carried out under project number M62 3 09339 in the framework of the Strategic Research Program of the Materials innovation institute (M2i) in the Netherlands (www.m2i.nl).

ISBN 978-94-91909-00-9

An electronic version of this dissertation is available at
`http://repository.tudelft.nl/`.

CONTENTS

1

INTRODUCTION

1.1 AIM OF THIS THESIS

1

SENSORS are devices that convert a chemical or physical phenomenon into a signal that can be used by an observer. Typical sensors consist of a sensing element, that is influenced by the chemical or physical parameter that needs to be measured, and a transducer, which translates the signal from the sensing element into a signal that is readable by the observer (Figure 1.1). A thermometer for example, will convert the temperature in a room (medium) into a number on a screen. In an old-fashioned mercury thermometer the liquid mercury is the sensing element as it will expand when it gets warmer. The transducer in this case is the glass tube in which the mercury level will rise which has been calibrated to indicate the right temperature. In a thermocouple thermometer, two conductors form the sensing element, while a voltmeter is used as the transducer that measures the (temperature-dependent) potential difference between the conductors and translates it into a number on a screen. When additional processing is required, a signal processor is added to the system.

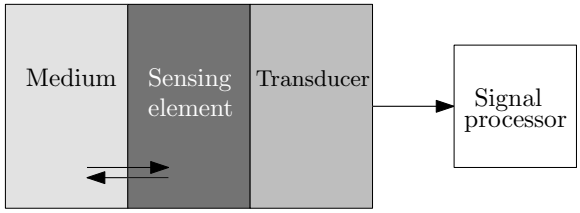

FIGURE 1.1: Schematic representation of a sensor. The sensing element interacts with a medium. The transducer translates the signal from the sensing agent into something that can be measured. When needed, this signal will go to a signal processer which changes the signal into the sensor output. (Figure adapted from [1])

Applications of sensors are numerous. Physical sensors can not only measure temperature, but also mass, distance or pressure, and chemical sensors are used to detect chemical substances like pH or specific chemical analytes (e.g. pregnancy tests, glucose tests for diabetics).

The aim of this thesis is to develop a sensor for the detection of ions. In such a sensor, several analytes play a role. It is aimed to show that pH and potassium ions can be detected using the developed device, because this will demonstrate the possibilities for other analytes as well, including heavy metal ions. Ion sensors are applied in a large number of fields, e.g. the pharmaceutical industry, medical applications, food, water quality, industry (waste water). The target here is to make a small, cheap, sensitive and selective sensor. The transducer of choice is the nanowire field-effect transistor (NW-FET). NW-FETs are devices where a nanowire

made of silicon exist between a source and drain contact. The conductivity of the nanowire can be influenced adsorbing charges near the nanowire surface. The change in the electrical conductivity can be read out electrically. By adjusting the surface of the nanowire (surface modification) selectivity towards specific analytes can be obtained. NW-FETs can be constructed using bottom-up grown nanowires, or via top-down etching, which has gained the most interest recently. The goal of this project is first to develop a cheap method for large-scale top-down production of these devices via complementary metal oxide semiconductor (CMOS) fabrication on silicon wafers. The working principles of the device will be studied which will be used in sensing experiments and the possibilities for ion sensing are investigated.

1.2 DETAILED OUTLINE

In this thesis an overview of the scientific work performed during this project is presented. The different parts of the project resulted in a number of publications/manuscripts and are presented here as individual chapters. Chapter 2 is largely based on a literature review, and Chapters 3-6 present experimental work. The final chapter gives the overall conclusions and discussion. In more detail:

Chapter 2 describes the theory behind the NW-FET and the state of the art of NW-FETs as sensors. Further, it gives an overview of the surface modifications that are reported in literature. The first part of this chapter starts from the theory behind ISFETs (the predecessor of the NW-FET), explains the differences and similarities between ISFETs and NW-FETs, discusses briefly what kind of NW-FETs have been developed and shows some typical properties of NW-FETs. The second part of this chapter (Section 2.2) was partly published in **Nanowires - Implementations and Applications** as *Organic Surface Modification of Silicon Nanowire-based Sensor Devices*, InTech, (2011) [2] and discusses the current status of surface modification of top-down, silicon NW-FETs in literature.

Chapter 3 gives a detailed description of the top-down fabrication process of the nanowire field-effect devices used in the this thesis. This was published in the **Journal of Nanoscience and Nanotechnoloy** as *Robust Fabrication Method for Silicon Nanowire Field Effect Transistors for Sensing Applications*, **13**, 8 (2013) [3]. The process is flexible in terms of the front oxide of the transistor, as it is applied in a separate, independent step from the application of the surrounding oxide. Furthermore, the use of a passivation layer opens possibilities for adding selectivity via surface modification on

SiO_2 and silicon. This process includes only six masks steps and uses only conventional processing techniques.

Chapter 4 utilizes devices similar to those fabricated in Chapter 3. The devices are exposed to deionized water and solutions of salt. It explains how a pulsed electrical characterization of the nanowire field-effect transistors is carried out when the sensor is exposed to liquid. Issues with instabilities of the sensor signal are reduced by applying a pulsed gate potential. This was not demonstrated in literature before. The chapter also shows how this method can be used in pH sensing experiments using the SiO_2 gate oxide. This work was presented at the **2010 International Conference on Microelectronic Test Structures** (ICMTS) in Hiroshima, Japan, and later published in **IEEE Transactions on Electron Devices** as *Pulsed Method for Characterizing Aqueous Media Using Nanowire Field Effect Transistors*, **58**, 7 (2011) [4].

Chapter 5 combines the devices from Chapter 3 and a measurement methodology comparable to that in Chapter 4. It compares the response of the NW-FET to back gating and liquid gating, and shows the influence of dioxane-water mixtures (with a range of dielectric constants) on the sensors characteristics. These experiments are performed to get a better understanding of the fundamental working principle behind the NW-FET and the way it is influenced by its surrounding medium. It is concluded that in these experiments not the dielectric constant of the medium is the determining factor for the response of the device, but that the electrical conductivity of the solution largely determines the device response. This chapter was published in **Sensors** as *Influence of Conductivity and Dielectric Constant of Water-Dioxane Mixtures on the Electrical Response of SiNW-FETs*, **14**, 2 (2014) [5].

Chapter 6 shows the results of potassium sensing experiments using a polymer membrane on the devices from Chapter 3. Methods from both Chapters 4 and 5 are used to work towards the sensing of potassium ions. Membranes of siloprene containing a valinomycin ionophore are prepared to ensure good adhesion of the membranes to the NW surface. The membranes are drop-casted on top of both plain SiO_2 substrates and nanowire devices. The response of the membrane to changes in potassium ion concentration is measured using a conventional ion-selective electrode setup and NW-FETs. The potassium ions function as a model analyte for further detection of ions, including heavy metal ions.

Chapter 7 discusses all the conclusions from the preceding chapters and gives recommendations for future work.

2

BACKGROUND

This chapter describes the theory behind ISFETs and NW-FETs, and gives some examples of the NW-FETs characteristics. Furthermore, it introduces the variety of surface modification techniques that have been used in literature to add selectivity to the NW-FET as sensor device.

Paragraph 2.2 of this chapter is an updated version of a review that has been published as a book chapter in Nanowires - Implementations and Applications, *Organic Surface Modification of Silicon Nanowire-Based Sensor Devices*, L.C.P.M. de Smet, D. Ullien, M. Mescher and E.J.R. Sudhölter, Intech, (2011) [2].

2.1 FIELD-EFFECT TRANSISTORS

FIELD-EFFECT transistors (FETs) are electronic devices that consist of semiconducting material between a source (S) and a drain (D) contact. The conductivity of this material is controlled by the potential on a third contact, the gate (G). The gate is capacitively coupled to the material. If a potential is applied to the gate, charge carriers in the material are moved to or from the surface creating a conductive channel between the source and the drain. When a (small) potential difference is applied between the source and the drain, the current at the drain (I_D) is a function of the gate potential (V_{GS}). The simplest form of a FET is shown in Figure 2.1.

A typical example of such an I_{SD}-V_G curve is shown in Figure 2.2. Although a small voltage bias is applied between the source and the drain, at first there flows no current between these two contacts. The gate voltage is applied and increased, and at a certain gate voltage a current starts to flow from the source to the drain. Initially, this current increases linearly with the gate voltage as the conductivity of the channel rises up to the point when the channel is saturated and the current does not increase further. The slope of the linear part of this curve is the transconductance (g_m), which is reciprocal to the resistance of the device. The point where this slope crosses the x-axis, and thus the point at which the channel is opened, is called the threshold voltage (V_T). This is the minimum gate voltage at which the FET starts conducting. The current through the materiel when this is saturated is called the saturation current (I_{sat}). The threshold voltage, transconductance and saturation current are important characteristics to describe the FET.

There are different types of FETs that have a different layout and a different way

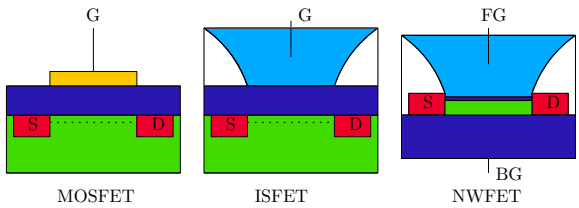

FIGURE 2.1: Schematic representations of the structure of three types of FETs: (a) MOSFET (b) ISFET (c) NW-FET. S and D are source and drain, respectively. G stands for gate, FG and BG are the front and back gate contacts. Green parts represent low-doped silicon, red high-doped silicon, yellow represents a metal layer, dark-blue is SiO_2, white parts are insulation and light-blue is liquid through which gating is achieved.

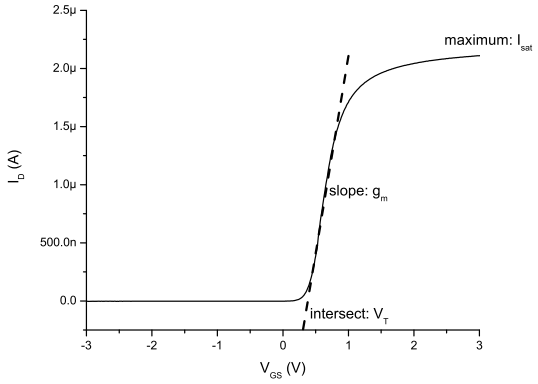

FIGURE 2.2: Typical I_D-V_{GS} characteristics of an n-type FET. The threshold voltage (V_T), transconductance (g_m) and saturation current (I_{sat}) are indicated.

of inducing a source-drain current. The most notable of these is the metal-oxide-semiconductor FET (or MOSFET, Figure 2.1a). In a MOSFET, the source and drain are composed of heavily doped silicon in an oppositely doped silicon substrate. The metal gate is electrically separated from this layer by an insulating oxide layer. When a potential is applied to the gate, a conductive channel is formed at the surface of the semiconductor substrate, below the insulating oxide layer. Note that a conductive channel can also be formed by applying a potential to the body, which capacitively coupled acts as a so-called back gate.

2.1.1 ION-SELECTIVE FIELD-EFFECT TRANSISTORS

AN ion-selective field-effect transistor (ISFET) is a FET which is specially designed to be used as a sensor for ions. It is first reported in the 70s by Bergveld [6]. In an ISFET, the metal layer has been removed and the insulating layer (e.g. SiO_2) is exposed to an electrolyte solution (Figure 2.1b). An electrical contact in the solution acts as gate. The gate potential is modulated by a boundary potential, which is the result of the proton dissociation of surface silanol groups. The device characteristics depend on this modulated gate potential. This changing density of charge carriers in the channel changes the ISFETS conductivity. This potential is described by the Nernst equation:

$$E = E_0 + \frac{RT}{zF} \ln a_i \tag{2.1}$$

where E is the potential at the solid-liquid interface, E_0 is the standard potential in the system, R is the gas constant, T the absolute temperature, z is the charge of the ions in the solution, F is the Faraday constant and a_i represents the activity of the primary, potential determining ion in the solution.

In a normal FET, the channel starts conducting when the applied gate voltage meets V_T. However, in the case of an ISFET, the potential of the oxide-electrolyte interface and variations of potential in the electrolyte add to the V_G thereby changing V_T [7, 8]. This makes it suitable for use as a sensor. Changes in the charge density at the sensor surface can be measured as a change in V_T. Advantages of the ISFET compared to conventional glass electrodes are the smaller size of the device and the smaller sample size that is needed, enabling application in medical and food applications [9].

An ISFET with a bare oxide layer is sensitive to pH [9], but the layer can be modified to specifically adsorb and thereby detect other compounds. Moss and coworkers constructed a K^+ sensor by combining well-known PVC membranes with valinomycin with the ISFET structure [10]. Other polymers were applied to solve problems with membrane adhesion [11]. Also covalent modification has been used to add selectivity to ISFETs [12]. Although the ISFET was developed 40 years ago, it is still used as the basis for recent research on sensors made from semiconducting materials, as will become clear in the following chapters.

2.1.2 NANOWIRE FIELD-EFFECT TRANSISTORS

In the case of nanowire FETs (NW-FETs), the conductive channel between the source and drain has been replaced by a (number of) nanowire(s) (Figure 2.1c). A nanowire is a structure that has a size in the nanometer range in two dimensions. Hence, essentially it is a really thin piece of semiconducting material. One effect of a smaller size is the increase in surface-to-volume ratio. As the sensing effect of sensor-FETs depends on surface potential, this effect increases with an increasing surface-to-volume ratio [13]. Furthermore, when the nanowire dimensions become very small, the presence of a small amount of charges near the surface might be able to locally influence the complete nanowire. This nanowire often has a gate oxide around it. Either a front gate in the solution or a back gate can be used to gate the device in addition to potentials which develop at the nanowire-liquid interface, similar to the ISFET configuration. Although there is a broad range of semiconducting materials from which nanowires are produced (e.g. (doped) silicon, carbon (carbon nanotubes), InP, GaN), the focus in this thesis is on silicon nanowires. There are different ways of producing the silicon nanowires: they can either be etched (top-down approach) or grown (bottom-up). Nanowire growth is usually done via VLS (vapor-liquid-solid) techniques, first reported in 1964 [14]. In this technique, a metal particle (e.g. gold) on a substrate (e.g. silicon)

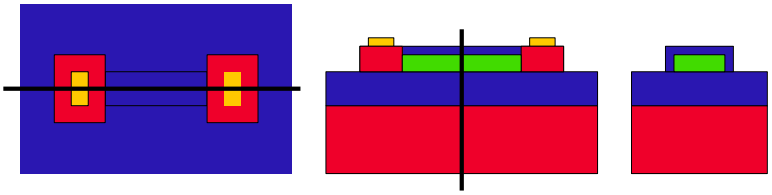

FIGURE 2.3: Schematic (not-to-scale) representations of the a NW-FET (left) from the top, (middle) along the line in the left scheme and (right) across the line in the middle scheme. The substrate consist of high-doped silicon (red) and a burried oxide layer (blue). The nanowire (green) is covered with a SiO_2 gate oxide (blue) and found between the highly conductive source and drain (red). Metal (yellow) contacts are deposited on the source and drain.

is heated. The particle melts and forms a liquid alloy with the substrate which acts as a catalyst for the growth of the nanowire. Precursors for the desired nanowire material are introduced in the gas phase, and adsorb in the catalyst droplet. When this saturates, crystal growth will start on the droplet-substrate interface, and a nanowire will grow. Although this method has been studied extensively, there is no reliable method yet for the integration of the grown nanowires in FET-like structures. The top-down method, which will be discussed later (Chapter 3), does offer this possibility, which is essential for the large-scale integration of these devices. Therefore, the focus in the thesis is on top-down silicon nanowires.

NW-FETs function in the same way as described in Section 2.1.1. A more detailed schematic of a NW-FET is shown in Figure 2.3. The silicon nanowire connects the source and drain contacts. These contacts consist of high-doped silicon with metal on top. The contacts are covered with insulating material to avoid the presence of leakage currents. For matters of clarity, this insulation is not shown in Figure 2.3. The current through the nanowire depends on the potential that is applied to the gate and to the charge that is present at its surface. For n-type NW-FETs, this means that with increasingly positive potentials and charges, the current through the nanowire will increase. Typical characteristics of n-type NW-FETs are shown in Figure 2.4. The current through the nanowire depends on the size of the nanowire as well: The current decreases with increasing nanowire length due to the larger resistance of the wires. As can be expected, a smaller number of parallel nanowires has the same effect on the current: they act as if they were separate individual resistors and fewer nanowires give less total current. As in the case of ISFETs, the surface of NW-FETs can be altered to obtain selectivity. In Section 2.2 an overview is presented of the broad range of surface modifications that have been used in literature to achieve selectivity on top-down Si NW-FETs.

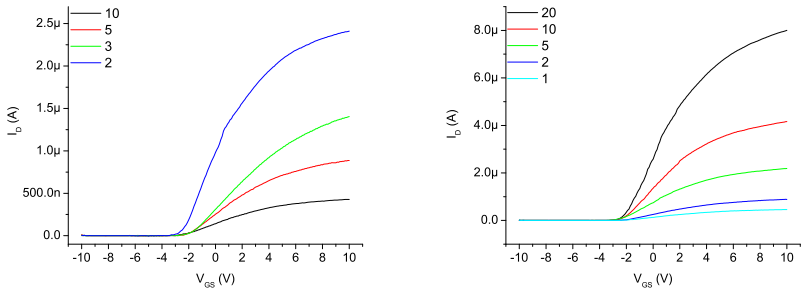

(a) (b)

FIGURE 2.4: The effect on the drain current of (a) the length of a nanowire in micrometer and (b) the number of nanowires in a single FET for n-type NW-FETs.

2.2 SURFACE MODIFICATION

SINCE their introduction in 2001 [15] SiNW-based sensor devices have gained considerable interest as a general platform for ultra-sensitive electrical detection of biological and chemical species (Figure 2.5). Although SiO_x coatings can be used for the detection of protons [13] and gases [16], the specific detection of other analytes, including ions and biomolecules, requires the presence of an affinity layer that interacts with the analyte of interest. Such a layer can be added on top of the nanowire by the modification of the nanowire surface. In this section we review the surface modification strategies that have been explored on SiNW-based devices over the past decade.

Scope and Organization of This Review

This section focuses on surface modification strategies of SiNW-based devices. This review concentrates on electrical devices that consist of in-plane orientated SiNWs, which are positioned between two ohmic contacts, often referred to as source and drain.

An extensive overview of different materials that have been explored to prepare NW-based sensors, including silicon, is found in the review of Ramgir et al. [17]. Several reviews on SiNW-based devices have been written with a clear focus on the chemical-vapour-deposition fabricated NWs by the Lieber and Zhou groups [18, 19, 20] or top-down fabricated SiNW-based sensors from the Reed group [21]. In this section we discuss issues related to the modification of SiNW-based devices with organic compounds. The topics of SiO_x [22] and Si-H [22, 23, 24] surface modification with covalently linked organic monolayers have been reviewed ex-

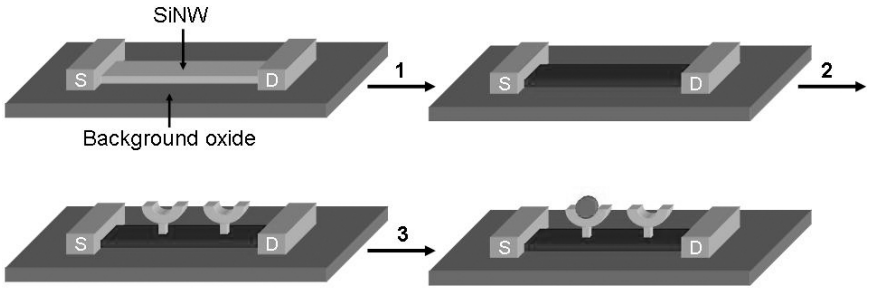

FIGURE 2.5: Schematic representation of a SiNW-based device (top left), of which the nanowire has been chemically modified (step 1), followed by the immobilization of receptors (step 2) and the binding of an analyte (step 3). S and D stand for source and drain, respectively.

tensively. However, the main focus of these reviews is on the modification of large planar substrates, while the focus of this section is on SiNW-based devices. A review by Wanekaya et al. contains a paragraph on the covalent functionalization of SiNWs with biomolecules [25]. Other reviews also include sections with brief schemes for SiNW functionalization [26, 27]. Very recently, our research group published a review paper focussing on the surface modification of SiNW-based FETs with gas-phase sensing applications [28].

The aim of this section is to give an overview of all the different surface modification strategies that have been explored to modify SiNW-based devices, including non-covalent immobilization strategies. The methods can be divided into different categories (Table 2.1). The first one is based on silanization chemistry, i.e., the reaction between hydroxylterminated surfaces and organosilanes. Also other compounds like activated esters or organophosphonates have been covalently attached to SiO_x surfaces. In addition, polyelectrolytes and bilayers have been physically adsorbed onto SiO_x surfaces. Polymer membranes were dropcasted on NW-FETs and metal nanoparticles and thin films were deposited on the nanowire surface. The last approach follows the route of oxide removal, followed by the reaction with (IETS-functionalized)-1-alkenes.

2.2.1 SiO_x-COVERED SiNW-BASED SENSOR DEVICES

Cleaned silicon surfaces exposed in an ambient environment such as air or solutions will oxidize spontaneously [29]. The silicon oxide layer, in this chapter referred to as SiO_x, either native oxide or oxide grown under controlled conditions, passivates the silicon surface. This allows the silicon to be used as an electronic material in processing and application environments. After fabrication, or at

TABLE 2.1: Overview of different strategies used in the modification of SiNW-based devices.

Surface (section)	Modification method	Type of binding	Nature film	# of papers (first year of report)	Section
SiO_2	Silanization	Covalent	Monolayer	>100 (2001)	2.2.2
SiO_2	Esterification	Covalent	Monolayer	1 (2004)	2.2.2
SiO_2	Phosphorization	Covalent	Monolayer	1 (2008)	2.2.2
SiO_2	Layer-by-Layer	Electrostatic	Multilayers	2 (2010)	2.2.3
SiO_2	Lipid membrane	Electrostatic	Bilayer	2 (2009)	2.2.3
SiO_2	PVC membrane	Physisorption	Membrane	2(2012)	2.2.3
SiO_2	Nanoparticles	Electrodeposition	Monolayer	1(2013)	2.2.3
Si-H	Hydrosilylation	Covalent	Monolayer	9 (2006)	2.2.4

least after exposure to ambient environment, also SiNWs contain a SiO_x layer. The thickness of this SiO_x layer on the NW is typically 1.5-10 nm, whereas the background oxide is usually >10 nm. It is important to note that, in terms of surface modification, one cannot discriminate between the oxide of the nanowire and background oxide; both are modified. The surface modifications described in Section 2.2.2 deal with SiO_x-coated SiNW devices.

2.2.2 COVALENT FUNCTIONALIZATION

Silanization

The most applied method to functionalize silica surfaces is through the self-assembly of organofunctional alkoxysilane and chlorosilane molecules. While early silane-based monolayer work is based on Langmuir-Blodgett techniques, the first silane-based self-assembled monolayer was reported by Sagiv in 1980 [30]. In general, a hydroxylated surface is introduced into a solution of a silane derivative in an organic solvent, but gas-phase methods have also been used [22]. In all cases, thorough cleaning of the substrate is a must for obtaining a clean and activated (hydroxylated) oxide layer with a high density of silanol groups on the surface ($\sim 10^{15}$ per cm^2) [22]. Figure 2.6 gives a schematic representation of the formation of a silane monolayer onto SiO_x surfaces. It should be noted that this chemistry is not limited to SiO_x surfaces; other hydroxylated oxides surfaces can be modified as well (e.g., Al_2O_3 [31]). Also in the case of the surface functionalization of the SiO_x surfaces of SiNW-based devices the most applied method is silanization. Figure 2.7 gives an overview of the different silane derivatives that have been used, while Table 2.2 gives a number of examples of surface silanization, together with the target analytes. It should be noted that on planar SiO_x substrates more compounds have been used; here it is aimed to give an overview for SiNW-based devices only. Table 2.2 summarizes the first papers on SiNW-based sensor devices and selected

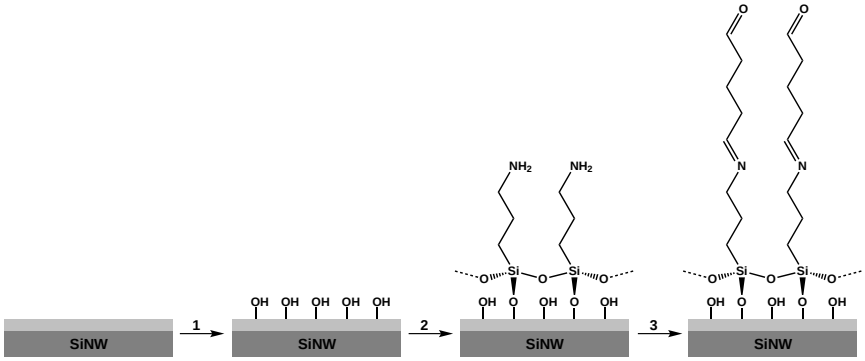

FIGURE 2.6: Schematic representation of the 1) cleaning/hydroxylation of the SiO_x surface, 2) silanization (here: silane 1a, Figure 2.7), and 3) further functionalization with glutaraldehyde. It should be noted that the exact structure of the bonded silanes is arbitrary as also two or three silanol groups per attached molecule may have reacted with the surface hydroxyl groups. Here we adapted the scheme from Aswal et al. [22].

papers that use other silanization methods. The references have been categorized in terms of pH sensors, biosensors, cation sensors and gas sensors. As such, the cited work does not only represent the diversity of silane compounds that have been used, it also shows the variation in the further (bio)functionalization of SiNW-based devices.

3-Aminopropyltriethoxysilane The first paper of the Lieber group on SiNW-based devices shows the utilization of silane-based functionalization of SiO_x-coated nanowires [13]. The devices were chemically modified with 3-aminopropyltriethoxysilane (APTES, Figure 2.7, silane 1a). The resulting devices showed a linear source-drain conductance versus pH-response for pH values from 2 to 9. The authors explained these results by the presence of both NH_3^+ and SiOH groups, which have different acid dissociation constants. At low pH, the amino group is protonated, and acts as a positive gate, which depletes hole carriers in the p-type SiNW and decreases the conductance. At high pH, the SiOH group is deprotonated, causing an increase in conductance. Ma et al. realized pH sensitivity via the enzymatic polymerization of aniline, which was templated by DNA on APTES [34] (Figure 2.8). The direct use of the stretched, immobilized DNA molecules as templates prevents the agglomeration of the polyaniline/DNA complexes formed in solution.

Besides its use as sensitive layer in the detection of protons, recently APTES has also been used as a sensing layer for the vapor-phase detection of 2,4,6-

TABLE 2.2: Examples of surface modifications on SiO_x-covered SiNW devices and target analytes. GA = Glutaraldehyde; EDC = 1-Ethyl-3-[3-dimethylaminopropyl]carbodiimide hydrochloride; PSA = Prostate specific antigen; ATP = Adenosine triphosphate; TNT = Trinitrotoluene; CRP = C-reactive protein; *The chemical structures of the silanes are given in Figure 2.7; **The silicon nanowires are covered with a layer of 10 nm Al_2O_3, grown by atomic layer deposition.

Sensor type	Surface modification*	Receptor	Analyte	Reference
pH	SiO_2	n.a.	H^+	
pH	APTES (1a)	n.a.	H^+	[13, 32, 33]
pH	APTES (1a)	DNA-templated polymerization of aniline	H^+	[34]
Bio		Biotin	Streptavidin	[13]
Bio	APTES (1a)	15-mer ss-DNA	Hybridization-induced charges in poly-T/ poly-A 15-mer DNA	[35]
Bio	APDMES (1b)	16-mer ss-DNA	Complementary DNA	[32]
Bio	MPTMS (4a)	12-mer ss-DNA	Single mismatch	[36]
Bio	APMS (3)	Monoclonal antibodies	PSA	[37]
Bio	APMS (3)	Antibody	Inluenza	[38]
Bio	APMS (3)	Tyrosine kinase	ATP	[39]
Bio	APTES (1a)/GA	Estrogen receptors protein	Estrogen response elements	[40]
Bio	APTES (1a)/GA	Anti-PSA	PSA	[41]
Bio	APTES** (1a)/GA	Glucose-oxidase	Glucose	[31]
Bio	APTES (1a)/GA	Anti-CRP	CRP	[42, 43]
Bio	APTES (1a)	EDC-supported carboxy-phenylboronic acid (CPBA)	Dopamine	[44]
Bio	AEAPS (2)	Gold nanoparticles	Thiol-terminated enzyme	[45]
Cations	SiO_2	Calmodulin	Ca^{2+}	[13]
Cations	MPTES (4b)	n.a.	Hg^+, Cd^+	[46]
Cations	AEAPS (2)	(phosphor)tyrosine	Ca^{2+}	[47]
Cations	APMS (3)	Gly-Gly-His	Cu^{2+}	[47]
Gas	APTES (1a)	n.a.	TNT	[48]

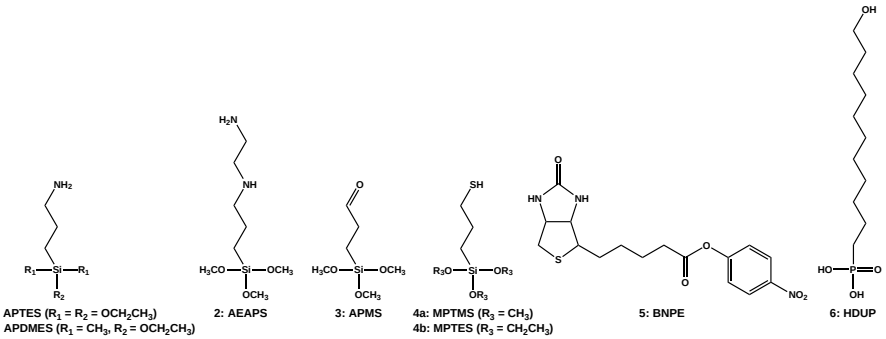

FIGURE 2.7: Compounds that have been used in the modification on SiO_x-coated NWs in NW-based devices: 3-aminopropyltriethoxysilane (APTES, 1a), (3-aminopropyl)-dimethylethoxysilane (APDMES, 1b), N-(2-aminoethyl)-3-aminopropyltrimethoxysilane (AEAPS, 2), 3-aldehydepropyltrimethoxysilane (APMS, 3), mercaptopropyltrimethoxysilane (MPTMS, 4a), mercaptopropyltriethoxysilane (MPTES, 4b), biotin 4-nitrophenyl ester (BNPE, 5) and 11-hydroxyundecyl-phosphonate (HDUP, 6).

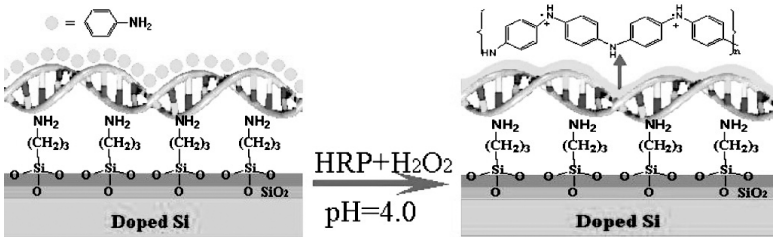

FIGURE 2.8: Fabrication of a polyaniline nanowire immobilized on a SiO_x surface with stretched double-stranded DNA as a guiding template, resulting in pH sensitivity. HRP stands for horseradish peroxidase. Figure from [34].

trinitrotoluene (TNT) [48]. The sensing mechanism is based on the acid-base interaction between the aminoterminated nanowire surface and the polarized TNT nitro-groups, which have a weak basicity. The binding of electron-deficient TNT molecules to the amino groups on the SiNW sensor surface is believed to result in the formation of charge-transfer complexes, which act as effective molecular gating elements. The conductance response of the resulting devices has a clear relation with the concentration of the explosive analytes and the device was found to be able to distinguish the target analyte from structurally related compounds. This example nicely shows that SiNW-based sensors are not only sensitive to changes in charges, but also to changes in charge density.

Given its reactivity towards aldehyde, carboxylic acid and epoxy functionalities, APTES has become the most frequently used linker compound for further (bio)functionalization of SiNWs. The activation procedure of the SiO_x nanowire surface using an oxygen plasma, followed by the immersion in a solution of APTES in ethanol and subsequent heating of the chip as reported by the Lieber group [13] is commonly used [43, 31]. Alternative approaches have been reported as well, e.g., the use of UV/ozone for the surface activation, followed by the use of neat APTES [44]. Also toluene [42] and acetone [35] have been used as a solvent in the silanization step. Because of the possibility of hydrogen-bond formation between the amine of APTES and the SiO_x surface, both head and tail groups can be oriented towards the surface, which can result in a large disorder in APTES layers [49]. Additionally, cross-linking between the alkoxy silane units may yield oligomerized silane structures on the surface, resulting in rough layers that are thicker than a monolayer. The optimal conditions for solvent-based silanization using APTES were investigated on planar surfaces [50]. The morphology and growth kinetics of APTES films deposited from solutions were found to be affected by reaction time, solution concentration, and temperature. Experiments with an APTES concentration of 1 % only produced good films when the reaction was time-limited (1 h). Increasing the reaction time increased the APTES film thickness. To overcome the problem of the disordered monolayers, Lin et al. performed a post-treatment of APTES-functionalized devices [35]. After the APTES modification, they aligned the internal dipoles of the APTES molecules using high electric fields, thus decreasing the disorder in the monolayer. In addition, it is shown that the source-drain conductance of the APTES-functionalized devices changes upon UV illumination. The authors explained this by a strengthening effect of the internal APTES dipoles by UV illumination. Additionally, UV illumination excites extra charge carriers in the nanowire. Depending on the size of both effects, the resistance of the nanowire can be increased or decreased, which was found to be measurable with the produced devices.

A modification that often follows the attachment of APTES to the SiO_x nanowire

surface is the reaction with glutaraldehyde (GA, Figure 2.6, right). This linker molecule is used to form an aldehyde-terminated surface, which increases the possibilities for further reactions, including the reaction with amine groups of, e.g., antibodies [41], proteins and enzymes [51, 31, 40]. Also amino-terminated, single-stranded DNA (ss-DNA) has been attached to APTES/GA-modified surfaces to measure hybridization-induced mismatches in 15-mer ss-DNA chains [35]. The addition of glutaraldehyde is, like that of APTES, both performed from solution [52, 40] and from the gas phase [31].

Li et al. reported the functionalization of an APTES-coated thin oxide gate with a dopamine receptor [44]. Although the devices do no belong to the class of SiNW-based sensors, the CMOS open-gate FET devices have (sub)micrometer gate dimensions. They have immobilized carboxyphenylboronic acid onto the APTES layer. The boronic acid group specifically reacts with the catechol functionality of, e.g., dopamine, which was detected in the femtomolar range.

Other Silane Derivatives Apart from APTES, also other amino-terminated silane derivatives have been used. For example, (3-aminopropyl)-dimethyl-ethoxysilane (APDMES, Figure 2.7, silane 1b) has been used in the modification of SiNW-based devices to bind a 16-mer ss-DNA [32]. In contrast to APTES (1a), APDMES (1b) is a mono-alkoxydimethylsilane, which is a crucial difference when it comes to the monolayer quality. Although silanes with only alkoxy group can react with each other, oligomerization can not take place. Consequently, the use of mono-alkoxydimethylsilanes results in the formation of a true monolayer. This issue was addressed in a detailed study by Dorvel et al. who synthesized an amino- and an epoxy-terminated mono-alkoxydimethylsilane, which were immobilized onto planer silicon oxide surfaces (Dorvel, 2010). In addition, N-(2-aminoethyl)-3-aminopropyltrimethoxysilane (AEAPS, Figure 2.7, silane 2) has been applied to immobilize an amino acid [52]. The nanowires devices were exposed to a solution of AEAPS in water, subsequently washed and finally dried to stimulate cross-linking of the molecules. This was followed by the reaction with GA to produce an aldehyde-terminated surface. Finally, tyrosine and phosphotyrosine were crosslinked with the aldehyde group through the formation of a Schiff base, which was further reduced to a stable secondary amine using sodium cyanoborohydride ($NaBH_3CN$). The studies, however, do not contain information on potential benefits of the alternative silanization agents used. Some other functionalities rather than amino groups have been employed in silane chemistry (Figure 2, silanes 3 and 4). Apart from APTES, the Lieber group used 3-aldehydepropyltrimethoxysilane (APMS, Figure 2.7, silane 3) [37] to directly obtain an aldehyde-terminated surface. Subsequently, monoclonal antibodies were attached to detect prostate-specific

antigens (PSA). The use of APMS enabled them to make a thinner organic layer as compared to combining APTES with glutaraldehyde. As oxygen in air will slowly oxidize aldehydes to acids or peracids, it is advisable to work with freshly prepared APMS surfaces or to make use of the reaction of glutaraldehyde with an APTES surface, directly prior to further functionalization. As a last example we mention the use of 3-mercaptopropyltriethoxysilane (MPTES, Figure 2.7, silane 4b) [46], which was applied to detect Cd^{2+} and Hg^{2+} ions. The thiol-terminated devices showed a linear relation between the logarithm of the Cd^{2+} and Hg^{2+} concentration and the source-drain conductance. The response towards K^+, Na^+, Ca^{2+}, Ba^{2+}, and Mg^{2+} (hard Lewis acids) was considerably smaller as compared to Cd^{2+} and Hg^{2+} (soft Lewis acids). This difference can be explained by the chemical softness of thiol groups, which hardly coordinate with hard Lewis acids. Since 2011, many more studies have been published on the covalent attachment of molecules on SiO_2, among which the extensive studies of the Haick-group [53, 54], who thoroughly study the effect of the chain length and functional groups on the electric characteristics of their sensors for the detection of volatile organic compounds.

Alternative Approaches

In this paragraph we address two different types of non silane-based compounds that have been used in the chemical modification of SiO_x surfaces of SiNW-based devices. Hahm and Lieber report on the 4-(dimethylamino)pyridine (DMAP)-catalyzed transesterification of biotin 4-nitrophenyl ester with the hydroxyl groups of SiO_x nanowire surface [55](Figure 2.9, left). Afterwards, the devices were exposed to phosphate-buffered saline (PBS) solution of avidin, which was followed by the addition of biotinylated peptide nucleic acid (PNA) capture probes. A general benefit of the use of PNA over DNA is that it enables sensing in an ultra-low background due to the lack of charges on the peptide backbone. In the work of Hahm and Lieber the surfaces were not analyzed after each modification step. However, based on the electrical characteristics of the modified devices it can be concluded that the PNA immobilization was successful. It has to be noted though that siloxane ester bonds (Si-O-(CO)) have a limited hydrolytic stability, at least lower than in the case of siloxane bonds (Si-O-Si). As a result, this immobilization technique is not often used.

Cattani-Scholz et al. investigated hydroxyalkylphosphonate monolayers as a platform for the biofunctionalization of SiNW-based field-effect sensor devices [56] (Figure 2.9, right). They employed a stepwise functionalization protocol using 11-hydroxyundecylphosphonate and a maleimide heterobifunctional linker system. The surface chemistry was also performed on planar surfaces, which made it possible to extensively analyze the surfaces after each step. It was found

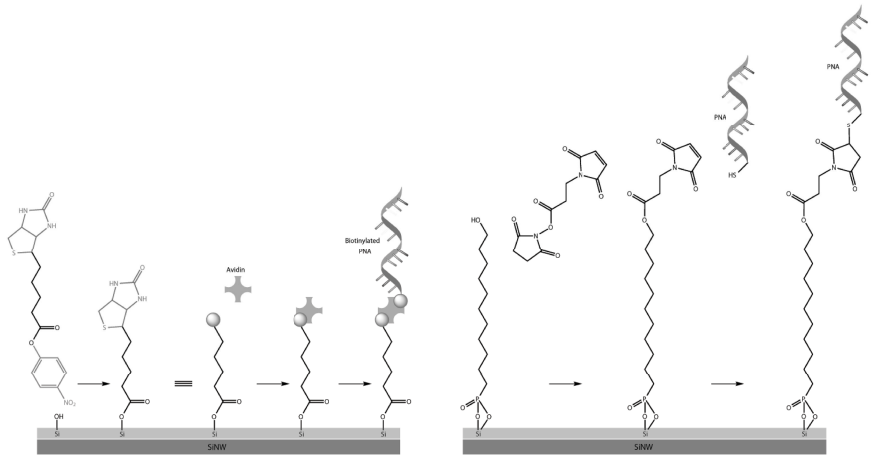

FIGURE 2.9: A schematic representation of two different surface chemistries that have been used to attach PNA onto SiO_x:(top) the use of biotin 4-nitrophenyl ester (the blue part of the structure indicates biotin molecule, whereas the red part of the structure indicates the 4-nitrophenyl group, which is used to activate the ester), the following steps involve the use of avidin and biotinylated PNA, and (bottom) the formation of organophosphonate monolayer, followed by the reactions with a maleimide heterobifunctional linker and subsequently with a thiolated PNA derivative.

that the hydroxyalkylphosphonate monolayer effectively passivates the Si surface against electrochemical leakage current into the electrolyte solution through the interface, with maximum currents of the order of 10 pA measured at an applied voltage of 200 mV. In a comparative study it has been shown that phosphonate monolayers on the native oxide of Ti-6Al-4V are hydrolytically more stable than the corresponding siloxane monolayers [57]. It is also reported that the monolayer growth is not limited by the surface OH content [58], making this type of surface modification an interesting alternative for silane-based chemistry.

2.2.3 NON-COVALENT FUNCTIONALIZATION

Adsorption of Polyelectrolytes

The negative nature of SiO_x at pH > 3.5 allows one to electrostatically immobilize positively charged polymers (polycations), also called generally polyelectrolytes (PEs). Subsequently, a negatively charged polymer (polyanion) can be adsorbed on top. Providing that each adsorption step of charged polymers leads to a charge inversion of the surface (charge overcompensation effect), the subsequent deposition finally results in a PE multilayer, stabilized by strong, multivalent electrostatic forces. This method is known as layer-by-layer (LbL) deposition [59].

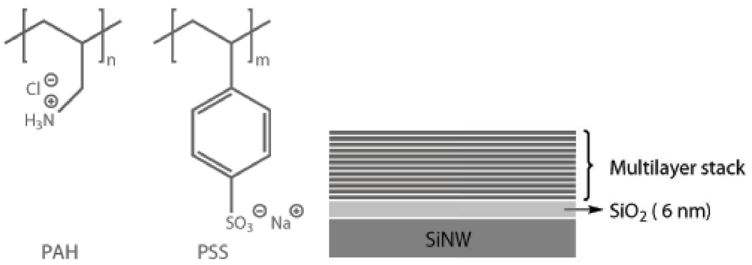

FIGURE 2.10: Structures of the polycation polyallylamine hydrochloride (PAH) and polyanion polystyrenesulphonate (PSS) used by Ingebrandt and coworkers to prepare layer-by-layer multilayers onto SiO_x-covered SiNW-based devices [60].

A variety of deposition methods can be used, including dip-coating, spin-coating, spray-coating and flow-based techniques. Ingebrandt and coworkers applied the LbL deposition technology onto SiNW-based devices [60]. They immobilized polyallylamine hydrochloride (PAH: MW 15,000) onto 6 nm thick, thermally grown SiO_x via dip coating. Subsequently, polystyrenesulphonate (PSS: MW 60,000-80,000) was immobilized and this sequence was repeated several times to make a stack of 6 bilayers (Figure 2.10). The thickness of the resulting multilayer has not been reported. Assuming a monolayer thickness of ~ 2 nm [59, 61] the multistack thickness would be ~ 24 nm. It has to be noted, however, that the salt concentration has an effect on the layer thickness [62], which makes it difficult to predict the thickness accurately. Although the noise level of PE-coated devices was slightly higher than that of their standard FET devices, the sensitivity for PE adsorption measurements was 3 to 4 times higher as compared to previous reports.

Dorvel and coworkers [63] reported on the electrostatic adsorption of poly-L-lysine (PLL) on HfO_2-covered NW surfaces. Atomic Layer Depoistion (ALD) was used to form the HfO_2 dielectric, followed by a wet etch-based process for releasing the device structure. After electrostatic deposition of the positively charged PLL-layer, negatively charged ssDNA was added, which adsorbs in a horizontal alignment [64]. This way, the charges are closer to the surface compared to vertically aligned ssDNA, and have a larger influence on the NW. After the electrostatic binding of the phosphate backbone of the probe DNA to the PLL, the complementary DNA target is introduced and sensed on the device (Figure 2.11). It was found that lower molecular-weight PLL results in a comparable layer thickness compared to high molecular-weight, and a larger density and a higher sensitivity in DNA sensing experiments. Moreover, a non-complementary DNA target strand showed very little response, indicating a highly sensitive and highly

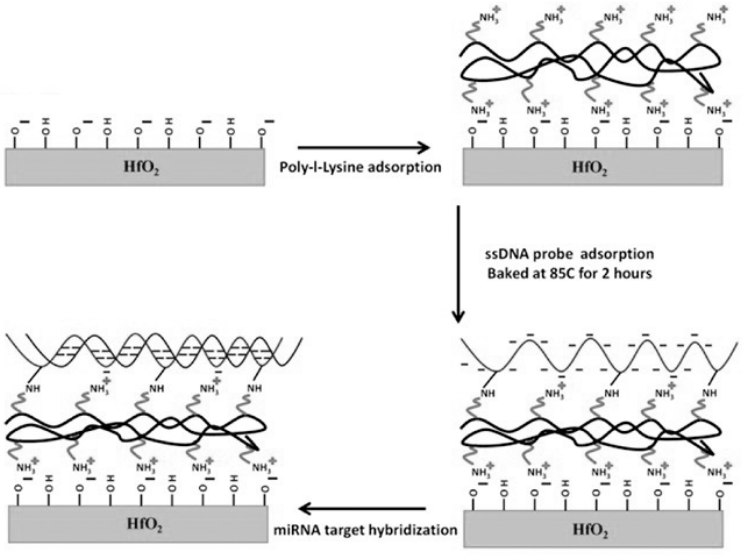

FIGURE 2.11: Schematic of the surface functionalization of the HfO_2 surface for ssDNA sensing [63].

selective biosensing platform.

Lipid Membranes
Silica surfaces have also been used as a platform to immobilize model membrane systems like supported lipid bilayers, which have been extensively used in understanding the fundamental properties of biological membranes. However, there have been only a few attempts to apply lipid membranes on nanoelectronic devices. Misra et al. incorporated lipid bilayer membranes into SiNW transistors (Figure 2.12). In more detail, they covered the NWs and the background oxide with a continuous lipid bilayer shell, forming a barrier between the SiO_x surface and solution species [65, 66]. The method is based on the fusion of spherical unilamellar vesicles onto a SiNW surface producing a planar conformal lipid bilayer coating [67].

Cyclic voltammetry using potassium ferrocyanide ($K_4Fe(CN)_6$) as a redox probe showed that the presence of a lipid bilayer on the NW surface reduced the limiting current by 85-95 % relative to the native oxide-covered NW device [66]. Subsequently, two different transmembrane peptides (gramicidin A and alamethicin) were incorporated in the vesicles, resulting in ion channel-containing lipid bilayers after fusion with SiNW-based devices. It was shown that the incorporation

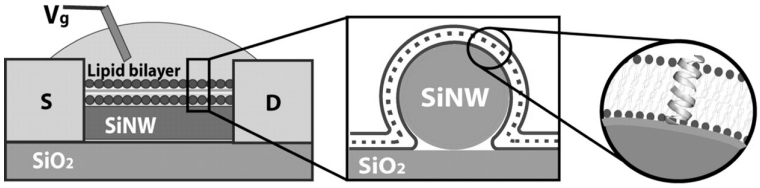

FIGURE 2.12: Device schematics showing a SiNW connected to microfabricated source (S) and drain (D) electrodes. Although this is not clear from the figure it should be noted that the source and drain are insulated with Si_3N_4. The insets show the configuration of the lipid bilayer and a pore channel placed in the bilayer membrane. Figure from [66].

of transmembrane peptide pores enabled ionicto electronic-signal-transduction by using voltage-gated and chemically gated ion transport through the membrane pores.

PVC Membranes

As a logical continuation of the work on membrane-covered ISFETs [10], ion-selective membranes have also been drop-casted on NW-FETs [68, 69]. The membranes consist of PVC which serves as a carrier for the valinomycin ionophore, which is able to bind potassium ions very specifically. Chang and coworkers [68] used these membranes to detect extracellular K^+ flux. After culturing, the cells were placed on top of the NW/membrane system, and stimulated using nicotine to release K^+ ions. Concentrations of 10^{-6} to 10^{-2} M have been measured, making this a suitable system for in-situ biological applications. The second study with PVC membranes drop-casted onto NW-FETs, by Wipf and coworkers [69], shows a high response of 38 mV per decade, using Al_2O_3-covered NWs as reference devices.

Palladium Nanoparticles and Thin Films

Extremely local modification of nanowires with metal nanoparticles is demonstrated by Yun and coworkers [70]. Joule heating (or Ohmic heating, the release of heat when current passes through a semiconductor) is used to modify the individual wires, making it possible to selectively modify only those wires that are targeted, while the other wires stay unheated and thus unmodified. Two approaches have been demonstrated, both depicted in Figure 2.13. In the first method, the chip is exposed to a precursor solution of 16 ml of 1 mM K_2PdCl_4 and 200 µl of 30 mM sodium citrate. An aqueous sodium hydroxide solution was added to the palladium precursor solution to set pH=11. The Joule heating of a SiNW generated a localized heat along the SiNW resulting in endothermic reactions such

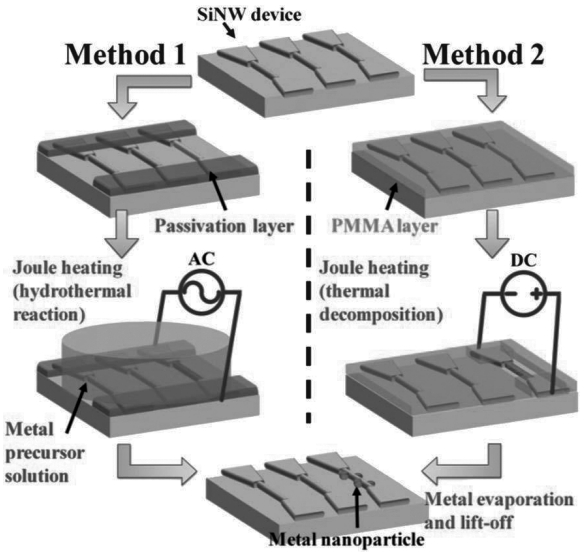

FIGURE 2.13: Schematic representation of the approaches used by Yun and coworkers. In method 1 the nanoparticles are formed on the nanowire by hydrothermal reaction via Joule heating of a SiNW. In method 2, a metal thin film is locally deposited on a SiNW through PMMA decomposition, metal evaporation and lift-off [70].

as hydrothermal synthesis of nanoparticles or thermal decomposition of polymer thin films.

The second method is similar to the method published by the same author a few years earlier [71]: the Joule heating creates an opening in a polymer layer on top of the devices (here: polymethyl methacrylate (PMMA)). After this local removal, a thin layer (<2 nm) of palladium has been evaporated on the sample. Lift-off is done subsequently by dipping in aceton and ultrasonication, resulting in a nanowire decorated with metal particles. Devices prepared using both methods are used in H_2 gas sensing experiments, and it was demonstrated that the conductiviy of the system changes upon H_2 exposure. This attributed to the formation of a PdH_2 complex. Joule heating was used to optimize the sensitivity and response time of this system, as a higher temperature leads to a faster response, but a lower detection limit. Recovery of the initial conductivity was obtained faster when larger potentials were applied to the devices.

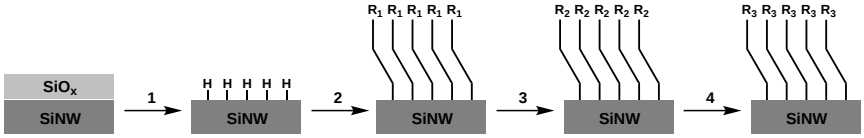

FIGURE 2.14: Schematic representation of the 1) etching of the SiO_x surface, yielding a H-terminated surface, 2) formation of Si-C monolayers via hydrosilylation (R_1 represents a functional group that is chemically protected towards the reaction with the H-terminated Si surface, e.g., an ester or amide), 3) deprotection the functional group (represented by R_2, e.g., a carboxylic acid or amine), 4) attachment of a receptor (represented by R_3).)

2.2.4 OXIDE-FREE SINW-BASED SENSOR DEVICES

Hydrosilylation

As an alternative to silane-based chemistry, silicon substrates can also be modified using so-called hydrosilylation chemistry, e.g., the reaction between a surface Si-H and an organic compound containing a terminal unsaturated carbon-carbon bond (alkenes and alkynes) to form a Si-C linked monolayer (Figure 2.14).

This work has been pioneered by Linford and Chidsey in the early 1990s [72, 73] and this type of monolayers has continued to attract attention ever since. Hydrosilylation chemistry requires removal of SiO_x, which in most cases is achieved using wet chemistry. On planar silicon surfaces diluted, aqueous HF and NH_4F solutions are used to etch Si(100) and Si(111) substrates, respectively, although a wide variety of etching methods has become available (Zhang, 2001a). This process results in hydrogen-terminated, oxide-free silicon substrates with Si-H groups. The reaction of H-terminated silicon surfaces with alkenes and alkynes can be performed by making use of high temperatures, UV and visible light irradiation, electrochemistry, hydrosilylation catalysts (e.g., $AlCl_3$), and chemomechanical scribing, as summarized in different reviews [74, 23, 24, 75].

Organic Monolayers: Si-C versus SiO_x-C

Si-C bonded monolayers have a number of advantages over silane-based monolayers on SiO_x surfaces. First, interface trap densities for Si-C bonded monolayers can be considered remarkably lower than in the case of alkyl chains organic monolayers on naturally oxidized silicon surfaces [76]. Also, as already mentioned in Section 2.2.2, silane oligomerization can result in rough layers that are thicker than a monolayer. In contrast, the reaction between a H-terminated Si surface and alkenes or alkynes results in a true monolayer. This is related to the involved zipper mechanism, in which each binding of an alkyl chain directly generates a new radical site on the next-nearest Si surface atom [73]. Moreover, the chemical stability of monolayers on SiO_x in aqueous media is poor since the exposure to wa-

ter pilots the destruction of the monolayer through hydrolysis of Si-O bonds [77]. Organic layers formed by hydrosilylation are stable in a number of environments, including air, boiling water, organic solvents, and acids [73]. In the field of SiNW-based devices, the application of Si-C monolayers has a number of other benefits as compared to silane-based surface modifications.

First, the removal of SiO_x brings a sensing event (target/analyte interaction) closer to the conducting surface, which increases the sensitivity of the device [32, 78]. Second, the selective functionalization of oxide-free SiNWs is considered to be a supplementary factor that improves the detection sensitivity by avoiding the binding competition between the SiNW and the oxide surface on the rest of the device. Third, several studies show improved electrical properties of Si-C linked monolayers over monolayers on SiOx, in terms of the flatband potential and source-drain conductance [79, 80].

A crucial difference between the silane-based and alkene-based approach becomes clear from, e.g., the preparation of amine-terminated monolayers. While in the case of SiO_x unprotected amines can be used (Section 2.2.2), e.g., APTES, amine-containing alkenes should be chemically protected as amines can react with H-terminated Si surfaces. The N-tertbutoxycarbonyl (t-BOC, Figure 2.15, alkenes 7a and 7b) is a commonly used protecting group for primary amines, but other protecting groups have been used as well [81]. Apart from amines, also carboxylic acid and alcohol functionalities should be protected before application in the hydrosilylation chemistry [74].

Characteristic of Si-C bonded monolayers is that the molecular cross-section of the attached alkyl chain prevents reaction of all individual Si-H bonds, i.e., upon formation of a monolayer on Si(111) about 50-55 % of the Si-H sites has reacted [82], while on Si(100) this is about 30-35 % [83]. The remaining, unreacted Si-H sites are a potential source for the formation of interface states, e.g., via oxidation, which is an unfavourable process in terms of device performance.

Hydrosilylation on SiNW-Based Sensor Devices

The reported chemistry for functionalizing the oxide-free, H-terminated SiNW sensor devices is mainly done via one method, i.e., hydrosilylation catalyzed by UV irradiation. This approach has been applied by different research groups using different etching conditions and probing different types of analytes (Table 2.3). The first report on the modification of oxide-free SiNW-based devices is by Heath and coworkers [32]. The authors followed an established, multistep protocol [84, 85] that starts with the hydrosilylation of H-terminated SiNWs with tert-butyl allylcarbamate (Figure 2.15, alkene 7a) irradiated at 254 nm. After deprotection, the researchers obtained a positively charged amine-terminated monolayer on the SiNWs, enabling the adsorption of negatively charged, oligo ss-DNA. Surface

TABLE 2.3: Overview of the references that report on the chemical modification of the SiNW-based devices via hydrosilylation chemistry. *The chemical structures of the alkenes are given in Figure 2.15.

Analyte	Receptor	Surface Binding Molecule*	Etching Conditions	Reference
ss-DNA	ss-DNA	7a	2 % HF (aq) (3 s)	[32]
K^+, Na^+	Crown Ether	7b	1 % HF(aq) (50 s) + NH_4F (aq) (60 s)	[86]
ss-DNA	ss-PNA	7b	1 % HF (aq) (50 s) + NH_4F (aq) (60 s)	[78, 87]
Avidin/ Streptavidin	Biotin	7b	10:1 v/v 40 % NH_4F (aq)/ 49 % HF (aq) (5s)	[88]
Antigen	Antibody	7b	10:1 v/v 40 % NH_4F (aq)/ 49 % HF (aq) (5s)	[88]
-	-	8,9a	10:1 v/v 40 % NH_4F (aq)/ 49 % HF (aq) (5s)	[88]
-	-	9b	1 %HF (aq) + 40 % HF (aq) (4-5 min)	[89]
DPCP		11	HF	[90, 91, 92]

characterization of the nanowires embedded in a device is a challenge, since conventional analytical tools used for surface characterization require substrates on the micro-scale. For that reason a widely used strategy is to perform the applied chemistry also on planar samples.

This strategy was also followed by Bunimovich et al. and planar Si(100) samples were analyzed by water contact angle measurements and X-ray Photoelectron Spectroscopy. Moreover, this interesting paper compares Si-C and SiO_x-based monolayers. It is shown that the electrical read-out of oxide-free SiNWs for sensing complementary 16-mer DNA was more profound than on modified, SiOx-covered SiNWs.

Also Zhang et al. used hydrosilylation chemistry to coat SiNW devices with ss-DNA, although a different strategy was chosen [78, 87]. The modification scheme starts with the UV-initiated attachment of 10-N-boc-amino-dec-1-ene (Figure 2.15, alkene 7b) to a device with H-terminated SiNWs. After the deprotection of the amino groups the surface was chemically modified with glutaraldehyde, allowing the covalent binding of amino-terminated compounds. Inspired by the work of others on devices with SiO_x nanowires [93, 55, 47], they subsequently immobilized

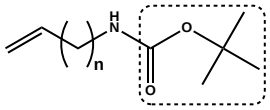

7a: Tert-butyl allylcarbamate (n=1)
7b: 10-*N*-Boc-amino-dec-1-ene (n=8)

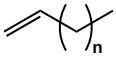

9a: 1-Decene (n = 7)
9b: 1-Octadecene (n = 15)

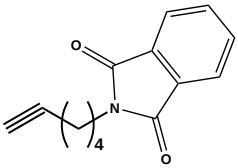

10: n-(5-Hexynyl)phthalimide precursor

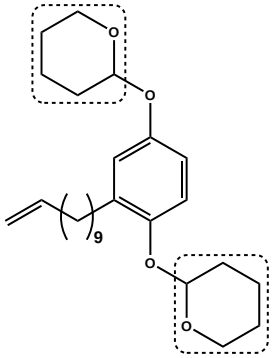

8: Tetrahydropyranyl-terminated alkene

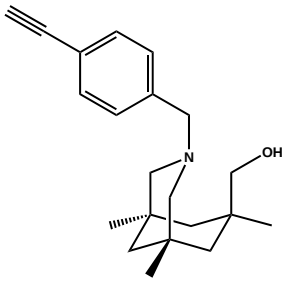

11: Alkyne derivative (receptor for diphenylchlorophosphate)

FIGURE 2.15: Examples of derivatives that have been chemically bound to oxide-free SiNW sensor devices. The protecting groups on various alkenes are marked in dashed rectangles. For alkene 7a and 7b the protecting group is N-tert-butoxycarbonyl (t-BOC), for alkene 8 it is the tetrahydropyranyl (THP) group. See text for further information.

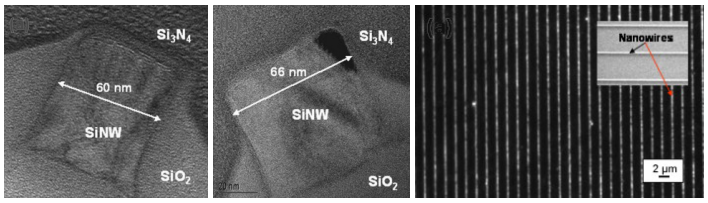

(a) (b) (c)

FIGURE 2.16: Alkene derivatives that have been chemically bound to oxide-free SiNW sensor devices. The protecting groups on various alkenes are marked in grey rectangles. For alkene 7a and 7b the protecting group is N-tert-butoxycarbonyl (t-BOC), for alkene 8 it is the tetrahydropyranyl (THP) group. See text for further information.

PNA. The benefit of this approach over the method reported by Bunimovich et al. is twofold: PNA is not only neutral (see also section 2.2.2), it is also bonded covalently. Although multivalent, ionic interactions might be stronger than one single covalent bond, the latter is independent of the salt concentration, making it more robust in wide range of chemically different environments.

As for sample characterization the research group was quite successful in depicting the chemistry performed on the SiNWs. Transmission electron microscopy (TEM) was performed for a morphological study of the non-oxidized SiNW surface. From the TEM data the authors concluded that the surface was nearly uniform, oxide free and did not show visible TEM-detectable defects (Figure 2.16b). In addition, binding of fluorescently labeled, complementary DNA was used to demonstrate the selectivity of the non-oxidized SiNW surface chemistry and the specificity of PNA-DNA hybridization. Indeed, strong fluorescent signals on the SiNWs were obtained and the bright arrays of SiNWs were clearly visible (Figure 2.16c).

Earlier work by Zhang et al. focused on the sensing of alkali metal ions by the chemical modification of SiNW-based devices with crown ethers [86]. Also in this case alkene 7b was used, followed by the reaction with glutaraldehyde, resulting in an aldehydeterminated monolayer. Subsequently, amine-terminated crown ethers were covalently attached. Based on the complexation selectivity of crown ethers to alkali metal ions, the resulting functionalized oxide-free SiNW-based devices could detect Na^+ and K^+.

The sensitivity of protein binding by oxide-free SiNW-based FETs was first reported by Stern et al. using biotin-avidin/streptavidin interactions and antibody-antigen sensing [22]. Three different functionalized alkene derivatives were used in the UV-initiated reaction with H-terminated SiNW devices: 10-N-boc-amino-dec-1-ene (7b), 2-[2-(undec-10-enyl)-4-(tetrahydro-2H-pyran-2-yloxy)phenoxy]-

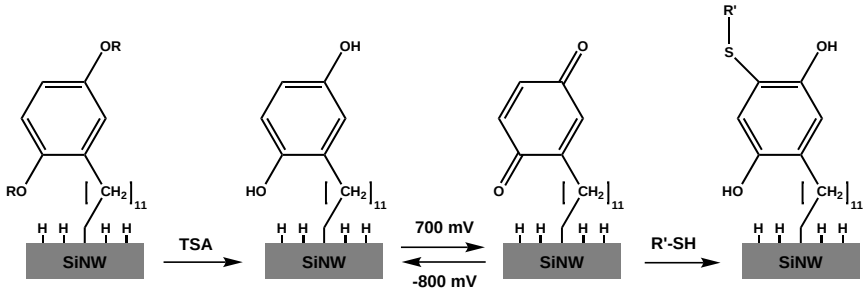

FIGURE 2.17: The strategy reported by the Heath group [84] and also investigated by the Reed group [88] for the selective immobilization of thiolated biotin (R'-SH) via a Michael addition. TSA stands for 1% toluene sulfonic acid. See text for further explanation.

tetrahydro-H-pyran containing a tetrahydropyranyl (THP) protecting group (8), and 1-decene (9). Only alkene 7b could be realized for sensing purposes, whereas modification with alkene 8 was ineffective for sensing and alkene 9 aimed as a control. Using alkene 7b, amino-terminated monolayers were obtained, followed by a common biotinylation protocol using N-hydroxysulfosuccinimide for capturing avidin and streptavidin. For antibody-antigen sensing the capture antibodies were bound to hydrosilylated SiNWs by N-hydroxysulfosuccinimide/ethylene dicarbodiimide coupling chemistry [94].

The strategy for protein binding using alkene 8 is different and more complicated, yet very appealing. That is because it creates electrochemically active monolayers on top of the SiNWs. Such electro-active monolayers ensure not only the monolayer formation qualitatively, but they also allow the quantification of the surface coverage. This is based on the fact that the required electrons for the reduction of the electro-active moiety can be measured. The number of electrons is directly proportional to the number of the electroactive groups present and hence to the coverage. As a first step THP-protected alkene 8 was photochemically bound to hydrogen-terminated SiNW. Removal of the protecting THP ethers under mild conditions of 1% toluene sulfonic acid (TSA) in methanol leads to the hydroquinone (Figure 2.17). Cyclic voltammetry (CV) in PBS oxidized the hydroquinone to quinone. Finally, they aimed to couple thiolated biotin selectively to the thus formed quinone moieties, but this was not successful, most likely due to the degradation of the device performance that was observed upon chemical modification.

While devices that were modified via UV-induced hydrosilylation using alkenes 7b and 9a experienced increased leakage currents, the use of compound 8 led to

loss of gating behavior, most likely due to the formation of redox-active surface traps. For compound 7b the authors report a device yield as low as <2 % after the deprotection. The work of Stern et al. highlights the importance of validating the device performance after chemical modification [88].

Attachment of molecules via the reaction of an alkyne with the Si-H surface is done by the group of Simonato and Raskin [90, 91, 92]. In this work, HF-pretreated Si-NWs and nanoribbons are modified with compound 11 from Figure 2.15, by reacting the alkyne group with the Si-H surface, forming a Si-C bond. Diphenylchlorophosphate (DPCP) can be used as mimic for warfare agents like Sarin or Soman and reacts with compound 11, making this a sensor for nerve agents.

Organic Monolayers on Oxide-Free SiNW Devices: Towards Sensing
The observation of changes in device performance upon chemical modification of its sensing area has not only been reported by Stern et al., but also in a few other cases. Yet there is evidence that even non-charged molecules adsorbed on the nanowire alter the device characteristics. Haick et al. showed an improved conductance of the H-terminated SiNWs upon the chlorination/alkylation of the nanowire [95]. They reported that methylterminated SiNWs exhibit higher source-drain conductance values, lower surface defect levels and higher on-off ratios than oxygenated SiNWs. Another example of characterizing the surface passivation of a NW prior to sensing is the work of Masood et al. [89]. An improved device behavior after hydrosilylation on SiNW with 1-octadecene and n-(5-hexynyl)phthalimide (Figure 2.15, compound 9b and 10) has been shown by means of capacitance-voltage and current-front gate voltage electrical measurements. Based on other studies showing that hydrogen-terminated Si(111) surfaces have the lowest reported surface recombination velocity and improved electronic performance as compared to Si(100) surfaces with SiO_2 interfaces, the authors stress the importance of using Si(111) surface to further improve the Si-NW biosensor performance.

Cyclic Voltametry
The only other method for hydrosilylation on SiNW surfaces reported in literature is cyclic voltametry (CV). CV is a method where a cyclic potential is applied to a system, in order to study redox reactions, that can also be used to graft molecules onto surfaces, including silicon. This alternative approach to the covalent functionalization of oxide-free NW surface is used by Azmi and coworkers [96] (see Figure 2.18). The authors use the NW chip array as working electrode, a Pt wire as a counter electrode and a Ag/AgCl electrode as reference electrode. A thin film of nitrophenyl groups is attached to the NW using a solution of

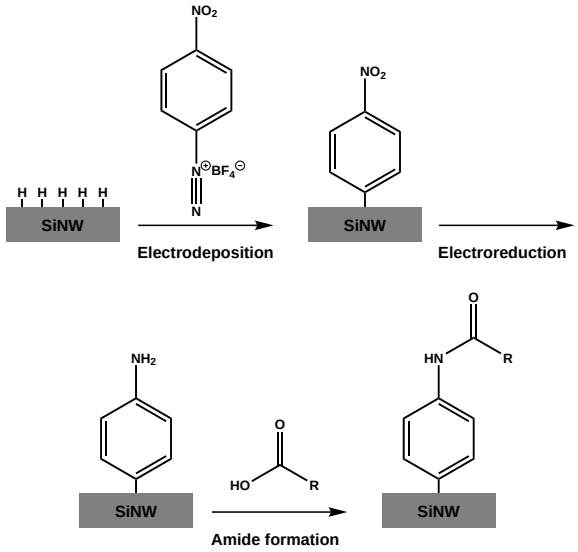

FIGURE 2.18: The strategy reported by the Azmi and coworkers [96] for the electografting of using diazonium compounds. See text for further explanation.

4-nitrobenzenediazonium tetrafluoroborate and a cyclic voltametry scan from +0.2 V to -0.9 V. The CV has to be repeated 20 times to ensure that the reduction reaction is completed. In the second step, the nitrobenzene groups are reduced to aniline ($PhNH_2$) molecules, using a constant voltage of -0.9 V. Antibodies against prostate cancer risk biomarker 8-hydroxydeoxyguanosine (8-OHdG) are subsequently attached to the amino group via the well-known reaction with the carboxyl group. The authors show consistent proof of the attachment of the modification using X-ray photoelectron spectroscopy, atomic force microscopy and contact angle measurements and are able to detect the 8-OHdG biomarkers down to 1 ng/ml, with a linear response over the 1-40 ng/ml concentration range.

2.2.5 CONCLUDING REMARKS AND OUTLOOK

In order to bind (bio)receptor molecules onto SiNW-based devices, most studies apply the silanization on the nanowire oxide layer. Clearly APTES is the most frequently used silane-based agent, enabling the subsequent immobilization of carboxylic acid- or aldehyde terminated biomolecules. More often, further derivativization with glutaraldehyde has been applied to chemically bind amine-terminated biomolecules. A disadvantage of silane compounds is their ability to

react with each other via cross-linking of the alkoxy units, resulting in rough, unordered multilayers. Based on the optimization studies on planar silica substrates that have become available [50] and reports on the quality differences between vapour- and wet chemistry-prepared APTES layers (Fiorilli, 2008), there is room for the improvement of silane chemistry on SiNW-based devices. Phosphonate monolayers are an interesting alternative for silane-based monolayers, due to their higher hydrolytical stability and the less critical pretreatment of the oxide surface that is required.

Apart from covalent functionalization of SiNW-based sensor devices also physisorption has been studied, which enabled the detection of several compounds and ions. Covalent attachment of (bio)molecules to sensor surfaces may be appealing in terms of device stability, but some systems, e.g., membrane receptors require a more dynamic environment. It has been shown that a phospholipid monolayer can be covalently immobilized on SiO_x [97] and Si-H [98] surfaces, enabling the noncovalent immobilization of a second phospholipid layer. However, this strategy may hamper the fluidic properties of the bilayer, which is vital for the incorporation of biologically active structures into the membrane. The fusion of spherical unilamellar vesicles onto surfaces overcomes this problem. So far, only two different transmembrane ion channels on SiNW-based devices have been reported [66], but lipid bilayers provide a matrix for a virtually unlimited number of transmembrane proteins that can accommodate different functionalities.

Physisorbed PE layers are not covalently attached; nevertheless they are very stable, due to the multivalent character of the interaction. The multivalency is also beneficial regarding the detection of a PEs that adsorbs onto the SiNW-based device. LbL films of PE have been employed for various applications, including electrochemical sensing and biosensing and they have also contributed to the investigation of fundamental studies in electrochemistry [99]. The work of Ingebrandt and coworkers [60] can now be extended to the use of biologically relevant PEs and perhaps also the incorporation of nanoparticles. Also the work on drop-casting of PVC membranes [68, 69] has shown that modifications similar to those on ISFETs are possible, which opens a broad range of available membranes, ready for their application on NW-FETs. The idea of using Joule heating [70] has also opened up a large number of possibilities, especially in the field of the fabrication of arrays with individually modified NWs, making it possible to attach different receptors on individual NWs without using mask technologies. Potentially this can also be achieved by the electrodeposition of diazonium compounds [96]. These developments are very important for multiplex analysis, i.e. to simultaneously measure multiple target compounds.

An interesting candidate to replace SiO_x layers on silicon surfaces is found in alkene-prepared organic monolayers. There are a number of benefits for

monolayers on oxide-free silicon over silane-based layers: a) no risk of oligomerization, resulting in a true monolayer, b) higher chemical stability, c) selective functionalization, i.e., the background surface is not functionalized, and d) a lower density of interface traps. Although a wide variety of preparation procedures for hydrosilylation surface chemistry are available, so far only UV initiated methods and cyclic voltametry have been used in the chemical modification of oxide-free H-terminated SiNW devices. This can be explained by the fact that the research in this direction is still in its early days, and it probably will not take long before some of the other available preparation methods will be explored on SiNW-based devices. An important issue in this regard is the surface orientation of the nanowire [84]. In addition, a very good monolayer quality is needed, reducing the number of interfacial defects [100]. In contrast to SiO_x-covered SiNW-based devices, the insulating properties in the case of oxide-free SiNW-based devices are exclusively to be realized by the organic monolayer itself. One possibility to improve the monolayer quality is by using alkynes instead of alkenes [101, 102, 103].

To conclude, selective functionalization of the nanowires is critical to retain sensitivity as the modification of the background oxide results in a reduced sensitivity. In addition, the modification of individual nanowires that are part of a larger array is essential to perform a multi-analysis using a single device. Continued advances in the preparation of well-defined, defect-free, organic-semiconductor interfaces will further improve the performance of SiNW-based devices. The combination of an increasingly growing number of interesting (bio)receptors, sophisticated device fabrication methods, improved electrical characterization procedures and advanced organic surface modification (e.g. the Joule heating [70] and the electrografting [96]) does not only provide unlimited research opportunities, it will also contribute significantly to diverse, highly usable sensor applications in a variety of fields.

3

FABRICATION

This chapter demonstrates a new method for the top-down production of silicon nanowire field-effect transistors for sensing applications. A simple and robust method for the fabrication of these devices is described, using only conventional CMOS processing techniques making it manufacturable on large scale in a broad range of production facilities. Moreover, the process is flexible in terms of the choice of the type of front oxide of the transistor, as it is applied in a separate, independent step from the application of the surrounding oxide. In case ultimate small dimensions are required that go beyond the wafer stepper resolution, the use of e-beam technology to produce even smaller structures can be easily integrated. Furthermore, the use of a passivation layer opens possibilities for adding selectivity via surface modification on silicon dioxide and silicon. After a detailed description of the process, the electrical characteristics of the devices are shown together with data on the device reliability, indicating that the process is easy to manufacture, has a large yield and results in sensor devices with electrical characteristics in the desired regime.

This chapter has been published in Journal of Nanoscience and Nanotechnoloy, *Robust Fabrication Method for Silicon Nanowire Field Effect Transistors for Sensing Applications*, M. Mescher, L.C.P.M. de Smet, E.J.R. Sudhölter and J.H. Klootwijk, **13**, 8 (2013) [3].

3.1 INTRODUCTION

OVER the past years, numerous papers have been published on silicon nanowires. Their large surface-to-volume ratio makes them potentially very useful for sensing purposes [19, 104, 105]. Integration of these nanowires into silicon nanowire field-effect transistors (Si NW-FETs) as sensors has been explored in a wide variety of applications, ranging from the detection of ions [46, 106, 107], proteins [108, 88, 13, 38, 109] and DNA [110, 78, 32, 36] in aqueous solutions to sensing of the presence of explosives [48] and other gas sensor applications [111, 112]. A broad range of chemical and physical modification methods is applied to obtain selectivity, starting from silicon oxide and silicon [2]. Besides the modification, other aspects of NW-FETs as sensors have been investigated as well. For example, the optimal working regime has been studied [113, 114, 115] and nanowires with different shapes and dimensions have been produced [116, 117]. Other studies focus on optimizing the sensor sensitivity by tuning the Debye length [118, 119] and the use of real biosamples such as whole blood instead of model solutions [120]. NW-FETs are primarily known from vertically grown nanowires, the so-called bottom-up approach [121]. However, the integration of these nanowires in in-plane devices on large scale has proven to be difficult, so many researchers moved to the top-down strategies. Here, the nanowires are etched from silicon on insulator (SOI) wafers following a CMOS-like approach, which enables an easier and more controlled formation of the contacts to the nanowire. What has not been explored in much detail is the large-scale production of these sensors. For industrial applications, e.g. water purifiers or medical devices, it is desired to manufacture the devices at high reproducibility and low cost. In this study we demonstrate an easy and cheap process for the production of the silicon nanowire devices. The process is CMOS compatible and flexible making it suitable for a broad range of applications. It also allows the use of other front oxides besides the common silicon oxide (e.g. Al_2O_3), which has been shown to be an important option [122]. The silicon nanowires are defined by etching the top silicon layer of an SOI wafer. This can be performed by wet methods, or by dry etching (deep reactive ion etching). In particular in the latter case the selectivity of etching towards the underlying silicon dioxide is not infinite. Stopping on the oxide layer without attacking the underlying layer may be an issue, although the etching technology is very mature and well developed. In order to prevent any negative consequence of this etching step, our process flow includes additional processing steps to compensate for and partially prevent this undesired effect. Furthermore, integration of e-beam techniques is possible, which provides a way to scale down the nanowire dimensions even further. A third advantage of the process described in this chapter has to do with the option to use different

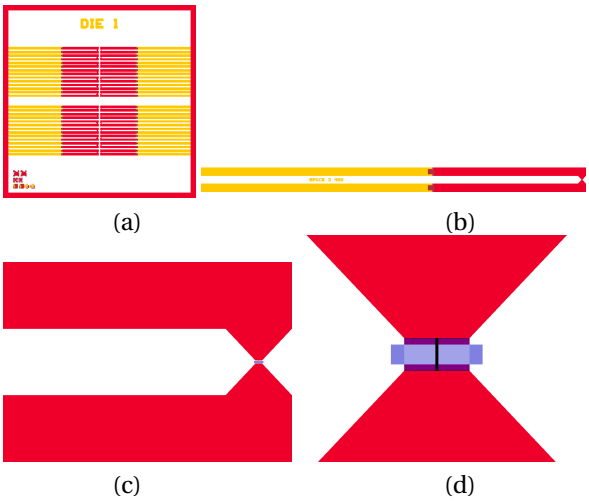

FIGURE 3.1: Details of the wafer stepper reticles used. Yellow parts are metal, red is silicon, blue is the no-implant mask. a) Is the overview of a complete die, where on both sides two times fourteen devices are placed. The lower left corner contains test structures used for process control. b) Shows a single nanowire device: the metal contact leads are connected to the (highly doped) silicon connections, which on the right sides connect the nanowire c) Shows how the leads come to the nanowire and d) Shows the no-implant wafer stepper reticle as it is used on top of the nanowire.

materials for the front oxide and surrounding oxide, which enables the selective modification of the nanowire only. Techniques that offer selectivity for (silicon) oxide compared to the passivation layer can be used to selectively modify the nanowire only, either by direct silanization of the front oxide, or by etching away the front oxide followed by hydrosilylation. In the following sections, a detailed description of processing these devices is presented; the electrical characteristics of the NW-FETs are shown and these results are discussed.

3.2 EXPERIMENTAL METHODS

THE layout of the chips containing the silicon nanowire field-effect transistors is shown in Figure 3.1.

Every die consists of an array of two times fourteen nanowire field-effect devices. The devices consist of a nanowire between two highly-doped silicon contact leads. These leads are connected to aluminum leads, which are used to connect the device to the external analyzing equipment. The important dimensions of the nanowire are determined by 1) the structure that is etched from the silicon and 2) by the no-implant wafer stepper reticle that is used to define the low-doped part

of the actual nanowire. The devices consist of a nanowire of typically 20-2000 nm in width and a low-doped (effective device) length of 3 μm.

The devices are produced from 150 mm SOI wafers. The wafers have a buried oxide (BOX) layer of 300 nm and a high-doped (10^{19} cm^{-3}) substrate (Figure 3.2b). The (low-doped p-type) device layer is thinned until a thickness of 50-100 nm. Alignment markers are lasered in the wafer and etched free. Subsequently, a screen oxide is applied before the wafer is implanted to protect the wafer during the implantation. A layer of resist is applied and patterned, after which the wafer is implanted with boron (Figure 3.2c-e). The resulting high-doped, p-type areas will eventually be part of the contact pads and will form the source and drain terminals. Ultralow contact resistance Ohmic contacts are thus formed. The low-doped area will become the actual nanowire, and thus the active and most important part of the device.

The resist and the screen oxide are then removed from the implanted wafer, after which a new layer of resist is patterned to form a mask during the subsequent silicon etch (Figure 3.2f-h). This step defines the dimensions of the nanowire and can be done by patterning using e-beam instead of a wafer stepper reticle to obtain even smaller nanowire dimensions. During this step over etching is a potential risk, which creates the possibility of device break down when the devices are used as a sensor in a liquid. The resist is removed and 20 nm thermal oxide is grown on top of the silicon. This is then covered with 80 nm TEOS (Figure 3.2i). The thermal oxide is used to ensure a good silicon-silicon dioxide interface, while the TEOS is used to thicken the silicon oxide layer. A passivation layer (silicon nitride in this specific example) of 100 nm is deposited afterwards (Figure 3.2j). The oxide and the passivation layer will form an insulating layer to prevent break down when over etching of the silicon took place. Furthermore, they will reduce leakage current over the nanowire surface and protect the wafer against mechanical damage. However, the most important reason to use the passivation top layer is the possibility it provides for further modification; the nanowire will be covered with an oxide layer, while the rest of the die has e.g. a parylene top layer, enabling selective modification. This can be obtained by, e.g. selectively removing the gate oxide using diluted HF followed by hydrosilylation [2]. It is noted that other passivation layers are also possible, as long as they either have a different surface termination than the front oxide, or are resistant to the etching with (diluted) HF, which is typically used in the formation of hydrogen-terminated silicon. This combination of protecting layers is covered with resist, which is patterned such that only the silicon nanowire is left exposed (Figure 3.2k-m). This step is followed by the growth of a front oxide layer on top of the nanowire (Figure 3.2m). In this process silicon dioxide was used, but other oxides are possible as well. A new layer of resist is deposited to protect the devices during the etching while defining the

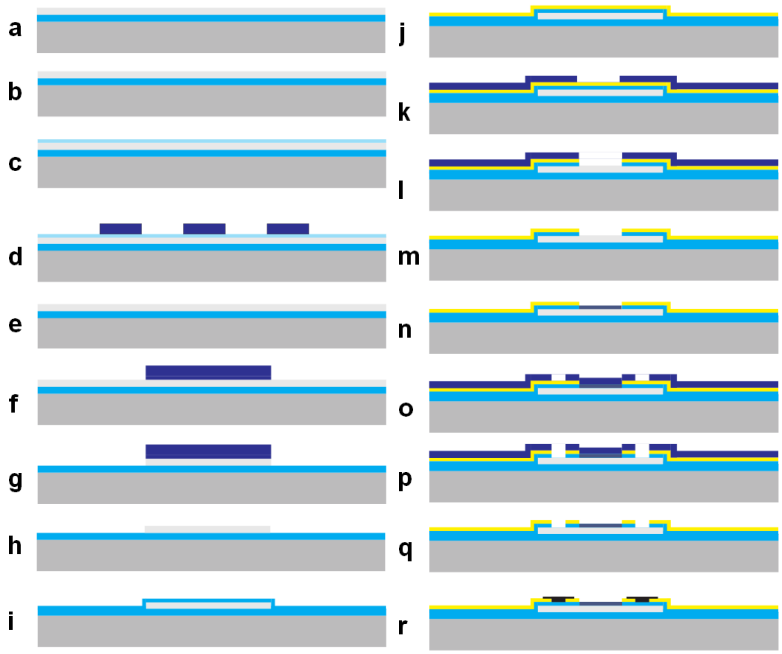

FIGURE 3.2: Schematic representation of the process flow. Dark grey: high-doped silicon, light grey: low-doped silicon, light blue: silicon oxide (see text for type), dark blue: photoresist, black: metal, yellow: passivation layer (a) SOI wafer (b) wafer with alignment marks (c) SOI wafer with screen oxide (d) no-implant mask on SOI wafer (e) removal of screen oxide and no-implant mask after implantation (f) mask for silicon etch (g) silicon etching (h) remaining silicon after etching (i) growth of 20 nm oxide followed by deposition of 80 nm TEOS (tetraethyl orthosilicate) (j) deposition of passivation layer (k) mask for opening silicon oxide/passivation layer around nanowire surface (l) etching to nanowire surface (m) removal of etching mask (n) front oxide growth (o) contact hole lithography (p) contact hole etching (q) removal of mask (r) metal deposition and patterning.

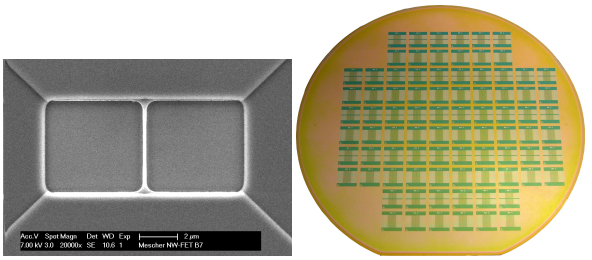

(a) (b)

3

FIGURE 3.3: (a) SEM image of one nanowire device. The nanowire (centre) connects the source (top) and drain (bottom) terminals. Only the nanowire and a part of the surrounding oxide are exposed to the environment, while the rest of the chip is covered with the passivation layer, here silicon nitride. (b) Picture of a processed wafer containing 84 devices.

contact holes (Figure 3.2o-q). Deposition of aluminium follows this step, creating the contact leads (Figure 3.2r). After the lift-off process, a final sintering step is performed to ensure good Ohmic contacts. Eventually the wafer can be diced to separate the individual dies, enabling characterization in gaseous or fluidic environment.

3.3 DEVICE CHARACTERIZATION

AFTER fabrication the devices have been characterized thoroughly. A Scanning Electron Microscopy (SEM) image of one nanowire in one of the devices is shown in Figure 3.3a. This is the same part of the device as depicted in Figure 3.1d. Figure 3.3b shows a picture of a wafer containing 84 dies with 28 NW-FETs. A standard Keithley 4200 Semiconductor Characterization System with pre-amps is used for the electrical characterization of the NW-FET. During all measurements, a potential of 50 mV is applied to the drain, while the source is connected to ground. The potential of the gate is swept (according to [4]), while the drain current is measured. In order to utilize nanowire field-effect devices as sensors, it is convenient when the threshold voltages and the transfer curves of the devices on one die are similar. Figure 3.4a shows the result of this characterization. The threshold voltages were determined by extracting the potential at which the current reaches 1 nA for each first device on a die, provided a pre-defined drain potential. When plotted on wafer scale, it is clear that, although there is some spread over the wafer due to the processing, neighboring dies show comparable characteristics. When all devices on a single die are measured, the typical transfer curves look like those presented in Figure 3.4b. For robust processes and for sensor applications in particular it is important that all these devices have a similar

threshold voltage and transconductance (g_m), which is the case for these devices. The spread observed in single dies is much smaller than observed on wafer scale, which is what matters for sensor applications. Quantification hereof is shown in Figure 3.4c.

An issue that exists during the production of nanowire field-effect devices is the attack of the oxide layer because of over etching of the silicon during the definition of the actual nanowire. This does not necessarily result in a problem for gas sensing applications, however, considering devices exposed to fluids, breakdown of these devices can occur at the edge of the nanowire, making these devices unusable. Figure 3.5 shows an example of this effect, as occurred when devices were processed as described in [4]. To avoid breakdown as a consequence of over etching and to create a reliable top-down fabrication method using conventional CMOS processing techniques, the authors developed the method presented in this chapter.

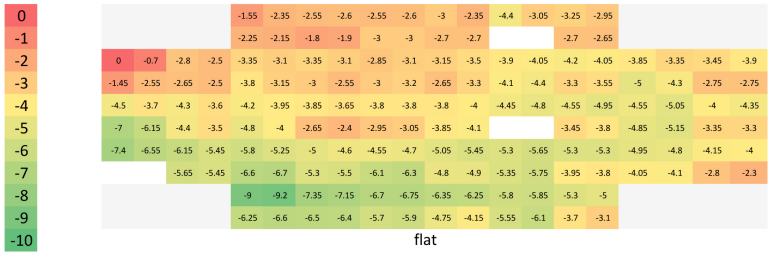

(a)

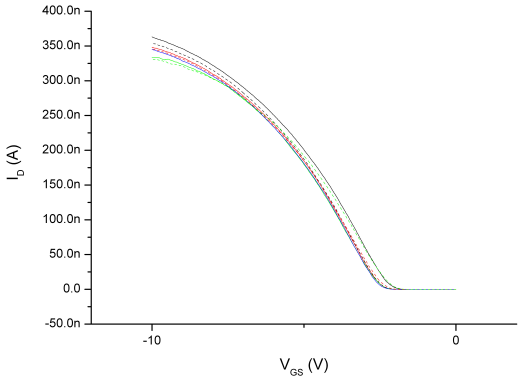

(b)

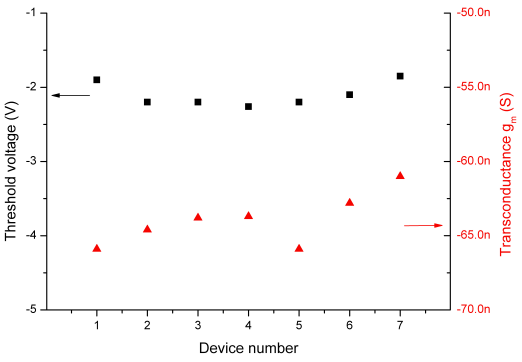

(c)

FIGURE 3.4: (a) Distribution of threshold voltages over a whole wafer in volt. For each die, the first device was measured and the threshold voltage was determined as the potential where the current reaches 1 nA. (b) I_D-V_{GS} curves of all devices on a single die (c) threshold voltages and transconductance of 7 NW-FETs on one die: the variation in threshold voltage is small (<0.5 V), as is the variation in transconductance (<5 nS)

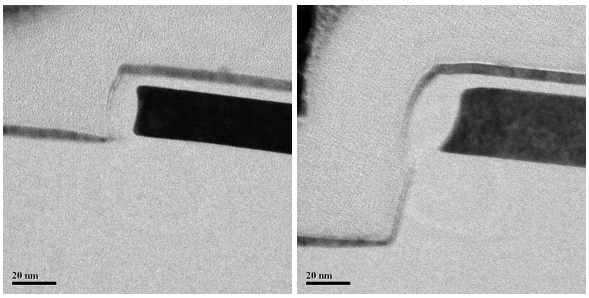

(a) (b)

FIGURE 3.5: Transmission Electron Microscopy (TEM) images of a cross section of the nanowire. The dark part is the silicon, the lighter part around it the silicon dioxide. The layer that appears to be thicker than the nanowire silicon and silicon oxide is the contrast layer which was added to make the over etching problem visible. In (a) no over etching occurred, while the over etching is clearly visible in (b). The arrow indicates the region where break down of the oxide will occur.

3.4 CONCLUSIONS

IN conclusion, we have demonstrated a new method for the top-down production of silicon nanowire field-effect transistors. This method is used to obtain devices that can be used as sensors. A single chip contains 28 NW-FETs, which allows for fingerprinting sensor applications or multiplexing [123, 37]. Besides solving the issue with over etching, this method gives flexibility in the use of other front oxides, provides selectivity in the use of passivation layers and thus modification and makes it possible to define the nanowires using e-beam technology. All steps used are based on standard CMOS processing techniques, which are available in standard clean rooms. We demonstrated that the variation in electrical characteristics of the device within a single die is small, providing the possibility for fingerprinting sensor applications and differential measurements.

4

PULSED CHARACTERIZATION

This chapter presents a method for using nanowire field-effect transistors (NW-FETs) as sensors in aqueous solutions without the need for a reference electrode. A pulsed-gate potential method is used to reduce instabilities related to the dynamics of ions and other charged species present in the solution. Application of this method results in a significant increase in the stability of the electrical properties of the devices, enabling reproducible characterization of aqueous media with NW-FETs. We show that this method can be applied to perform pH measurements with a silicon NW-FET.

A slightly modified version of this chapter has been published in IEEE Transactions on Electron Devices, *Pulsed Method for Characterizing Aqueous Media Using Nanowire Field Effect Transistors*, M.Mescher, B.Marcelis, L.C.P.M.de Smet, E.J.R. Sudhölter and J.H. Klootwijk **58**, 7 (2011) [4].

4.1 INTRODUCTION

IT is widely recognized that semiconducting nanowire field-effect transistors (NW-FETs) have promising applications as sensitive sensors for chemical and biological species, [13, 36, 88, 18]. NW-FETS exhibit enhanced sensitivity, compared with regular planar field-effect transistors (FETs), originating from their advantageous surface-to-volume ratio [124] (as explained in Chapter 2). Moreover, their 1-D character offers the possibility to detect single-molecule events [18]. Modification of the nanowire surface is used to adjust the selectivity to a broad range of target species, including DNA [36], protons and antibodies [88], and metal ions [106, 46].

Previously, planar FETs have been used as sensors, which generally include a reference electrode to control the electrical potential of the contacting solution [125]. However, instabilities and drift are well-known problems for immersed FET sensors. These issues remain when a planar FET is reduced in size to a NW-FET [126, 127].

The electrical characteristics (threshold voltage (V_T) and drain current (I_D)) of the NW-FET are influenced by both the potential of the gate and by its environment. In fact, changes in the environment of the NW surface, including adsorption of species, can be monitored via a change in the electrical properties of the NW-FET, which is the sensing principle of this device. Before applying a device in a complex aqueous solution containing ions and/or (charged) (bio)molecules, initial characterization of NW-FETs is performed in a dry and well-controlled environment. This enables the determination of the FET threshold voltage and drain current. Afterward, NW-FET devices can be characterized in controlled aqueous solutions, e.g., an aqueous salt solution without the presence of any additional analyte. When the device is exposed to an aqueous salt solution that does contain additional analytes, electrical readout of the NW-FET characteristics is used to detect the modulation of the drain current due to the presence and/or adsorption of analytes. However, the immersion of NW-FETs in these (rather complex) media results in a number of new challenges during characterization, compared with dry conditions, as ions and other charged species are present. These charged species can be attracted to the nanowire surface, particularly when potentials are applied. This leads to the screening of the electric fields induced by the gate and the target species and results in an additional and nonselective modulation of the drain current. It is obvious that the nonselective modulation complicates the use of the NW-FET as a reliable and selective (bio)chemical sensor. Although several papers have been published on the use of NW-FETs as (bio)chemical sensors [13, 18, 36, 88] and comparable instabilities are observed in these papers, methods that address the type of instabilities induced by these

charged species have not been explored in much detail until now.

In this chapter, we present a new method for the electrical characterization of NW-FETs in aqueous solutions. We introduce the use of a pulsed and alternating gate potential to reduce the nonspecific attraction of charged species to the surface. This results in an improved stability of the electrical characteristics of the sensor, enabling the use of the device as a (bio)chemical sensor. We demonstrate that, when appropriate pulse durations are used, a stable situation is achieved. This enables one to sense the pH of a solution with silicon NW-FETs without the need of a reference electrode.

4.2 EXPERIMENTAL METHODS

SILICON NW-FETs are fabricated on silicon-on-insulator wafers. A schematic representation of the structures used is shown in Figure 4.1a. Typically, the samples consist of 20 parallel low-doped, n-type nanowires of 4 μm length and 50 nm width (Figure 4.1b). The height of the silicon is 80 nm. The nanowires are covered with a silicon oxide layer of approximately 8 nm in thickness. An Ohmic contact between the nanowire and the source and drain contacts is formed by contact implantation. Source and drain are isolated from the gate (substrate) via a 300-nm-thick buried oxide layer.

The devices in this chapter differ on a number of points from the devices described in Chapter 3. The devices in Chapter 3 consist of single nanowires, with individual sources and drains. In this chapter however, the devices each consist of 20 parallel nanowires, sharing a common source and drain. In either way, when a device is mentioned, the characteristics of the wire or wires between an individual source and drain are discussed, whether this is a single wire or a number of parallel wires. Furthermore, the type of dopant used in this chapter is n-type, compared to the p-type devices in the rest of this thesis. A third difference is size of the nanowire. Here, we use 50 nm wide wires, while the devices in the other chapters typically have a width of 300 nm. The length is approximately the same: 4 μm vs. 3-5 μm. The height of the nanowires used in this chapter is somewhat larger compared to the other devices: 80 nm vs. 15 nm.

The mode of operation is accumulation (i.e., no inversion layer), where optimal sensitivity is achieved by using the subthreshold behavior of the transistor (steepest slope, see Figure 4.3) [120, 114]. In this paper, we used a constant device architecture to avoid the introduction of too many variables [128]. To allow the characterization of the sensors exposed to liquids, a fluidic in/outlet is placed on top of the transistor, as shown in Figure 4.1c. The fluidics are designed such that contact between source and drain connections and the liquid is prevented, whereas the complete nanowire surface is exposed to it. Later in the project, these

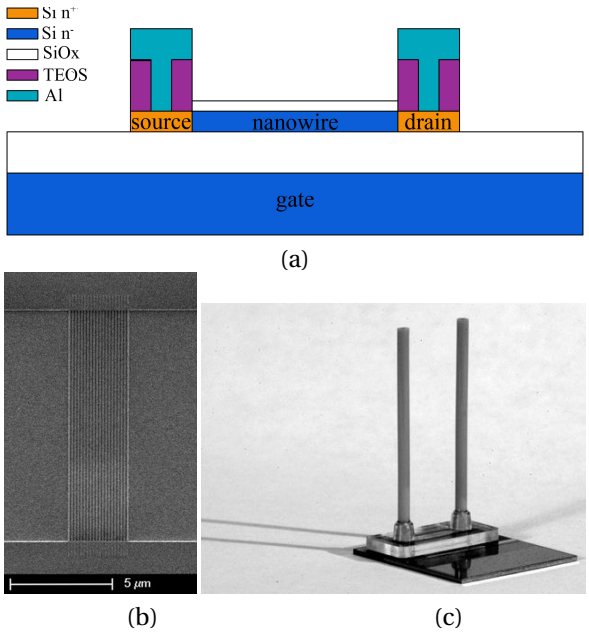

FIGURE 4.1: (a) Schematic not to scale representation of NW-FET. Aluminum source and drain contacts are shown in black. The back gate (dark gray) consists of highly doped silicon. The nanowire (light gray) consists of low-doped silicon, which is connected to the source and drain contact via highly doped regions (dark gray) to ensure Ohmic contacts. (b) Scanning electron microscopy image of NW-FET containing 20 parallel nanowires (top view). Source and drain contacts are shown and connected via the nanowire. (c) NW-FET carrier with fluidic inlet and outlet mounted on top of the sensor. Solutions enter the sample at the left, flow over the nanowires, and leave the sample at the right-hand side. Typically, a flow speed of 0.1 ml/min is used.

fluidics were further optimized (Chapter 6).

Wet characterization of the NW-FET is carried out using a solution of 0.01 M NaCl in de-ionized water. A flow of 0.1 ml/min is used and applied via a Harvard Syringe pump. A standard Keithley 4200 semiconductor characterization system combined with a Cascade M150 Probestation is used for the electrical characterization of the NW-FET. The pH sensing experiments are performed using solutions with a fixed NaCl concentration. Aqueous solutions of NaOH and HCl are used to adjust the pH, which is measured with an Eutech/Oalton Instruments pHTestr30 pH meter.

To use a NW-FET as a chemical sensor, it is first biased by applying a drain voltage (V_{DS}) and measuring the drain current as a function of the applied gate

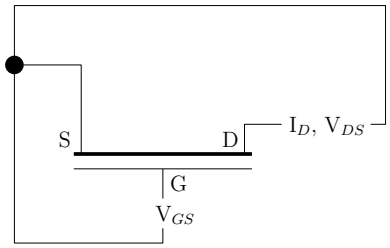

FIGURE 4.2: Schematic representation of the realized structure. V_{DS} is 50 mV, I_D is determined as a function of V_{GS}.

voltage (V_{GS}). When the NW-FET is subsequently exposed to a target species, this induces a change in the surface potential, e.g., an additional electric field due to the binding of the target to the nanowire surface. This induced electric field can be considered to act as a second gate, which modulates the conduction in the NW-FET. The presence of target species can thus be monitored as a shift in the I_D versus V_{GS} characteristics, e.g., a different V_{GS} has to be applied to achieve the same I_D. The selectivity of the nanowire sensor to various targets can be adapted by surface modification of the nanowire. For instance, FET sensors with a silicon oxide surface are known to be sensitive to changes in pH [129]. During all measurements, a potential of 50 mV is applied to the drain, whereas the source is connected to ground. The potential of the gate is swept, whereas the current through the drain is measured (Figure 4.2). The threshold voltage is determined from the intersect of the linear part of the I_D versus V_{GS} characteristics with the V_{GS}-axis.

4.3 RESULTS

THE initial experiments were performed with NW-FETs exposed to air. The potential of the gate was swept from -10 to 10 V while measuring the drain current. Subsequently, the NW-FET was exposed to an aqueous solution of 0.01 M NaCl, whereas the same characterization was carried out. The change in the NW-FET's environment resulted in a steeper slope of the I_D-V_{GS} plot at a potential slightly higher than V_T (Figure 4.3), which can be rationalized as follows: When the NW-FET is exposed to an aqueous solution instead of to air, the relative permittivity (ε_r) of the devices environment changes from 1 to 80. This increases the capacitive coupling of the gate potential via this solution to the NW-FET. As a result, the number of charge carriers in the nanowire induced by the applied potential is larger, which leads to an increased conductivity and, thus, an increased slope of I_D versus V_{GS}. For high applied V_{GS} a plateau is observed for the current

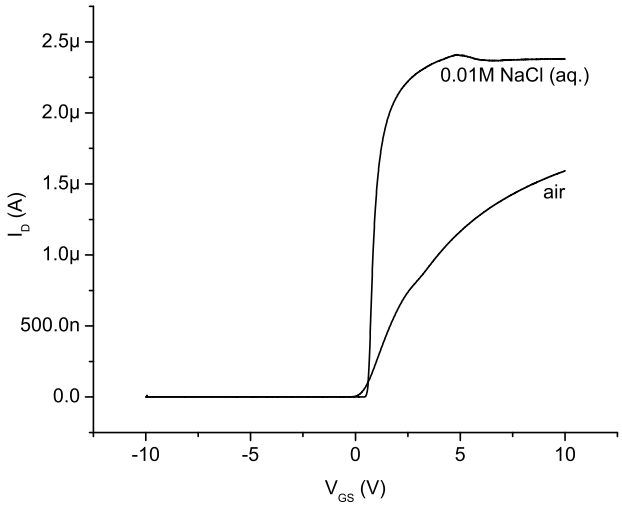

FIGURE 4.3: NW-FET I_D versus V_{GS} characteristics in air and 0.01 M NaCl (aq.) showing a clear difference in the slope of the I_D versus V_{GS} plot at a potential slightly higher than V_T.

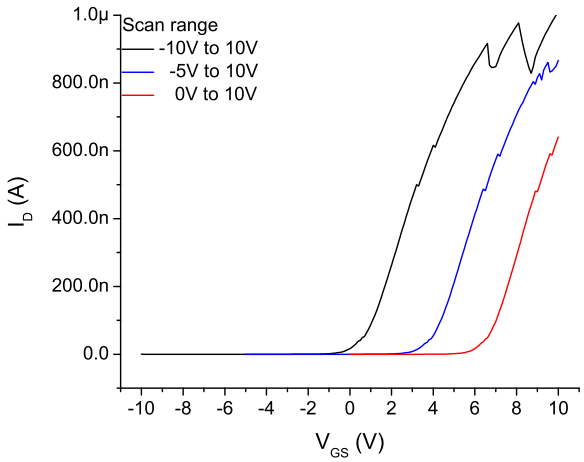

(a)

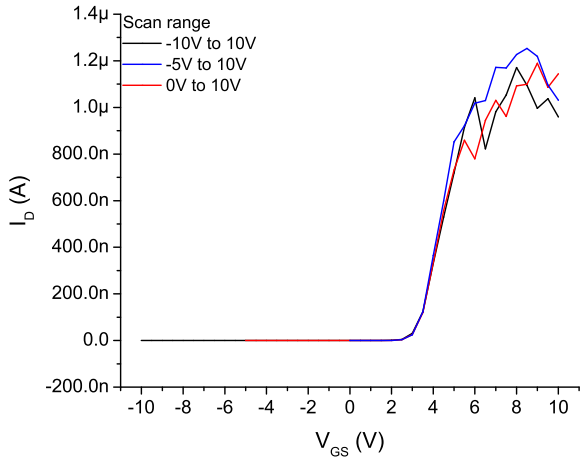

(b)

FIGURE 4.4: I_D versus V_{GS} characteristics as a function of the range over which the potential of the gate is scanned (a) using a conventional gate sweep with a small increment and (b) using a larger increment (pulse method A).

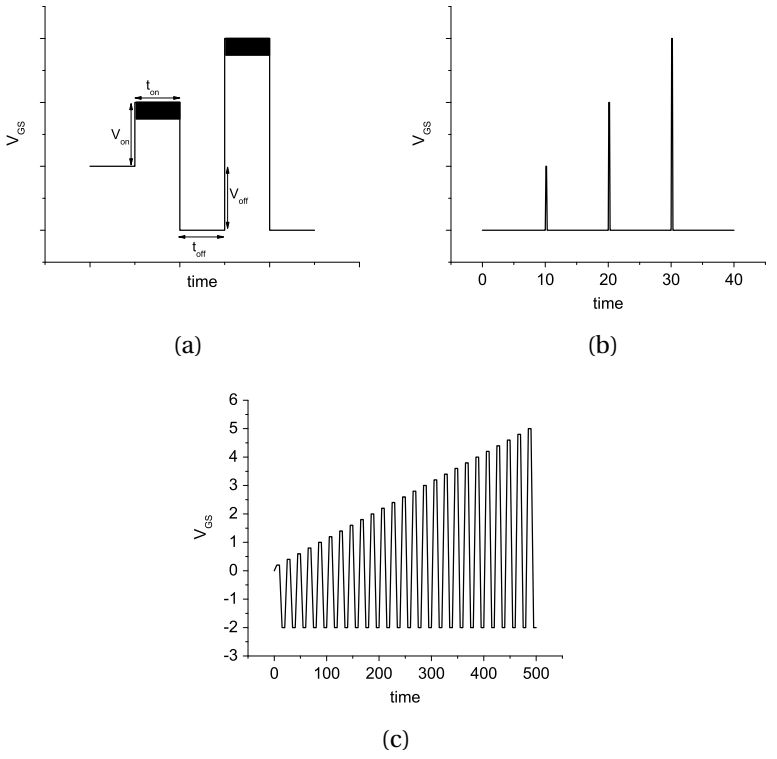

FIGURE 4.5: (a) Schematic representation of the parameters that are adjusted to optimize the measurement: V_{on}, t_{on}, V_{off}, and t_{off}. Typical potential values of the gate as a function of time during the measurements for (b) method A and (c) method B.

TABLE 4.1: Typical values for parameters in methods A and B, as discussed in the text. The values depend on the characteristics of the device used. Therefore, the optimal setting may differ from sample to sample.

Symbol	Method A	Method B
t_{on}	20 ms	10 ms
V_{on}	-10 to 10 V	-5 to 10 V
t_{off}	10 s	10 ms
V_{off}	0 V	5 V
Result	Independency of scan range	Stable V_T

I_D, which is caused by the resistance of the nanowire contacts. These highly doped regions limit the maximum current that can flow through the nanowire, as also explained in [130]. In the case of the measurement in air, no plateau value for the current is reached as the current through the nanowire was not sufficiently large.

A remarkable observation is that the results of device characterization depend on the voltage scan range. This effect is shown in Figure 4.4a: the threshold voltage depends on the initial gate potential. This is a problem when a time-resolved measurement is done, where a constant gate potential is applied while the drain current is measured as a function of time. This should result in a single value for the drain current. In order to obtain an independence of the scan range, the measurement was adjusted such that V_{GS} (V_{on} in Figure 4.5a) was applied in short pulses (t_{on}=10 ms), alternated with long periods (t_{off}=10 s) without gate voltage (V_{off}=0 V). This indeed resulted in a stabilized threshold value for these NW-FETs exposed to a sodium chloride solution (Figure 4.6b). This method will be referred to as method A (Table 4.1).

In addition to the shift in the threshold voltage as a function of the scan range, a second effect is observed. When a NW-FET in air is subsequently measured 20 times during a period of 15 min, the characteristics are reproduced 20 times. It has been observed that no drift takes place on time scales up to hours. However, when this experiment is carried out with a NW-FET in aqueous NaCl, a drift of the characteristics is observed, as shown in Figure 4.6a. This drift might be caused by the diffusion of Na^+ ions into the silicon oxide layer around the nanowire or by inappropriate timing. Although long waiting periods between the pulses of the gate improved the stability, the results of the NW-FET in aqueous NaCl solution were not as stable as of the NW-FET in air. An additional adjustment to the gate potential was therefore applied: the period between the pulses of the gate potential was shortened until the on and off pulses (t_{on} and t_{off} in Table 4.1) had an equal duration, and a negative potential was applied to the gate during these periods. This resulted in a typical shape of the gate potential as a function of time, as

demonstrated in Figure 4.5b and c.

The amplitude of the pulse during the periods in between the positive pulses (t_{off}) was adjusted such that use of the applied pulse resulted in reproducible I_D-V_{GS} characteristics on time scales that are appropriate for sensing experiments. Typically, these can take up to several hours. Figure 4.6b shows the result of this method, which is referred to as method B (Table 4.1). The presented I_D-V_{GS} characteristics are measured with different devices, which explain the differences in V_T and output current among the individual plots. The optimal timing depends on the individual devices, and this method is not independent of the scanning range.

To demonstrate the improved sensor stability resulting from the pulsed gate method, method B has been used to measure the pH with an immersed NW-FET sensor device. The device was exposed to solutions in a wide pH range, without the use of a reference electrode in the solution. The resulting I_D-V_{GS} characteristics are shown in Figure 4.7a, demonstrating that the I_D versus V_{GS} curves shift to more positive voltages with larger pH. Without the use of method B, the instabilities in the characteristics were larger than the observed effect. A plot of the measured threshold voltage against the pH confirms this trend, as shown in Figure 4.7b. The slope is slightly larger than the theoretical value of 59 mV per pH unit. This is due to the capacitive coupling of the gate potential through the 300 nm thick BOX layer, which makes the gate potential experienced by the nanowire effectively smaller than the applied value.

4.4 DISCUSSION

THE use of a pulsed method offers the possibility to stabilize the I_D versus V_{GS} characteristics of the NW-FET in aqueous solution. A possible reason for the observed instability is the presence of charged species, other than the target species, in the solutions to which the device is exposed. These species screen the desired selective electric fields induced by the gate and by target species and lead to an undesired nonselective modulation of the drain current. In order to use the device as a chemical sensor, it is necessary to obtain selective and reproducible I_D versus V_{GS} characteristics on the typical time scales of an experiment.

The method presented in this paper demonstrates that the specific time scales involved in the screening of the gate potential are larger than the duration of the gate potential pulses used in method B. The pulsed-gate method is applied to immersed field-effect sensors without the use of an additional reference electrode in the solution. Although the use of a reference electrode is recommended by Carlen and Van den Berg [20], the pH-sensing experiment presented in this paper shows that it is feasible to measure the pH of a solution with a NW-FET sensor

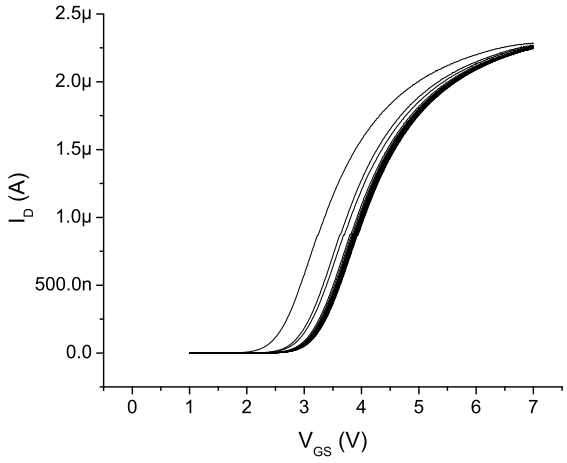

(a)

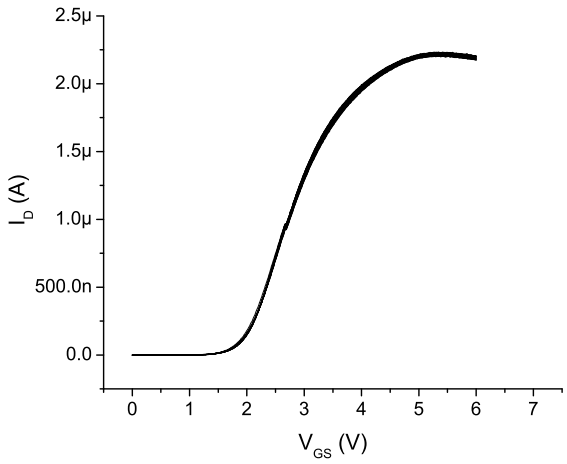

(b)

FIGURE 4.6: (a) I_D versus V_{GS} characteristics of the NW-FET exposed to a NaCl solution during 20 subsequent measurements. The lines represent the results of the series using the conventional method, which leads to significant drift of the characteristics. (b) I_D versus V_{GS} characteristics of the NW-FET exposed to a NaCl solution during 20 subsequent measurements. The lines show the outcome of 20 subsequent measurements using method B, largely reducing the drift on typical timescales.

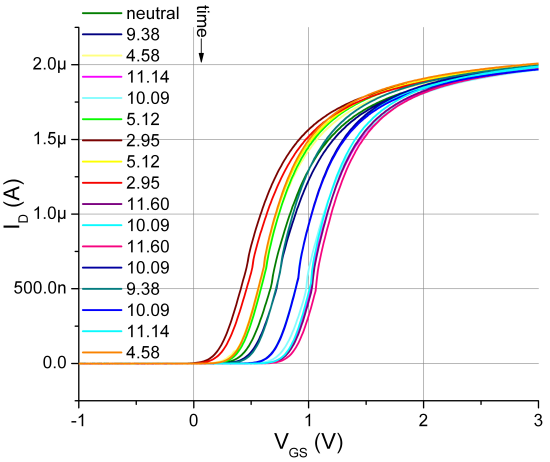

(a)

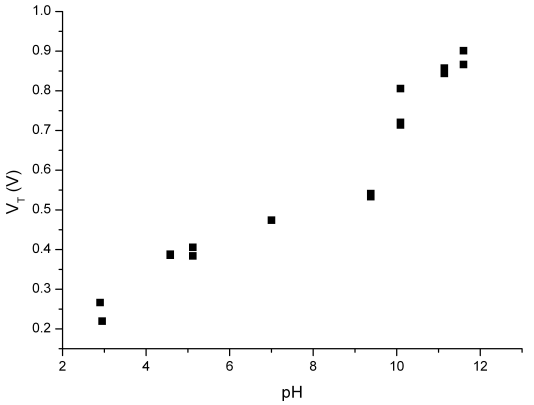

(b)

FIGURE 4.7: (a) I_D versus V_{GS} characteristics as a function of the pH of the solution to which the device is exposed. (b) For each of the I_D versus V_{GS} characteristics, the threshold voltage is determined, which belongs to a specific pH. This plot shows the threshold voltage as a function of the pH to which the sensor is exposed.

without the use of a reference electrode, when a controlled environment is used.

The control over the timing is essential in the stabilization of the characteristics of the NW-FETs. This control is not yet optimal in the current setup. Furthermore, the pulse duration cannot be smaller than 15 ms because of the restrictions on the integration time in the current measurement device used in these experiments (Keithley 4200). It is however an interesting avenue for future research to improve the set up to obtain shorter pulse durations and increase the control that exists on the timing.

Having developed a method that enables the stable characterization of NW-FETs, the next steps will include experiments on the surface modification of the nanowires and the use of these devices as sensors for other analytes.

4.5 CONCLUSIONS

A new method for characterization of aqueous solutions using NW-FETs has been described in this chapter. It has been shown that a pulsed gate potential improves the stability of the device. The initially observed drift of the threshold voltage has been reduced by short positive pulses combined with long periods of neutral potential (method A in Table 4.1). Furthermore, a method to improve the stability of the NW-FETs on typical time scales as used during measurements has been demonstrated (method B in Table 4.1). Alternating positive and negative pulses lead to increased stability of the I_D versus V_{GS} characteristics in time. This method can be used to detect changes in pH and facilitates, combined with the appropriate surface modification, the application of the NW-FET as chemical sensor platform.

5

GATING AND WATER-DIOXANE MIXTURES

In this study, we report on the electrical response of top-down, p-type silicon nanowire field-effect transistors exposed to water and mixtures of water and dioxane. First, the capacitive coupling of the back gate and the liquid gate via an Ag/AgCl electrode were compared in water. It was found that for liquid gating smaller potentials are needed to obtain similar responses of the nanowire compared to back gating. In the case of back gating, the applied potential couples through the buried oxide layer, indicating that the associated capacitance dominates all other capacitances involved during this mode of operation. Next, the devices were exposed to mixtures of water and dioxane to study the effect of these mixtures on the device characteristics, including the threshold voltage (V_T). The V_T dependency on the mixture composition was found to be related to the decreased dissociation of the surface silanol groups and the conductivity of the mixture used. This latter was confirmed by experiments with constant conductivity and varying water-dioxane mixtures.

This chapter has been published in Sensors, *Influence of Conductivity and Dielectric Constant of Water-Dioxane Mixtures on the Electrical Response of SiNW-FETs*, M.Mescher, A.G.M. Brinkman, D. Bosma, J.H. Klootwijk, E.J.R. Sudhölter and L.C.P.M. de Smet **14**, 2 (2014) [5].

5.1 INTRODUCTION

SILICON-BASED nanowire devices have been the subject of extensive research in the last decade. Most of the work focuses on different aspects of device fabrication and on (potential) sensor applications for the label-free detection of (bio)chemical species [88, 89, 17, 104]. Studies on (bio)chemical sensing typically require (bio)chemical modification of the nanowire surface [2]. In addition, there is a large series of studies on the description of fundamental performance limits of nanowire-based devices [131, 132], charge screening effects [133, 134, 123], improvement of the signal-to-noise ratio [135, 4, 136], the effect of surface modification on the nanowire electrical properties [32, 137], and work on the incorporation of a reference electrode [20, 138].

Soon after their introduction in 2001 [13], devices based on silicon nanowires (SiNWs) were applied in sensing experiments, addressing the pH sensitivity of silicon oxide-covered SiNWs as well as the detection of streptavidin binding on biotin-modified nanowires. The sensing mechanism was rationalized by considering the type of doping present in the SiNW and the changes in charge density at the sensor interface. The surface potential as a result of the surface charge density offsets the front and/or back gate potential and leads to a change of majority charge carriers in the SiNW. By far, most of the studied target compounds are charged and studied in an aqueous environment. Examples include not only protons and antibodies/antigens [13], but also deoxyribonucleic acid (DNA) [32, 110], polyelectrolytes [139] and ions [86]. Recently it was shown that the response of so-called nanoISFET pH sensors can be described by analytical models [122], similar to those developed for describing the operation of ISFETs [129].

Since 2007, also the responses of SiNW-based devices-which behave like field-effect transistors (FETs)-to uncharged target species in the gas or vapour phase have been studied. This was first shown by Heath and his co-workers who studied the exposure of NO_2, acetone and hexane in nitrogen (N_2) to bare and silane-modified SiNWs [140]. Later, Engel et al. prepared amino propyl-terminated SiNWs to detect trinitrotoluene (TNT) in N_2 [48]). Over the past few years, Haick and co-workers reported an interesting series of research papers on the fundamentals and applications of functionalized SiNW-based FETs for the detection of polar (water, ethanol, 1-butanol, 1-hexanol, 1-octanol and 1-decanol) and nonpolar (n-hexane, n-octane and n-decane) volatile organic compounds (VOCs) in oil-free air having 15% relative humidity [111, 141, 142, 143, 53, 54]. This in-depth work shows that one of the sensing mechanisms involved is related to the changes in the surrounding dielectric medium due to the condensation of VOCs on the functionalized SiNW surface [53]. The surrounding dielectric effect is also believed to play a role in an interesting contribution of the Nokia Research Center in which

etched SiNW-based devices were exposed to (neat) vapours of water, acetone, methanol, ethanol and 2 propanol in air [144].

In the present study we investigate the effect of exposure of the SiNWs to different solvents and the dielectric coupling in more detail. We use well-defined, top-down prepared, p-type SiNW-based devices. The SiNWs are covered with SiO_2 and were not further modified. Their electrical response to binary, liquid mixtures of water and dioxane, having a range of dielectric constants (ε_r varies between 2 and 80), is studied. In contrast to the detection of vapours or gases described in the previous paragraph, the analysis of the FET responses in the liquid environment, allows one to apply liquid gating (i.e. front gating) next to back gating. In this chapter we compared and discussed the influence of type of gating in aqueous solution. Several papers have discussed the use of back gating and methods for liquid gating (e.g. on-chip Au and Pt electrodes, Ag/AgCl electrodes, extended off-chip gates [114, 145, 146]), but a direct comparison on the influence of the type of gating on the I_D-V_{GS}-characteristics has not been made before. Next, the devices were exposed to two different types of water-dioxane mixtures: as-prepared and mixtures with a constant electrical conductivity achieved by the controlled addition of a salt. The electrical characteristics of the devices when exposed to these conditions were investigated and discussed.

5.2 EXPERIMENTAL SECTION

SiNW-FETs were produced as reported previously [3]. Briefly, the nanowires (p-doped at a concentration of 10^{16} cm^{-3} to assure semiconducting behaviour) are 3 μm in length, 300 nm in width and 40 nm in height and are covered with a silicon dioxide gate oxide with a thickness of 8 nm. The thickness of the buried oxide (BOX) layer is 300 nm. The devices were wire bonded and covered with a micro fluidic device. The setup is shown in Figure 5.1.

In order to investigate the difference between the use of a back gate (BG) and a liquid gate (LG), a Ag/AgCl electrode was inserted in the beaker containing the solution to which the nanowire was exposed. The solutions were sucked into the microfluidic cell with a syringe pump (Harvard Apparatus, Holliston, MA, USA) using Silastic Q7-4750 tubing (Dow Corning, Midland, MI, USA). The devices were exposed to the solutions in a random order. The target solution was sucked from the beaker into the microfluidic cell after which the flow was stopped and the measurements were performed under stagnant conditions at room temperature. The measurement was started immediately after exposure to the liquid. Each exposure continued for approximately 10 min using the liquid gate as described previously.

A standard Keithley 4200 semiconductor characterization system (Keithley

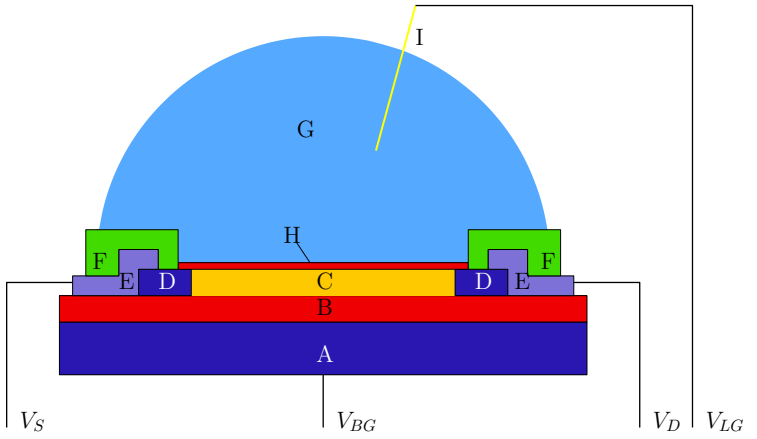

(a)

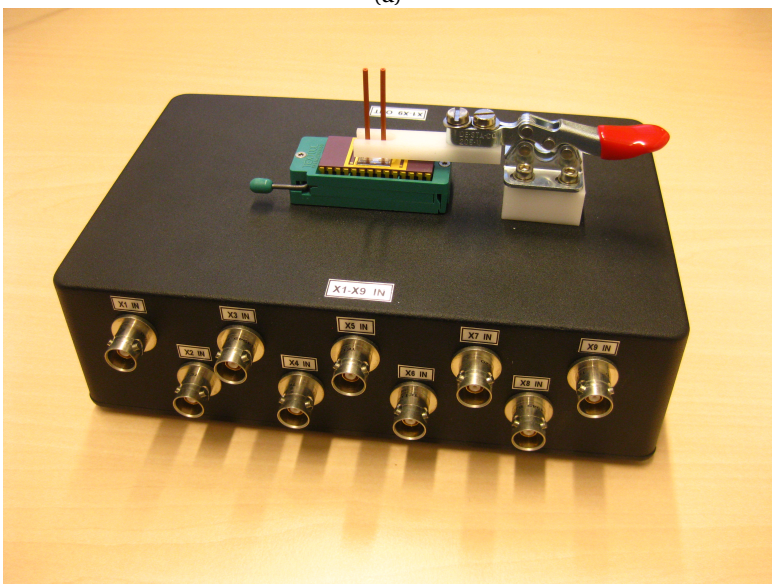

(b)

FIGURE 5.1: (a) Schematic representation of the experimental setup (not to scale). Atop of the high-doped (10×10^{20} cm^{-3}) silicon back gate (A) and a 300 nm thick buried oxide layer (B), the low-doped (10×10^{16} cm^{-3}) silicon nanowire is located (C). The ends of the nanowire consist of high-doped (10×10^{20} cm^{-3}) silicon and form the source and drain contacts (D), which were contacted next via aluminum contacts (E). The source, drain and contact were insulated using a 100 nm thick silicon nitride passivation layer (F), such that the nanowire and an area around it can be exposed to the solution used (G). Furthermore, the nanowire is covered with an 8 nm thick thermal silicon dioxide layer (H). An Ag/AgCl electrode (I) was placed at a fixed position in the solution; (b) Photograph of the box used for the electrical characterization. The cables and tubing are left out for clarity.

Instruments BV, Gorinchem, The Netherlands) equipped with eight source measurement units was used for the electrical characterization of the device during exposure. A 50 mV source-drain bias was applied and V_{GS} was applied such that the device is operated in depletion mode in the linear regime ($V_{SD} \ll V_{GS}$). The drain current (I_D) was measured while the gate potential (V_{GS}) was swept. This can be applied either via the back gate or the liquid gate. From these characteristics the threshold voltage (V_T) was determined.

To study the influence of the liquid medium in contact with the SiNW on the device characteristics, 1,4-dioxane (anhydrous, 99.8%, Sigma-Aldrich Chemie B.V., Zwijndrecht, The Netherlands) (ε_r = 2.25) and de-ionized water (ε_r = 80.1; ρ = ~20 kΩcm) were used as solvent because they mix in all ratios and make it possible to change the dielectric constant gradually in the range of 2-80. They were mixed as described by Åkerlöf et al. [147] to obtain mixtures with a range of dielectric constants (2-80). To adjust the electrical conductivity, tetramethylammonium chloride (≥98%, Sigma Aldrich Chemie B.V., Zwijndrecht, The Netherlands) was dissolved in the solvent mixtures where mentioned. The conductivity and pH of the solutions were measured using a Metrohm 712 Conductometer and a Metrohm 827 pH lab meter, respectively (Metrohm equipment was purchased from Applikon Analytical B.V., Schiedam, The Netherlands).

5.3 RESULTS AND DISCUSSION

FIRST the devices were exposed to water and the electrical characteristics were determined using the back gate and the liquid gate. The results of this comparison are discussed in Section 5.3.1. Subsequently, the devices were exposed to water-dioxane mixtures with a range of dielectric constants and the electrical characteristics were determined using liquid gating via an Ag/AgCl electrode (Section 5.3.2). In addition, the conductivity of some mixtures was adjusted to obtain solutions with similar conductivities.

5.3.1 BACK GATE VS. LIQUID GATE IN DE-IONIZED WATER

Figure 5.2 shows a schematic representation of the back-gated and liquid-gated situation and the capacitances that are present. In both cases the C_{liquid} was present, although it has a different value for the two cases, while C_{box} only plays a role in the case of back gating. The I_D-V_{GS} characteristics that were obtained using three different types of modes of operation are given in Figure 5.3a: (1) the back gate was swept while no electrode is inserted in the solution, (2) the gate potential was applied via the Ag/AgCl electrode while the back gate is connected to ground and (3) the gate potential was applied to the back gate and liquid gate simultaneously. In more detail, the figure shows the comparison between the use

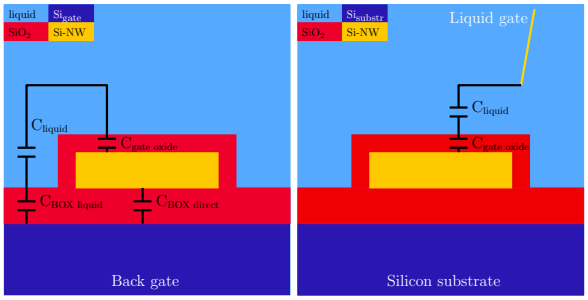

(a) (b)

FIGURE 5.2: (a) Schematic representations (not to scale) of the coupling of the potential when applying the potential to the back gate and (b) the liquid gate.

of the back gate and the liquid gate when the device is exposed to de-ionized water (red squares vs. blue circles). As expected for p-type nanowires in depletion mode, a more negative gate bias leads to an increase in the drain current, for both types of gating. It is clearly visible that a smaller potential on the liquid gate has to be used compared to the back-gate mode of operation in order to obtain a similar drain current through the nanowire. The addition of the BG to the LG did not have much influence on the characteristics of the device compared to the LG only (blue circles vs. green triangles).

To quantify this difference, the total capacitance of the system was estimated for both back and liquid gating as schematically shown in Figure 5.2, excluding C_{liq}. Exclusion is justified because this capacitance is not dominating the system, as the electrical conductivity of the de-ionized water is ~15-30 µS/cm and thus much higher than the conductivity of the SiO_2 layers (~10^{-16} S/cm [29]). After calculation of the total capacitances, the threshold voltage can be determined using the estimated total capacitance and the MOSFET (metal oxide semiconductor field-effect transistor) formula for V_T [148],

$$V_T = 2\varphi_B - \frac{\sqrt{2\varepsilon_S q N_A 2\varphi_B}}{C_{\text{total}}} \tag{5.1}$$

where φ_B is the difference between of the Fermi levels of doped and the intrinsic silicon, ε_S the relative permittivity of the silicon, N_A the acceptor density, q the elementary charge (1.6×10^{-19} C), and C_{total} the capacitance of the combined dielectric layers. Using estimated values of the total capacitance of 2.0×10^{-16} F and 3.1×10^{-15} F for the back-gate and front-gate situations, respectively, threshold voltages of -2.8 V and -0.8 V for BG and LG, respectively were calculated. In the

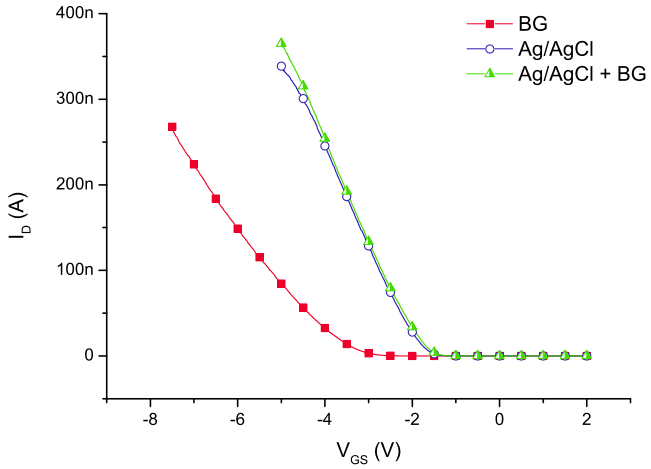

(a)

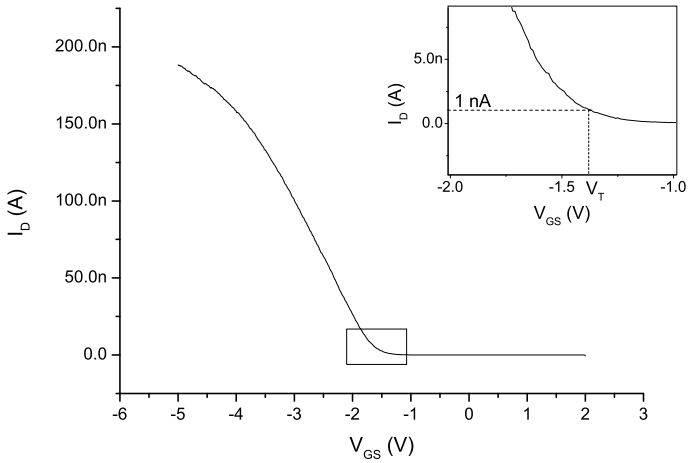

(b)

FIGURE 5.3: (a) I_D-V_{GS} characteristics of a device when exposed to water, showing three different types of modes of applying a gate potential. The gate potential was either applied via the back gate without using the liquid gate (red squares), via an Ag/AgCl electrode/liquid gate (blue circles) with the back gate at ground, or via both the back gate and liquid gate via an Ag/AgCl electrode (green triangles). (b) Example of the analysis of the curves in de-ionized water (here: liquid-gate swept and back-gate grounded): the threshold voltage (V_T) is the potential at which the current threshold of 1 nA is crossed.

experiments a difference of approximately 2 times was found between the BG and LG. The calculated V_T of the BG configuration is about 3.5 times larger than the one of the LG configuration. This discrepancy can be related to the parallel-plate assumption that was made in the calculation, while the system under study consists of a more complicated geometry. Different densities of trapped charges in the two oxide layers (i.e., BOX and gate oxide) may also contribute to the observed difference.

It is noted that an LG can only be used when there is a continuous electrical path between the Ag/AgCl electrode and the NW-FET via the liquid, as is the present case. Thus, when studying gas or vapour environments one is forced to use the BG or performing differential measurements, while in the case of a liquid contact one can choose. As the BG is not directly exposed to the solvent, its potential will not be influenced by interactions with this solvent. This can be a reason to prefer BG over LG. Furthermore, in terms of fabrication, it is cheaper and easier to use the BG, since no extra processing is needed, while integration of an on-chip electrode does. However, because of the smaller potentials that can be used and the concomitant longer device life times we observed, it was decided to use the LG in the following experiments.

5.3.2 WATER-DIOXANE MIXTURES

Subsequent to the experiments with the different modes of applying the gate potential, the device was exposed to water-dioxane mixtures and the I_D-V_{GS} characteristics are measured as described above by applying a variable potential to the Ag/AgCl electrode and the back gate connected to ground. The results are shown in Figure 5.4. Increasing dioxane content of the water-dioxane mixture requires the application of a more negative gate potential to arrive at the same drain current. From the I_D-V_{GS} curves the threshold voltages were determined and plotted as a function of the dioxane content in Figure 5.5. A more negative V_T is observed with increasing dioxane content.

The origin of this observation can be attributed to a decrease of capacitance of the liquid with increasing dioxane content, resulting in an increased negative gate potential to keep the source-drain current constant. However, it is also possible that the reduced dielectric constant of the liquid reduces the dissociation of the surface silanol groups at the oxide interface. This results in a decreased surface charge at a certain proton concentration in the solution. In that case an apparent lower pH value is measured. To compensate for this reduced negative surface potential a more negative potential has to be applied on the gate electrode. To estimate the effect we compare the pK_a values of protonated water and protonated dioxane, which are -1.74 and -2.92, respectively [149]. Therefore, protonated dioxane is slightly more acidic than protonated water, and concordially water is

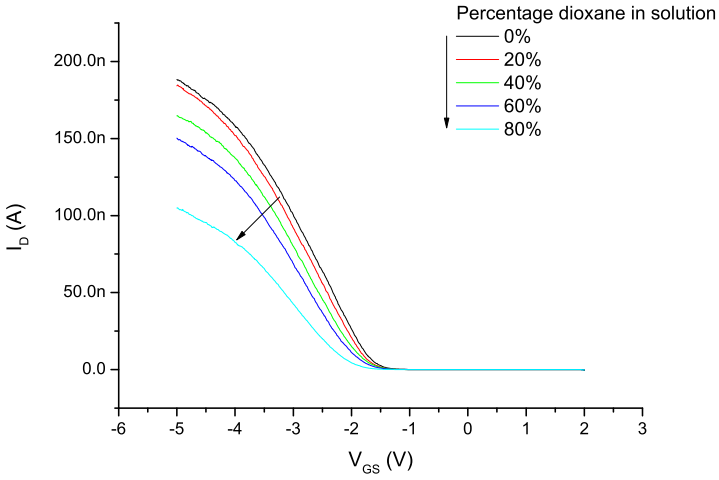

FIGURE 5.4: I_D-V_{GS} characteristics of a single nanowire device when exposed to the water-dioxane mixtures with varying dielectric constants. An Ag/AgCl electrode was used as liquid gate in this experiment.

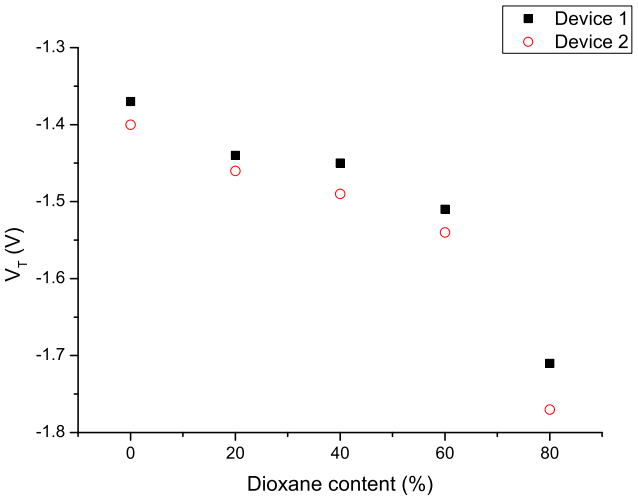

FIGURE 5.5: Average threshold voltage of two typical devices as a function of the dioxane content in the water-dioxane mixture exposed to the device

a stronger base than dioxane.

It is thus expected that upon increasing the content of dioxane in the water-dioxane mixtures, proton dissociation of the surface silanol groups is reduced. This is in line with an experimental study on the acid dissociation constants of several acids in water-dioxane mixtures [150]. We measured the pH of water-dioxane mixtures using a glass electrode and found that the pH meter reading decreased upon the addition of dioxane. This decrease can also be explained by the decreased dissociation of silanol groups now at the glass electrode surface [151]. In addition, the ionic product of water (pK_w) will also decrease upon increasing dioxane fraction [152]. However, that effect reduces the proton concentration, and -if dominant- will increase the surface silanol group dissociation. Since that was not observed in the nanowire experiments, it is concluded that this effect is not dominant. Returning now to our observations on the SiNW-based devices, both the reduced dielectric constant of the water-dioxane medium, i.e., a lower capacitance of that medium, and the reduced dissociation of the surface silanol groups explain the increase V_T necessary to restore the nanowire conductance.

To discriminate between these two possibilities we have investigated the change of the medium capacity, by changing the electrolyte concentration and therefore the electrical conductance. A higher fraction of dioxane decreases the

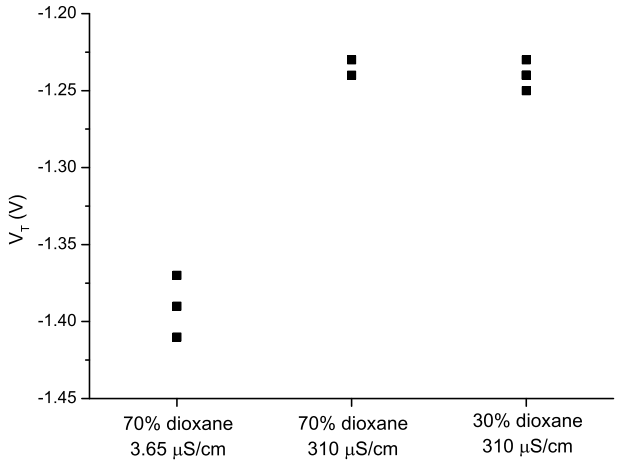

FIGURE 5.6: The threshold voltages of the device when exposed to three different water/dioxane solutions.

conductance and decreases the capacity. A less negative V_T is thus expected for a higher capacity. We have performed the experiments with the following solutions: (a) water/dioxane (30:70 v/v) with a conductivity of 3.65 μS/cm; (b) water/dioxane (30:70 v/v) with tetramethylammonium chloride added to obtain a conductivity of 310 μS/cm; and (c) water/dioxane ratio (70:30 v/v) with tetramethylammonium chloride added to obtain a conductivity of 310 μS/cm. It was observed (Figure 5.6) that changing the dioxane/water ratio from 30/70 to 70/30 (v/v) at a constant conductivity of 310 μS/cm did not influence the threshold voltage. Reduction of the conductivity to 3.65 μS/cm for a water/dioxane ratio 30/70 (v/v), resulted in a decrease of the threshold voltage. This shows that the conductivity has a larger effect on the gate potential to be applied for maintaining the drain current than changing only the ratio of water to dioxane. Therefore we come to the conclusion that the effect of water-dioxane ratios on the electrical properties of SiNW are induced by differences in the capacities of the medium between the nanowire and fate electrode as well as by a reduced dissociation of the surface silanol groups.

5.4 CONCLUSIONS AND OUTLOOK

In In this study, it was demonstrated that there is a different coupling of the gate potential to the SiNW-based device when this potential is applied via the back gate compared to application via a liquid gate. This difference is explained by the BOX layer through which the potential is coupled in the case of the back-gate configuration. This capacitance plays a dominant role over the other relevant capacitances involved. The capacitance of the solution is much less relevant because of its conductivity. Consequently, a reasonable approximation of the system is obtained, even when this layer is not taken into account in the capacitance of the system. Local addition of an individual back gate, which only acts through the area right below the SiNW and which has no capacitive coupling through the liquid, could make a quantitative description of the BG easier. It would also make it possible to individually gate the devices, providing more possibilities for sensor arrays with individual properties.

Furthermore, it was shown that the device characteristics, and most importantly the threshold voltage, are influenced by the solution to which the device is exposed. It is concluded that the change in the threshold voltage as function of dioxane fraction in the medium is determined by a decreased dissociation of the surface silanol groups and a reduced conductivity. Studying the dielectric coupling through the solution will thus only be possible when (1) the surface is passivated with a modification layer which has no interaction with the used solutions and (2) the solutions have a constant conductivity.

When the complete characteristics are taken into account (V_T and the slope of the I_D-V_{GS}-characteristics, i.e. the transconductance) an even more complete picture of the device characteristics and the influence of certain solvents could be obtained. Combined with assisted computer learning as demonstrated previously by Niskanen et al. [144] a sensor can be constructed from this device. A more detailed approach is needed to explain the observed effects quantitatively, which is beyond the scope of this article. This approach should include a better definition of the capacitance of the solution layer, the charges at the solvent-oxide interface should be taken into account, and adjustments for the absence of a pn-junction need to be added as well as including the presence of mobile charges in the solvent. However, with the simple approach presented in this study it is demonstrated that it is possible to distinguish the different solutions, depending on their conductivity.

To summarize, the results in this article: (1) lead to a better understanding of the electrical response of SiNW-based devices for BG vs. LG modes of operation; and (2) show that working in constant ionic strength is required in aqueous solutions and that corrections for the conductivity of mixed-media solutions are essential.

6

POTASSIUM-ION SENSING

This chapter present the preliminary results of experiments using a combination of a siloprene membrane and the potassium-selective ionophore valinomycin on NW-FETs.

A manuscript based on this chapter is in preparation, by M.Mescher, A. Cao, D. Bosma, J.H. Klootwijk, E.J.R. Sudhölter and L.C.P.M. de Smet.

6.1 INTRODUCTION

In 1975 the first potassium selective ISFET was reported [10]. It used a plasticized polyvinylchloride (PVC) membrane combined with a valinomycin ionophore (Figure 6.1). An ionophore is a molecule that very selectively forms a complex with an analyte, in this case with potassium ions. This membrane was well known from the ion selective electrode (ISE) field, and was in that year for the first time applied on ISFETs. In the following years, a large number of other publications followed this first one with a broad variety of membranes and sensor properties.

Chang and coworkers presented in 2011 the first NW-FET with a similar PVC membrane, again used for potassium ion sensing [68]. The PVC membrane was put on a NW-FET and used to monitor the potassium flux from cells when stimulated with nicotine. This paper was followed by an article by the group of Schonenberger [69], who were also able to combine these well-known membranes with the enhanced sensitivity of NW-FETs.

It is known that the lifetime of FETs with a PVC membrane is limited due to the low adherence of PVC membranes to SiO_2 surfaces [153]. Further the presence of a plasticizer in the membrane can cause degradation of the membrane. Several modification methods were used among which the replacement of the PVC membranes by a completely different rubber: siloprene [11, 154]. Siloprene is a polydimethylsiloxane which is cross-linked and can be used without an additional plasticizer. It can be prepared by cross-linking the silanol terminated polydimethylsiloxane K-1000 copolymer via condensation reaction of the silanol end groups with tetraethoxysilane present in the siloprene cross-linking agent K-11. In this chapter, experiments with siloprene membranes on ISEs and on NW-FETs are described. Besides the siloprene, the membrane consists of valinomycin, the ionophore, and potassium tetrakis(4-chlorophenyl)borate (Figure 6.1), which is used as an anionic additive. This additive ensures a high cationic concentration inside the membrane. This is essential for a proper functioning membrane, as membranes containing valinomycin and the additive in contact with an aqueous potassium ion solution possess a boundary potential. This potential depends on both concentrations. It is important that the concentration inside the membrane is constant. This is realized by the proper choice of valinomycin and additive concentrations in the membrane. When the potassium-ion concentration inside the membrane is high enough, it can be considered a constant and the measured potential will only depend on the concentration outside the membrane.

Wipf and coworkers [69] used an unmodified NW-FET as reference device in experiments. In this work a membrane without valinomycin is used to eliminate issues related to swelling, pH and other possible interactions of the target solution with the polymer matrix. The membranes are first tested using a conventional ISE

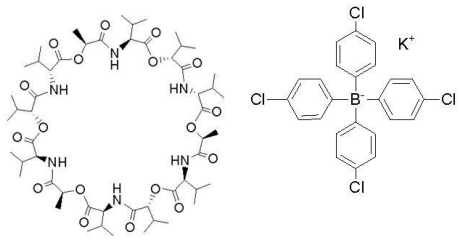

FIGURE 6.1: Active compounds in the well-known PVC membrane: valionmycin (potassium ionophore) and potassium tetrakis(4-chlorophenyl)borate (anionic additive)

setup. After this, membranes with an identical composition are tested using the NW-FETs as transducer. The results from both experiments are shown and the response is discussed.

6.2 EXPERIMENTAL

NANOWIRE field-effect transistors were produced according to [3] as described in Chapter 3. They were wirebonded using conductive glue and 25 μm thick gold wire with four functional devices per chip.

Two types of siloprene membranes were prepared: ion-selective membranes (ISMs) and reference membranes (RMs). These membranes were prepared according to [154]: For the ISMs approximately a 5:1 mass ratio of valinomycin and potassium tetrakis (4-chlorophenyl)borate (PTCB) was dissolved in CH_2Cl_2. After this, siloprene K-1000 (a silanol terminated polydimethylsiloxane) and K-11 (cross-linking agent) in a 10:1 wt% ratio were added. The solution for reference membranes was contained siloprene K-1000, cross-linker K-11 and anionic additive and was prepared in a similar way. The exact composition can be found in Table 6.1.

After stirring the membrane solutions for five minutes, the polymer solution was pipetted into a mold for experiments using the ISE setup. Reference membranes for the ISE experiments were prepared in the same way. After the solvent was evaporated overnight, the ISE membranes were placed on the ISE tip filled with a 3 M KCl filling solution.

Membranes for the nanowire experiments were drop-casted from the membrane solution on the nanowire devices, as were reference membranes. A chip with two drop-casted membranes is shown in Figure 6.2a. The fluidics were placed on the chips and sealed to prevent leakage of water (Figure 6.2b). To study the dimensions of the membranes on the NW-FETs, similar droplets are placed on

TABLE 6.1: Exact composition of the ISM and RM.

Compound	Ion-selective membrane	Reference membrane
Valinomycin	3.3 mg	-
PTCB	0.63 mg	0.69 mg
CH_2Cl_2	3 ml	3 ml
Cross-linker K-11	35.4 mg	35.5 mg
Siloprene K-1000	351.0 mg	355.5 mg

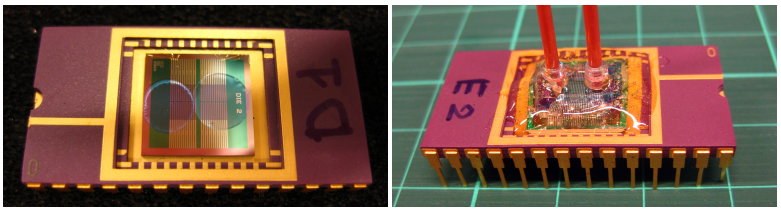

(a) (b)

FIGURE 6.2: (a) Wire bonded chip modified with two polymer membranes (the circles in the middle): the membrane on the left is the ISM. The droplet on the right is the RM. (b) Wire bonded chip after fluidics are placed and the system is glued to prevent leakage.

6

SiO_2 substrates. After curing of these membranes step height measurements are performed using a Dektak 6M with a stylus with a 12.5 µm radius. The applied force was 9.8 µN.

The ISE tests are performed using a Metrohm 278 pH lab system with a Metrohm Ag/AgCl reference electrode and custom made working electrode. The ion-selective electrode has a tip in which the membrane can be placed.

A standard Keithley 4200 semiconductor characterization system equipped with eight source measurement units is used for the electrical characterization of the NW device during exposure. The device was placed in a special designed measurement box (Figure 6.3) to ensure more stable source and drain contacts compared to the use of a probe station. A 50 mV source-drain bias is applied. The drain current (I_D) is measured while the gate potential (V_{GS}) is swept with $V_{SD} \ll V_{GS}$ in order to operate the device in depletion mode in the linear regime. The gate potential can be applied either via the back gate contact (V_{BG}) or an Ag/AgCl electrode in the solution: the fluid gate (V_{FG}). All experiments shown in this chapter were performed using the fluid gate.

The sensing experiments are conducted using solutions with a constant ionic strength of 0.1 M, prepared using KCl (99.0 %, Fluka) and NaCl (99,5 %, Merck Suprapur). The potassium concentration was varied from 10^{-5} M to 0.1 M and

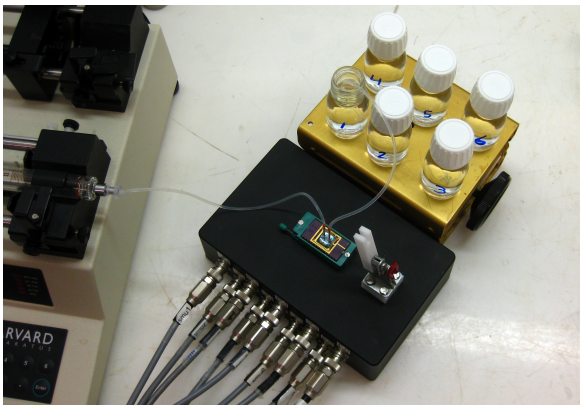

FIGURE 6.3: The setup in which the NW-FETs are tested. The sample is placed on top of the black box, after which the tubing is connected. The solutions are sucked into the system from the bottles in the top-right corner using the pump on the left. The Ag/AgCl electrode is placed in the bottle from which the solution is sucked.

NaCl was added to make the total ionic strength 0.1 M.

6.3 RESULTS AND DISCUSSION

Before electrical characterization, the dimensions and properties of the membranes were studied. Figure 6.4 shows the results of the investigation of the dimensions of the drop-casted membranes on plain SiO_2 samples. It is observed that all membranes have comparable dimensions: the diameters are 6-7 mm. The thickness of the ISMs is approximately 85-90 μm, and the RM are slightly thinner: 50-60 μm. Visual inspection of the membranes also showed a small difference: the ISMs were less transparent than the RMs. A difference between the membranes was also observed during the preparation of the ISE-tip: the ISMs were stronger than the RM, which turned out to be too fragile to handle.

6.3.1 ISE EXPERIMENTS

THE ISMs were first tested using the ISE-setup. Figure 6.5 shows the linear response of this membrane, i.e. a slope of 55 mV/decade. This is very close to the ideal response of 59 mV/decade predicted by the Nernst equation 2.1 and literature. During the second test series however, the response was significantly smaller: when the most diluted point is ignored, a slope of only 15 mV/decade is found.

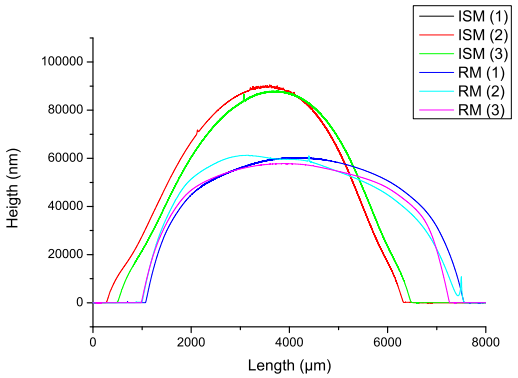

FIGURE 6.4: Results of the step height measurements on the SiO_2 substrates.

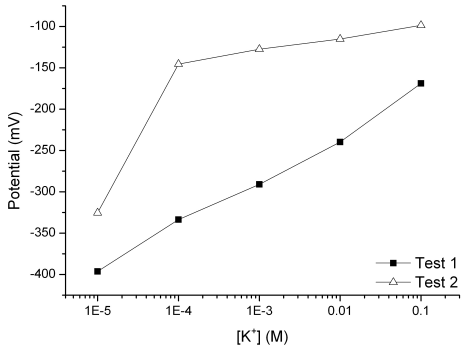

FIGURE 6.5: Response of the ISM in the ISE-setup

6.3.2 NW-FET EXPERIMENTS

Sensing experiments were performed using the modified chips as well. The (typical) result of one of the devices which was modified with an ISM is shown in Figure 6.6. This graph shows a clear shift of the curves towards more negative fluid gate potentials when the concentration of the potassium ions increases. The device modified with the RM showed no response, except for a small drift. This experiment was repeated several times with two ISM-modified devices on the chip. A quantification of these experiments is shown in Figure 6.7. Here, the V_T was obtained by taking the potential which was needed to cross the 1 nA current threshold. The shift in threshold voltage was normalized for all devices. The average values and the associated standard deviations were calculated and plotted for all series and devices. It was observed that the timing of the experiments is very important. Although the response of the system at higher concentrations is almost instantaneous (<1 min), the response at the lowest concentrations is much slower (~ 10 min may be needed for the system to stabilize). This type of membranes is known to have a detection limit of 10^{-5} M, below which the potassium ions can leach out of the membrane. The slow response rate can be explained by the equilibration rate from the membrane surface through the stagnant layer into the bulk of the solution: this in known the be a slow process. During the measurements it was also observed that some time is needed for the membrane to stabilize when going from the highest to the lowest concentration. This might be caused by the large difference between those two solutions. The slope of the to devices is 47 and 57 mV/decade, which is reduced to 36 and 45 mV/decade when the response is corrected for the drift observed in the reference membrane. For a better comparability of the response, the experiments with the ISE and the NW-FET should be repeated, so that more statistical data is obtained. The lifetime of the membranes on the NW-FET is an interesting subject for further experiments.

6.4 CONCLUSIONS AND OUTLOOK

In this chapter, siloprene membranes containing valinomycin have been used to selectively detect changes in potassium-ion concentration. In these first experiments it was found that the response of the NW-FETs is comparable to the response using an ISE setup. Having optimized the devices and setup opens up a large number of possibilities. What has not not been investigated here is the selectivity of the membrane. Therefore, it would be interesting to expose the devices to other ions and determine the exact selectivity. Experiments using the back gate instead of an Ag/AgCl electrode would be of interest as well: the possibility of sensing pH using the back gate only was demonstrated in Chapter 4. Combining the pulsed measurement techniques with potassium-selective membranes would

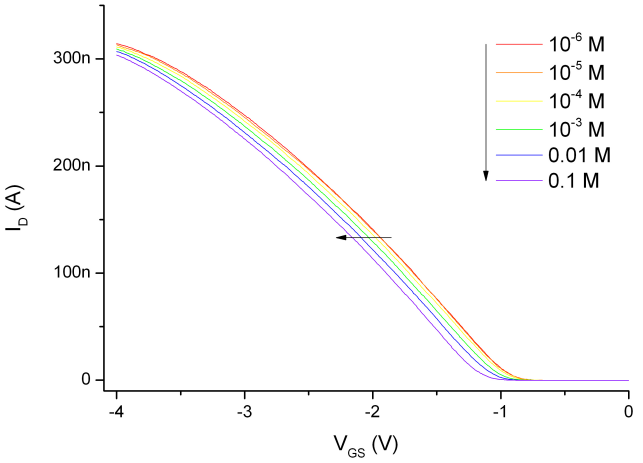

FIGURE 6.6: Typical I_D-V_{GS} characteristics of one of the devices modified with an ISM when exposed to solutions with a range of potassium-ion concentrations.

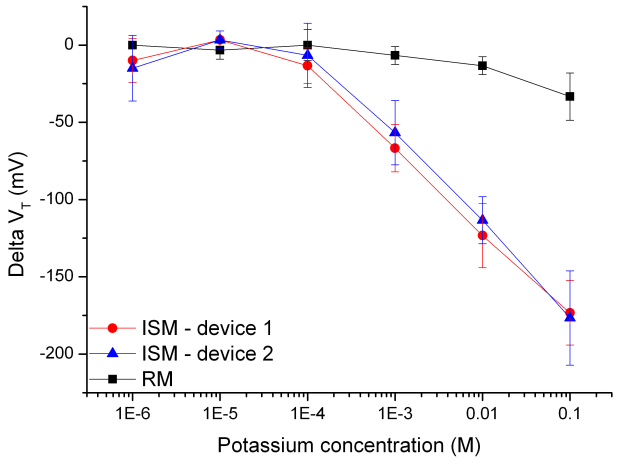

FIGURE 6.7: Response of the ISM and RM using the NW-FETs.

therefor be a valuable addition to this project. At the same time this can be used for another research question: is it possible to reduce the response rate of the membrane by selective application of positive or negative potential pulses?

The next step with this system could be to deposit three different membranes: one with and K^+-selective ionophore, a second membrane which is selective towards another type of ions, e.g. Na^+ and a reference membrane. This can be used to demonstrate the detection of two different ion-species on a single chip. The detection of multi-valent ions e.g. Hg^{2+} and Cd^{2+} is a good opportunity for future research, especially considering the original application of this project in drinking water applications.

7

CONCLUSIONS

7.1 CONCLUSIONS

THIS thesis describes the work that has been done in the project on the 'Sensitive and Selective Sensor for Water Sensing Applications'. The experiments presented in the preceding experimental chapters have lead to a number of conclusions.

In Chapter 3 a new method for the top-down fabrication of silicon nanowire field-effect transistors was demonstrated. This method was used to obtain sensor devices. A single chip contains 28 NW-FETs, which allows for fingerprinting sensor applications or multiplexing. Besides solving the issue with over etching, the presented method gives flexibility in the use of other front oxides. It provides selectivity in the use of passivation layers and thus modification. Furthermore also offers the possibility to further reduce the nanowires width using e-beam technology. All steps used are based on standard CMOS processing techniques. It was demonstrated that the variation in electrical characteristics of the device within a single die is small, providing the possibility for fingerprinting sensor applications and differential measurements

Chapter 4 presents a new method for characterization of the NW-FETs in aqueous solutions. It was shown that a pulsed back-gate potential improves the stability of the device in aqueous environments. The initially observed drift of the threshold voltage has been reduced by short positive pulses combined with long periods of neutral potential. Furthermore, a method to improve the stability of the NW-FETs on typical time scales as used during measurements was demonstrated. Alternating positive and negative pulses lead to increased stability of the I_D versus V_{GS} characteristics in time. It was shown that the pH can be detected using only back gating and this method, without any additional electrodes.

Chapter 5 demonstrates that there is a different coupling of the gate potential to the SiNW-based device when applied via the back gate compared to that applied via a liquid gate configuration. This difference is explained by the BOX layer through which the potential is coupled first, which plays a dominant role over the other relevant capacitances. The capacitance of the solution is much less relevant because of its conductivity.

Furthermore, it is shown that the device characteristics, and most importantly the threshold voltage, are influenced by the solution to which the device is exposed. It is concluded that the difference in the threshold voltage for the different solvent mixtures is related to differences in the conductivity, rather than the differences in the dielectric constant. The experiments in this chapter therefore show that working in constant ionic strength is required in aqueous solutions and that corrections for the conductivity of mixed-media solutions are essential.

In Chapter 6, siloprene membranes containing valinomycin have been used

to selectively detect changes in potassium-ion concentration. It was found that the response of the NW-FETs is comparable to the response using an ion selective electrode setup. Although this means that the increased sensitivity of NW-FETs compared to ion selective field-effect transistors has not been demonstrated, it does prove that modification of the surface results in a working sensor.

7.2 DISCUSSION

THE experiments in Chapter 3 were performed using the back gate, while in Chapters 5 and 6 a fluid gate via Ag/AgCl electrode was used. Both methods proved to work, and both have their advantages and disadvantages. The first method, i.e. the application of the potential using the back gate, was demonstrated using a pulsed measurement method. This requires extra measurements to determine the optimal settings for the device under test, which takes some time. However, this method does not need an additional Ag/AgCl electrode or an on-chip electrode. The back-gating experiments were performed in a very controlled environment: switching between solutions was done using a computer-controlled, pressure-operated switch, in order to maintain the semi-stable working mode of the device. Using this method, successful detection of changes in pH was performed.

The second method for gating presented in this thesis is liquid gating using an Ag/AgCl reference electrode, used for the water-dioxane experiments (Chapter 5) and the sensing of potassium (Chapter 6). The method obviously requires the integration or addition of this electrode, but no special measurement settings are applied. Switching can be done by hand and it doesn't influence the devices characteristics. In both cases a reference device can be used to correct for the drift.

It can be argued that depending on the situation an optimal gating-principle can be found. The sensor which is easiest to produce is the one where back-gating is used, but for fast and stable measurements the use of liquid gating via a reference electrode is recommended.

7.3 OUTLOOK

HAVING studied the properties of the NW-FET devices in air, de-ionized water, water with salts and water-dioxane mixtures, an improved understanding of the working principles of these devices has been obtained. Examples include the expanded knowledge about timing resulting from the work on the pulsed gate potential, the study on the influence of the conductivity of solutions on the device characteristics and the experimental experience obtained with the use of fluidics. There are a number of possible next steps to study the sensor behavior of these devices.

First, based on the process flow in Chapter 3 the different gate oxides can be studied. It would be interesting to see whether the addition of a different gate oxide can improve the sensitive of the device towards the pH, comparable to the one reported for Al_2O_3 by Chen et al. [122]. The work presented in Chapter 6 with polymer membrane-modified devices could be expanded by studying the cross-selectivity towards other ions, e.g. Na^+. Replacing the valinomycin ionophore with an ionophore which has a selectivity towards other ions can be carried out to expand this work even further. Finally, the deposition of multiple, different membranes on a single chip is an interesting topic for expanding the current research.

To answer the question in the title of this thesis, it has been demonstrated that sensing using nanowire field-effect transistors is not simple and straight forward. A large number of details in the production of the devices, the measurement setup, the methods for measuring, modification and the complexity of fluid samples play an essential role in the response obtained from the devices. Sensing simplicity can therefor only be reached after thorough study of these factors.

REFERENCES

[1] B. R. Eggins, *Biosensors: an Introduction.* Wiley, 1996.

[2] L. C. P. M. De Smet, D. Ullien, M. Mescher, and E. J. R. Sudhölter, *Organic Surface Modification of Silicon Nanowire-Based Sensor Devices*, ch. 13, pp. 267–288. InTech, 2011.

[3] M. Mescher, L. C. P. M. de Smet, E. J. R. Sudhölter, and J. H. Klootwijk, "Robust Fabrication Method for Silicon Nanowire Field Effect Transistors for Sensing Applications," *Journal of Nanoscience and Nanotechnology* **13** no. 8, (2013) 5649–5653.

[4] M. Mescher, B. Marcelis, L. C. P. M. de Smet, E. J. R. Sudhölter, and J. H. Klootwijk, "Pulsed Method for Characterizing Aqueous Media Using Nanowire Field Effect Transistors," *IEEE Transactions on Electron Devices* **58** no. 7, (2011) 1886–1891.

[5] M. Mescher, A. G. M. Brinkman, D. Bosma, J. H. Klootwijk, E. J. R. Sudhölter, and L. C. P. M. de Smet, "Influence of Conductivity and Dielectric Constant of Water-Dioxane Mixtures on the Electrical Response of SiNW-Based FETs," *Sensors* **14** no. 2, (2014) 2350–2361.

[6] P. Bergveld, "Development of an Ion-Sensitive Solid-State Device for Neurophysiological Measurements," *IEEE Transactions on Biomedical Engineering* (1970) 70–71.

[7] L. Bousse, N. F. de Rooij, and P. Bergveld, "Operation of Chemically Sensitive Field-Effect Sensors as a Function of the Insulator-Electrolyte Interface," *IEEE Transactions on Electron Devices* **30** no. 10, (1983) 1263–1270.

[8] M. J. Madou and S. R. Morrison, *Chemical Sensing with Solid State Devices.* Academic Press, Inc., 1988.

[9] P. Bergveld, "Development, Operation, and Application of the Ion-Sensitive Field-Effect Transistor as a Tool for Electrophysiology," *IEEE Transactions on Biomedical Engineering* (1972) 342–351.

[10] S. D. Moss, J. Janata, and C. C. Johnson, "Potassium Ion-Sensitive Field Effect Transistor," *Analytical Chemistry* **47** no. 13, (1975) 2238–2243.

[11] P. D. van der Wal, M. Skowronska-Ptasinska, A. van den Berg, P. Bergveld, E. J. R. Sudhölter, and D. N. Reinhoudt, "New Membrane Materials for Potassium-Selective Ion-Sensitive Field-Effect Transistors," *Analytica Chimica Acta* **231** (1990) 41–52.

[12] A. van den Berg, P. Bergveld, D. N. Reinhoudt, and E. J. R. Sudhölter, "Sensitivity Control of ISFETs by Chemical Surface Modification," *Sensors and Actuators* **8** no. 2, (1985) 129–148.

[13] Y. Cui, Q. Wei, H. Park, and C. M. Lieber, "Nanowire Nanosensors for Highly Sensitive and Selective Detection of Biological and Chemical Species," *Science* **293** no. 5533, (2001) 1289–1292.

[14] R. S. Wagner and W. C. Ellis, "Vapor-Liquid-Solid Mechanism of Single Crystal Growth," *Applied Physics Letters* **4** no. 5, (1964) 89–90.

[15] Y. Cui and C. M. Lieber, "Functional Nanoscale Electronic Devices Assembled Using Silicon Nanowire Building Blocks," *Science* **291** no. 5505, (2001) 851–853.

[16] J. Wan, S.-R. Deng, R. Yang, Z. Shu, B.-R. Lu, S.-Q. Xie, Y. Chen, E. Huq, R. Liu, and X.-P. Qu, "Silicon Nanowire Sensor for Gas Detection Fabricated by Nanoimprint on SU8/SiO_2/PMMA Trilayer," *Microelectronic Engineering* **86** no. 4-6, (2009) 1238–1242.

[17] N. S. Ramgir, Y. Yang, and M. Zacharias, "Nanowire-Based Sensors," *Small* **6** no. 16, (2010) 1705–1722.

[18] F. Patolsky, G. Zheng, and C. M. Lieber, "Nanowire Sensors for Medicine and the Life Sciences," *Nanomedicine* **1** no. 1, (2006) 51–65.

[19] Y. Li, F. Qian, J. Xiang, and C. M. Lieber, "Nanowire Electronic and Optoelectronic Devices," *Materials Today* **9** no. 10, (2006) 18–27.

[20] E. Carlen and A. Van den Berg, "Nanowire Electrochemical Sensors: Can We Live Without Labels?," *Lab on a Chip* **7** no. 1, (2007) 19–23.

[21] E. Stern, A. Vacic, and M. A. Reed, "Semiconducting Nanowire Field-Effect Transistor Biomolecular Sensors," *Electron Devices, IEEE Transactions on* **55** no. 11, (2008) 3119–3130.

[22] D. Aswal, S. Lenfant, D. Guerin, J. Yakhmi, and D. Vuillaume, "Self Assembled Monolayers on Silicon for Molecular Electronics," *Analytica Chimica Acta* **568** no. 1, (2006) 84–108.

[23] M. Stutzmann, J. A. Garrido, M. Eickhoff, and M. S. Brandt, "Direct Biofunctionalization of Semiconductors: A Survey," *Physica Status Solidi (A)* **203** no. 14, (2006) 3424–3437.

[24] R. J. Hamers, "Formation and Characterization of Organic Monolayers on Semiconductor Surfaces," *Annual Review of Analytical Chemistry* **1** no. 1, (2008) 707–736.

[25] A. K. Wanekaya, W. Chen, N. V. Myung, and A. Mulchandani, "Nanowire-Based Electrochemical Biosensors," *Electroanalysis* **18** no. 6, (2006) 533–550.

[26] M. Shao, D. D. D. Ma, and S.-T. Lee, "Silicon Nanowires - Synthesis, Properties, and Applications," *European Journal of Inorganic Chemistry* **2010** no. 27, (2010) 4264–4278.

[27] J. N. Tey, I. P. M. Wijaya, J. Wei, I. Rodriguez, and S. G. Mhaisalkar, "Nanotubes-/Nanowires-Based, Microfluidic-Integrated Transistors for Detecting Biomolecules," *Microfluidics and Nanofluidics* **9** no. 6, (2010) 1185–1214.

[28] A. Cao, E. J. R. Sudhölter, and L. C. P. M. de Smet, "Silicon Nanowire-Based Devices for Gas Phase Sensing," *Sensors* **1** no. 1, (2014) 1–2.

[29] X. G. Zhang, *Electrochemistry of Silicon and Its Oxide*. Kluwer Academic Publishers, 2004.

[30] J. Sagiv, "Organized Monolayers by Adsorption. 1. Formation and Structure of Oleophobic Mixed Monolayers on Solid Surfaces," *Journal of the American Chemical Society* **102** no. 1, (1980) 92–98.

[31] X. Wang, Y. Chen, K. A. Gibney, S. Erramilli, and P. Mohanty, "Silicon-Based Nanochannel Glucose Sensor," *Applied Physics Letters* **92** no. 1, (2008) 013903–013903–3.

[32] Y. L. Bunimovich, Y. S. Shin, W. S. Yeo, M. Amori, G. Kwong, and J. R. Heath, "Quantitative Real-Time Measurements of DNA Hybridization with Alkylated Nonoxidized Silicon Nanowires in Electrolyte Solution," *Journal of American Chemical Society* **128** (2006) 16323–16331.

[33] Y. Chen, X. Wang, S. Erramilli, P. Mohanty, and A. Kalinowski, "Silicon-Based Nanoelectronic Field-Effect pH Sensor with Local Gate Control," *Applied Physics Letters* **89** no. 22, (2006) 223512–223512–3.

[34] Y. Ma, J. Zhang, G. Zhang, and H. He, "Polyaniline Nanowires on Si Surfaces Fabricated with DNA Templates," *Journal of the American Chemical Society* **126** no. 22, (2004) 7097–7101.

[35] M. C. Lin, C. J. Chu, L. C. Tsai, H. Y. Lin, C. S. Wu, Y. P. Wu, Y. N. Wu, D. B. Shieh, Y. W. Su, and C. D. Chen, "Control and Detection of Organosilane Polarization on Nanowire Field-Effect Transistors," *Nano Letters* **7** no. 12, (2007) 3656–3661.

[36] Z. Li, Y. Chen, X. Li, T. I. Kamins, K. Nauka, and R. S. Williams, "Sequence-Specific Label-Free DNA Sensors Based on Silicon Nanowires," *Nano Letters* **4** no. 2, (2004) 245–247.

[37] G. Zheng, F. Patolsky, Y. Cui, W. U. Wang, and C. M. Lieber, "Multiplexed Electrical Detection of Cancer Markers with Nanowire Sensor Arrays," *Nature biotechnology* **23** (2005) 1294–1301.

[38] F. Patolsky, G. Zheng, O. Hayden, M. Lakadamyali, X. Zhuang, and C. M. Lieber, "Electrical Detection of Single Viruses," *Proceedings of the National Academy of Sciences* **101** no. 39, (2004) 14017–14022.

[39] W. U. Wang, C. Chen, K.-h. Lin, Y. Fang, and C. M. Lieber, "Label-Free Detection of Small-Molecule-Protein Interactions by Using Nanowire Nanosensors," *Proceedings of the National Academy of Sciences of the United States of America* **102** no. 9, (2005) 3208–3212.

[40] G.-J. Zhang, M. J. Huang, Z. H. H. Luo, G. K. I. Tay, E.-J. A. Lim, E. T. Liu, and J. S. Thomsen, "Highly Sensitive and Reversible Silicon Nanowire Biosensor to Study Nuclear Hormone Receptor Protein and Response Element DNA Interactions," *Biosensors and Bioelectronics* **26** no. 2, (2010) 365–370.

[41] A. Kim, C. S. Ah, H. Y. Yu, J.-H. Yang, I.-B. Baek, C.-G. Ahn, C.-W. Park, M. S. Jun, and S. Lee, "Ultrasensitive, Label-Free, and Real-Time Immunodetection Using Silicon Field-Effect Transistors," *Applied Physics Letters* **91** no. 10, (2007) 103901–103901–3.

[42] P. E. Lobert, D. Bourgeois, R. Pampin, A. Akheyar, L. M. Hagelsieb, D. Flandre, and J. Remacle, "Immobilization of DNA on CMOS Compatible Materials," *Sensors and Actuators B: Chemical* **92** no. 1-2, (2003) 90–97.

[43] F. Patolsky, G. Zheng, and C. M. Lieber, "Fabrication of Silicon Nanowire Devices for Ultrasensitive, Label-free, Real-Time Detection of Biological and Chemical Species," *Nature Protocols* **1** no. 4, (2006) 1711–1724.

[44] L. Dong-Che, Y. Po-Hung, and M. S. C. Lu, "CMOS Open-Gate Ion-Sensitive Field-Effect Transistors for Ultrasensitive Dopamine Detection," *Electron Devices, IEEE Transactions on* **57** no. 10, (2010) 2761–2767.

[45] J. T. Sheu, C. C. Chen, P. C. Huang, Y. K. Lee, and M. L. Hsu, "Selective Deposition of Gold Nanoparticles on SiO_2/Si Nanowires for Molecule Detection," *Japanese Journal of Applied Physics* **44** no. 4B, (2005) 2864.

[46] L. B. Luo, J. S. Jie, W. F. Zhang, Z. B. He, J. X. Wang, G. D. Yuan, W. J. Zhang, L. C. M. Wu, and S. T. Lee, "Silicon Nanowire Sensors for Hg^{2+} and Cd^{2+} Ions," *Applied Physics Letters* **94** no. 19, (2009) 3.

[47] X. Bi, A. Agarwal, N. Balasubramanian, and K.-L. Yang, "Tripeptide-Modified Silicon Nanowire Based Field-effect Rransistors as Real-Time Copper Ion Sensors," *Electrochemistry Communications* **10** no. 12, (2008) 1868–1871.

[48] Y. Engel, R. Elnathan, A. Pevzner, G. Davidi, E. Flaxer, and F. Patolsky, "Supersensitive Detection of Explosives by Silicon Nanowire Arrays," *Angewandte Chemie International Edition* **49** no. 38, (2010) 6830–6835.

[49] E. T. Vandenberg, L. Bertilsson, B. Liedberg, K. Uvdal, R. Erlandsson, H. Elwing, and I. Lundström, "Structure of 3-Aminopropyl Triethoxy Silane on Silicon Oxide," *Journal of Colloid and Interface Science* **147** no. 1, (1991) 103–118.

[50] J. A. Howarter and J. P. Youngblood, "Optimization of Silica Silanization by 3-Aminopropyltriethoxysilane," *Langmuir* **22** no. 26, (2006) 11142–11147.

[51] M.-H. Lee, K.-N. Lee, S.-W. Jung, W.-H. Kim, K.-S. Shin, and W.-K. Seong, "Quantitative Measurements of C-Reactive Protein Using Silicon Nanowire Arrays," *International Journal of Nanomedicine* **3** no. 1, (2008) 117–124.

[52] X. Bi, W. L. Wong, W. Ji, A. Agarwal, N. Balasubramanian, and K.-L. Yang, "Development of Electrochemical Calcium Sensors by Using Silicon Nanowires Modified with Phosphotyrosine," *Biosensors and Bioelectronics* **23** no. 10, (2008) 1442–1448.

[53] B. Wang and H. Haick, "Effect of Functional Groups on the Sensing Properties of Silicon Nanowires toward Volatile Compounds," *ACS Applied Materials & Interfaces* **5** no. 6, (2013) 2289–2299.

[54] B. Wang and H. Haick, "Effect of Chain Length on the Sensing of Volatile Organic Compounds by means of Silicon Nanowires," *ACS Applied Materials & Interfaces* **5** no. 12, (2013) 5748–5756.

[55] J. Hahm and C. M. Lieber, "Direct Ultrasensitive Electrical Detection of DNA and DNA Sequence Variations Using Nanowire Nanosensors," *Nano Letters* **4** no. 1, (2004) 51–54.

[56] A. Cattani-Scholz, D. Pedone, M. Dubey, S. Neppl, B. Nickel, P. Feulner, J. Schwartz, G. Abstreiter, and M. Tornow, "Organophosphonate-Based PNA-Functionalization of Silicon Nanowires for Label-Free DNA Detection," *ACS Nano* **2** no. 8, (2008) 1653–1660.

[57] B. M. Silverman, K. A. Wieghaus, and J. Schwartz, "Comparative Properties of Siloxane vs Phosphonate Monolayers on A Key Titanium Alloy," *Langmuir* **21** no. 1, (2005) 225–228.

[58] E. L. Hanson, J. Schwartz, B. Nickel, N. Koch, and M. F. Danisman, "Bonding Self-Assembled, Compact Organophosphonate Monolayers to the Native Oxide Surface of Silicon," *Journal of the American Chemical Society* **125** no. 51, (2003) 16074–16080.

[59] G. Decher, "Fuzzy Nanoassemblies: Toward Layered Polymeric Multicomposites," *Science* **277** no. 5330, (1997) 1232–1237.

[60] X. T. Vu, R. Stockmann, B. Wolfrum, A. Offenhäusser, and S. Ingebrandt, "Fabrication and Application of a Microfluidic-Embedded Silicon Nanowire Biosensor Chip," *Physica Status Solidi (A)* **207** no. 4, (2010) 850–857.

[61] A. Poghossian, M. H. Abouzar, F. Amberger, D. Mayer, Y. Han, S. Ingebrandt, A. Offenhäusser, and M. J. Schöning, "Field-Effect Sensors with Charged Macromolecules: Characterisation by CapacitanceŰVoltage, Constant-Capacitance, Impedance Spectroscopy and Atomic-Force Microscopy Methods," *Biosensors and Bioelectronics* **22** no. 9-10, (2007) 2100–2107.

[62] G. Decher and J. Schmitt, *Fine-tuning of the Film Thickness of Ultrathin Multilayer Films Composed of Consecutively Alternating Layers of Anionic and Cationic Polyelectrolytes*, vol. 89 of *Progress in Colloid & Polymer Science*, ch. 36, pp. 160–164. Steinkopff, 1992.

[63] B. R. Dorvel, B. Reddy, J. Go, C. Duarte Guevara, E. Salm, M. A. Alam, and R. Bashir, "Silicon Nanowires with High-k Hafnium Oxide Dielectrics for Sensitive Detection of Small Nucleic Acid Oligomers," *ACS Nano* **6** no. 7, (2012) 6150–6164.

[64] A. V. Saprigin, C. W. Thomas, C. S. Dulcey, C. H. Patterson, and M. S. Spector, "Spectroscopic Quantification of Covalently Immobilized Oligonucleotides," *Surface and Interface Analysis* **37** no. 1, (2005) 24–32.

[65] J. A. Martinez, N. Misra, Y. Wang, P. Stroeve, C. P. Grigoropoulos, and A. Noy, "Highly Efficient Biocompatible Single Silicon Nanowire Electrodes with Functional Biological Pore Channels," *Nano Letters* **9** no. 3, (2009) 1121–1126.

[66] N. Misra, J. A. Martinez, S.-C. J. Huang, Y. Wang, P. Stroeve, C. P. Grigoropoulos, and A. Noy, "Bioelectronic Silicon Nanowire Devices using Functional Membrane Proteins," *Proceedings of the National Academy of Sciences* **106** no. 33, (2009) 13780–13784.

[67] S.-C. J. Huang, A. B. Artyukhin, J. A. Martinez, D. J. Sirbuly, Y. Wang, J. Ju, P. Stroeve, and A. Noy, "Formation, Stability, and Mobility of One-Dimensional Lipid Bilayers on Polysilicon Nanowires," *Nano Letters* **7** no. 11, (2007) 3355–3359.

[68] K.-S. Chang, C.-J. Sun, P.-L. Chiang, A.-C. Chou, M.-C. Lin, C. Liang, H.-H. Hung, Y.-H. Yeh, C.-D. Chen, C.-Y. Pan, and Y.-T. Chen, "Monitoring Extracellular K^+ Flux with a Valinomycin-Coated Silicon Nanowire Field-Effect Transistor," *Biosensors and Bioelectronics* **31** no. 1, (2012) 137–143.

[69] M. Wipf, R. L. Stoop, A. Tarasov, K. Bedner, W. Fu, M. Calame, and C. Schonenberger, "Potassium Sensing with Membrane-Coated Silicon Nanowire Field-Effect Transistors," in *Solid-state Sensors, Actuators and Microsystems, The 17th International Conference on Transducers & Eurosensors XXVII* , pp. 1182–1185. 2013.

[70] J. Yun, C. Y. Jin, J.-H. Ahn, S. Jeon, and I. Park, "A Self-Heated Silicon Nanowire Array: Selective Surface Modification with Catalytic Nanoparticles by Nanoscale Joule Heating and its Gas Sensing Applications," *Nanoscale* **5** no. 15, (2013) 6851–6856.

[71] I. Park, Z. Li, A. P. Pisano, and R. S. Williams, "Selective Surface Functionalization of Silicon Nanowires via Nanoscale Joule Heating," *Nano Letters* **7** no. 10, (2007) 3106–3111.

[72] M. R. Linford and C. E. D. Chidsey, "Alkyl Monolayers Covalently Bonded to Silicon Surfaces," *Journal of the American Chemical Society* **115** no. 26, (1993) 12631–12632.

[73] M. R. Linford, P. Fenter, P. M. Eisenberger, and C. E. D. Chidsey, "Alkyl Monolayers on Silicon Prepared from 1-Alkenes and Hydrogen-Terminated Silicon," *Journal of the American Chemical Society* **117** no. 11, (1995) 3145–3155.

[74] J. M. Buriak, "Organometallic Chemistry on Silicon and Germanium Surfaces," *Chemical Reviews* **102** no. 5, (2002) 1271–1308.

[75] S. Ciampi, J. B. Harper, and J. J. Gooding, "Wet Chemical Routes to the Assembly of Organic Monolayers on Silicon Surfaces via the Formation of Si-C Bonds: Surface Preparation, Passivation and Functionalization," *Chemical Society Reviews* **39** no. 6, (2010) 2158–2183.

[76] S. Kar, C. Miramond, and D. Vuillaume, "Properties of Electronic Traps at Silicon/1-Octadecene Interfaces," *Applied Physics Letters* **78** no. 9, (2001) 1288–1290.

[77] M. Calistri-Yeh, E. J. Kramer, R. Sharma, W. Zhao, M. H. Rafailovich, J. Sokolov, and J. D. Brock, "Thermal Stability of Self-Assembled Monolayers from Alkylchlorosilanes," *Langmuir* **12** no. 11, (1996) 2747–2755.

[78] G. J. Zhang, J. H. Chua, R. E. Chee, A. Agarwal, S. M. Wong, K. D. Buddharaju, and N. Balasubramanian, "Highly Sensitive Measurements of PNA-DNA Hybridization using Oxide-Etched Silicon Nanowire Biosensors," *Biosensors and Bioelectronics* **23** no. 11, (2008) 1701–1707.

[79] E. J. Faber, L. C. P. M. de Smet, W. Olthuis, H. Zuilhof, E. J. R. Sudhölter, P. Bergveld, and A. van den Berg, "Si-C Linked Organic Monolayers on Crystalline Silicon Surfaces as Alternative Gate Insulators," *ChemPhysChem* **6** no. 10, (2005) 2153–2166.

[80] A. Vilan, O. Yaffe, A. Biller, A. Salomon, A. Kahn, and D. Cahen, "Molecules on Si: Electronics with Chemistry," *Advanced Materials* **22** no. 2, (2010) 140–159.

[81] A. B. Sieval, R. Linke, G. Heij, G. Meijer, H. Zuilhof, and E. J. R. Sudhölter, "Amino-Terminated Organic Monolayers on Hydrogen-Terminated Silicon Surfaces," *Langmuir* **17** no. 24, (2001) 7554–7559.

[82] A. B. Sieval, B. van den Hout, H. Zuilhof, and E. J. R. Sudhölter, "Molecular Modeling of Covalently Attached Alkyl Monolayers on the Hydrogen-Terminated Si(111) Surface," *Langmuir* **17** no. 7, (2001) 2172–2181.

[83] A. B. Sieval, R. Linke, H. Zuilhof, and E. J. R. Sudhölter, "High-Quality Alkyl Monolayers on Silicon Surfaces," *Advanced Materials* **12** no. 19, (2000) 1457–1460.

[84] Y. L. Bunimovich, G. Ge, K. C. Beverly, R. S. Ries, L. Hood, and J. R. Heath, "Electrochemically Programmed, Spatially Selective Biofunctionalization of Silicon Wires," *Langmuir* **20** no. 24, (2004) 10630–10638.

[85] A. S. Jeremy, K. Heesuk, M. N. Beth, and J. H. Robert, "Covalent Functionalization and Biomolecular Recognition Properties of DNA-Modified Silicon Nanowires," *Nanotechnology* **16** no. 9, (2005) 1868.

[86] G.-J. Zhang, A. Agarwal, K. D. Buddharaju, N. Singh, and Z. Gao, "Highly Sensitive Sensors for Alkali Metal Ions Based on Complementary-Metal-Oxide-Semiconductor-Compatible Silicon Nanowires," *Applied Physics Letters* **90** no. 23, (2007) 233903–233903–3.

[87] G.-J. Zhang, G. Zhang, J. H. Chua, R.-E. Chee, E. H. Wong, A. Agarwal, K. D. Buddharaju, N. Singh, Z. Gao, and N. Balasubramanian, "DNA Sensing by Silicon Nanowire: Charge Layer Distance Dependence," *Nano Letters* **8** no. 4, (2008) 1066–1070.

[88] E. Stern, J. F. Klemic, D. A. Routenberg, P. N. Wyrembak, D. B. Turner-Evans, A. D. Hamilton, D. A. LaVan, T. M. Fahmy, and M. A. Reed, "Label-Free Immunodetection with CMOS-Compatible Semiconducting Nanowires," *Nature* **445** no. 7127, (2007) 519–522.

[89] M. N. Masood, S. Chen, E. T. Carlen, and A. v. d. Berg, "All-(111) Surface Silicon Nanowires: Selective Functionalization for Biosensing Applications," *ACS Applied Materials & Interfaces* **2** no. 12, (2010) 3422–3428.

[90] S. Clavaguera, A. Carella, L. Caillier, C. Celle, J. Pécaut, S. Lenfant, D. Vuillaume, and J.-P. Simonato, "Sub-ppm Detection of Nerve Agents Using Chemically Functionalized Silicon Nanoribbon Field-Effect Transistors," *Angewandte Chemie International Edition* **49** no. 24, (2010) 4063–4066.

[91] S. Clavaguera, N. Raoul, A. Carella, M. Delalande, C. Celle, and J.-P. Simonato, "Development of an Autonomous Detector for Sensing of Nerve Agents Based on Functionalized Silicon Nanowire Field-Effect Transistors," *Talanta* **85** no. 5, (2011) 2542–2545.

[92] V. Passi, F. Ravaux, E. Dubois, S. Clavaguera, A. Carella, C. Celle, J. P. Simonato, L. Silvestri, S. Reggiani, D. Vuillaume, and J. P. Raskin, "High Gain and Fast Detection of Warfare Agents Using Back-Gated Silicon-Nanowire MOSFETs," *Electron Device Letters, IEEE* **32** no. 7, (2011) 976–978.

[93] T. Strother, R. J. Hamers, and L. M. Smith, "Covalent Attachment of Oligodeoxyribonucleotides to Amine-Modified Si(001) Surfaces," *Nucleic Acids Research* **28** no. 18, (2000) 3535–3541.

[94] G. T. Hermanson, *Bioconjugate Techniques*, ch. 11. Elsevier Science and Technology Books, 2nd edition ed., 2008.

[95] H. Haick, P. T. Hurley, A. I. Hochbaum, P. Yang, and N. S. Lewis, "Electrical Characteristics and Chemical Stability of Non-Oxidized, Methyl-Terminated Silicon Nanowires," *Journal of the American Chemical Society* **128** no. 28, (2006) 8990–8991.

[96] M. A. Mohd Azmi, Z. Tehrani, R. P. Lewis, K. A. D. Walker, D. R. Jones, D. R. Daniels, S. H. Doak, and O. J. Guy, "Highly Sensitive Covalently Functionalised Integrated Silicon Nanowire Biosensor Devices for Detection of Cancer Risk Biomarker," *Biosensors and Bioelectronics* **52** (2014) 216–224.

[97] S. Heyse, H. Vogel, M. Sänger, and H. Sigrist, "Covalent Attachment of Functionalized Lipid Bilayers to Planar Waveguides for Measuring Protein Binding to Biomimetic Membranes," *Protein Science* **4** no. 12, (1995) 2532–2544.

[98] A. Charrier, T. Mischki, and G. P. Lopinski, "Direct Stabilization of a Phospholipid Monolayer on H-Terminated Silicon," *Langmuir* **26** no. 4, (2009) 2538–2543.

[99] F. N. Crespilho, V. Zucolotto, O. N. Oliveira Jr, and F. C. Nart, "Electrochemistry of Layer-by-Layer Films: a Review," *International Journal of Electrochemical Science* **1** no. 5, (2006) 194–214.

[100] O. Seitz, T. Böcking, A. Salomon, J. J. Gooding, and D. Cahen, "Importance of Monolayer Quality for Interpreting Current Transport through Organic Molecules: Alkyls on Oxide-Free Si," *Langmuir* **22** no. 16, (2006) 6915–6922.

[101] A. B. Sieval, R. Opitz, H. P. A. Maas, M. G. Schoeman, G. Meijer, F. J. Vergeldt, H. Zuilhof, and E. J. R. Sudhölter, "Monolayers of 1-Alkynes on the H-Terminated Si(100) Surface," *Langmuir* **16** no. 26, (2000) 10359–10368.

[102] E. J. Faber, L. C. P. M. de Smet, W. Olthuis, H. Zuilhof, E. J. R. Sudhölter, P. Bergveld, and A. van den Berg, "Covalently Attached 1-Alkynes on Silicon Surfaces Provide Superious Insulators," in *8th Annual Workshop on Circuits, Systems and Signal Processing*, pp. 17–18. Veldhoven, the Netherlands, November, 2005.

[103] L. Scheres, M. Giesbers, and H. Zuilhof, "Self-Assembly of Organic Monolayers onto Hydrogen-Terminated Silicon: 1-Alkynes Are Better Than 1-Alkenes," *Langmuir* **26** no. 13, (2010) 10924–10929.

[104] G.-J. Zhang and Y. Ning, "Silicon Nanowire Biosensor and its Applications in Disease Diagnostics: A Review," *Analytica Chimica Acta* **749** (2012) 1–15.

[105] D. Narducci, "Biosensing at the Nanoscale: There's Plenty of Room Inside," *Science of Advanced Materials* **3** no. 3, (2011) 426–435.

[106] X. Y. Bi, A. Agarwal, and K. L. Yang, "Oligopeptide-Modified Silicon Nanowire Arrays as Multichannel Metal Ion Sensors," *Biosensors and Bioelectronics* **24** no. 11, (2009) 3248–3251.

[107] Y. S. Yu and S. W. Hwang, "Analytic Model of a Silicon Nanowire pH Sensor," *Journal of Nanoscience and Nanotechnology* **11** no. 12, (2011) 10809–10812.

[108] H. Kim, J.-H. Lee, E. J. Chae, J.-W. Choi, and B.-K. Oh, "Detection of Dopamine Using a Silicon Nanowire Patterned by Nanoimprint Lithography," *Journal of Nanoscience and Nanotechnology* **11** no. 8, (2011) 7516–7519.

[109] S. M. Kwon, G. B. Kang, Y. T. Kim, Y.-H. Kim, and B.-K. Ju, "In-Situ Detection of C-Reactive Protein Using Silicon Nanowire Field Effect Transistor," *Journal of Nanoscience and Nanotechnology* **11** no. 2, (2011) 1511–1514.

[110] S. Ingebrandt and A. Offenhäusser, "Label-Free Detection of DNA using Field-Effect Transistors," *Physica Status Solidi (A)* **203** no. 14, (2006) 3399–3411.

[111] Y. Paska, T. Stelzner, S. Christiansen, and H. Haick, "Enhanced Sensing of Nonpolar Volatile Organic Compounds by Silicon Nanowire Field Effect Transistors," *ACS Nano* **5** no. 7, (2011) 5620–5626.

[112] M. C. McAlpine, R. S. Friedman, S. Jin, K. H. Lin, W. U. Wang, and C. M. Lieber, "High-Performance Nanowire Electronics and Photonics on Glass and Plastic Substrates," *Nano Letters* **3** no. 11, (2003) 1531–1535.

[113] N. K. Rajan, D. A. Routenberg, and M. A. Reed, "Optimal Signal-to-Noise Ratio for Silicon Nanowire Biochemical Sensors," *Applied Physics Letters* **98** (2011) 264107 1–3.

[114] X. P. A. Gao, G. F. Zheng, and C. M. Lieber, "Subthreshold Regime has the Optimal Sensitivity for Nanowire FET Biosensors," *Nano Letters* **10** no. 2, (2010) 547–552.

[115] Y. Hashim and O. Sidek, "Nanowire Dimensions Effect on ON/OFF Current Ratio and Sub-Threshold Slope in Silicon Nanowire Transistors," *Journal of Nanoscience and Nanotechnology* **12** no. 9, (2012) 7101–7104.

[116] S. Y. Chen, J. G. Bomer, W. G. van der Wiel, E. T. Carlen, and A. van den Berg, "Top-Down Fabrication of Sub-30 nm Monocrystalline Silicon Nanowires Using Conventional Microfabrication," *ACS Nano* **3** no. 11, (2009) 3485–3492.

[117] H. D. Tong, S. Chen, W. G. van der Wiel, E. T. Carlen, and A. van den Berg, "Novel Top-Down Wafer-Scale Fabrication of Single Crystal Silicon Nanowires," *Nano Letters* **9** no. 3, (2009) 1015–1022.

[118] E. Stern, A. Vacic, C. Li, F. N. Ishikawa, C. W. Zhou, M. A. Reed, and T. M. Fahmy, "A Nanoelectronic Enzyme-Linked Immunosorbent Assay for Detection of Proteins in Physiological Solutions," *Small* **6** no. 2, (2010) 232–238.

[119] R. Elnathan, M. Kwiat, A. Pevzner, Y. Engel, L. Burstein, A. Khatchtourints, A. Lichtenstein, R. Kantaev, and F. Patolsky, "Biorecognition Layer Engineering: Overcoming Screening Limitations of Nanowire-Based FET Devices," *Nano Letters* **12** (2012) 5245–5453.

[120] E. Stern, A. Vacic, N. K. Rajan, J. M. Criscione, J. Park, B. R. Ilic, D. J. Mooney, M. A. Reed, and T. M. Fahmy, "Label-Free Biomarker Detection from Whole Blood," *Nature Nanotechnology* **5** no. 2, (2010) 138–142.

[121] T. Moh, G. Pandraud, d. S. L.C.P.M., C. van Rijn, E. Sudhölter, and P. Sarro, *Fabrication of Nanowires for Biosensing Applications*, ch. 1, pp. 1–31. Pan Stanford Publishing Pte. Ltd., 2012.

[122] S. Chen, J. G. Bomer, E. T. Carlen, and A. van den Berg, "Al_2O_3 Silicon NanoISFET with Near Ideal Nernstian Response," *Nano Letters* **11** no. 6, (2011) 2334–2341.

[123] A. Vacic, J. M. Criscione, E. Stern, N. K. Rajan, T. Fahmy, and M. A. Reed, "Multiplexed SOI BioFETs," *Biosensors and Bioelectronics* **28** no. 1, (2011) 239–242.

[124] J. F. Klemic, E. Stern, and M. A. Reed, "Hotwiring Biosensors," *Nature Biotechnology* **19** no. 10, (2001) 924–925.

[125] U. Guth, F. Gerlach, M. Decker, W. Oelßner, and W. Vonau, "Solid-State Reference Electrodes for Potentiometric Sensors," *Journal of Solid State Electrochemistry* **13** no. 1, (2009) 27–39.

[126] P. Bergveld, "ISFET, Theory and Practice," in *IEEE Sensor Conference*. 2003. Proceeding of IEEE Sensor Conference.

[127] E. Krommenhoek, M. van Leeuwen, H. Gardeniers, W. van Gulik, A. van den Berg, X. Li, M. Ottens, L. van der Wielen, and J. Heijnen, "Lab-Scale Fermentation Tests of Microchip with Integrated Electrochemical Sensors for pH, Temperature, Dissolved Oxygen and Viable Biomass Concentration," *Biotechnology and Bioengineering* **99** no. 4, (2008) 884–892.

[128] N. Elfstrom, A. E. Karlstrom, and J. Linnrost, "Silicon Nanoribbons for Electrical Detection of Biomolecules," *Nano Letters* **8** no. 3, (2008) 945–949.

[129] P. Bergveld, "Thirty Years of ISFETOLOGY What Happened in the Past 30 Years and What May Happen in the Next 30 Years," *Sensors & Actuators: B. Chemical* **88** no. 1, (2003) 1–20.

[130] M. M. H. Iqbal, H. Yi, P. Garg, F. Udrea, P. Migliorato, and S. J. Fonash, "The Nanoscale Silicon Accumulation-Mode MOSFET - A Comprehensive Numerical Study," *IEEE Transactions on Electron Devices* **55** no. 11, (2008) 2946–2959.

[131] P. R. Nair and M. A. Alam, "Performance Limits of Nanobiosensors," *Applied Physics Letters* **88** no. 23, (2006) 233120.

[132] P. R. Nair and M. A. Alam, "Screening-Limited Response of NanoBiosensors," *Nano Letters* **8** no. 5, (2008) 1281–1285.

[133] M. H. Sorensen, N. A. Mortensen, and M. Brandbyge, "Screening Model for Nanowire Surface-Charge Sensors in Liquid," *Applied Physics Letters* **91** no. 10, (2007) 102105.

[134] E. Stern, R. Wagner, F. J. Sigworth, R. Breaker, T. M. Fahmy, and M. A. Reed, "Importance of the Debye Screening Length on Nanowire Field Effect Transistor Sensors," *Nano Letters* **7** no. 11, (2007) 3405–3409.

[135] N. K. Rajan, D. A. Routenberg, C. Jin, and M. A. Reed, "1/f Noise of Silicon Nanowire BioFETs," *IEEE Electron Device Letters* **31** no. 6, (2010) 615–617.

[136] T. Moh, M. Nie, G. Pandraud, L. C. P. M. de Smet, E. Sudhölter, Q. Huang, and P. Sarro, "Effect of Silicon Nanowire Etching on Signal-to-Noise Ratio of SiNW FETs for (Bio) Sensor Applications," *Electronics Letters* **49** no. 13, (2013) 782–784.

[137] M. Y. Bashouti, R. T. Tung, and H. Haick, "Tuning the Electrical Properties of Si Nanowire Field-Effect Transistors by Molecular Engineering," *Small* **5** no. 23, (2009) 2761–2769.

[138] A. Tarasov, M. Wipf, K. Bedner, J. Kurz, W. Fu, V. A. Guzenko, O. Knopfmacher, R. L. Stoop, M. Calame, and C. Schönenberger, "True Reference Nanosensor Realized With Silicon Nanowires," *Langmuir* **28** no. 25, (2012) 9899–9905.

[139] V. Xuan Thang, R. Stockmann, B. Wolfrum, A. Offenhäusser, and S. Ingebrandt, "Fabrication and Application of a Microfluidic-Embedded Silicon Nanowire Biosensor Chip," *Physica Status Solidi A* **207** no. 4, (2010) 850–857.

[140] M. C. McAlpine, H. Ahmad, D. Wang, and J. R. Heath, "Highly Ordered Nanowire Arrays on Plastic Substrates for Ultrasensitive Flexible Chemical Sensors," *Nature Materials* **6** no. 5, (2007) 379–384. 10.1038/nmat1891.

[141] Y. Paska and H. Haick, "Interactive Effect of Hysteresis and Surface Chemistry on Gated Silicon Nanowire Gas Sensors," *ACS Applied Materials & Interfaces* **4** no. 5, (2012) 2604–2617.

[142] Y. Paska, T. Stelzner, O. Assad, U. Tisch, S. Christiansen, and H. Haick, "Molecular Gating of Silicon Nanowire Field-Effect Transistors with Nonpolar Analytes," *ACS Nano* **6** no. 1, (2012) 335–345. Paska, Yair Stelzner, Thomas Assad, Ossama Tisch, Ulrike Christiansen, Silke Haick, Hossam.

[143] R. Ermanok, O. Assad, K. Zigelboim, B. Wang, and H. Haick, "Discriminative Power of Chemically Sensitive Silicon Nanowire Field Effect Transistors to Volatile Organic Compounds," *ACS Applied Materials & Interfaces* **5** no. 21, (2013) 11172–11183.

[144] A. O. Niskanen, A. Colli, R. White, H. W. Li, E. Spigone, and J. M. Kivioja, "Silicon Nanowire Arrays as Learning Chemical Vapour Classifiers," *Nanotechnology* **22** no. 29, (2011) 295502.

[145] S. Chen and S.-L. Zhang, "Contacting versus Insulated Gate Electrode for Si Nanoribbon Field-Effect Sensors Operating in Electrolyte," *Analytical Chemistry* **83** no. 24, (2011) 9546–9551.

[146] W. Guan, N. K. Rajan, X. Duan, and M. A. Reed, "Quantitative Probing of Surface Charges at Dielectric-Electrolyte Interfaces," *Lab on a Chip* (2013) 1431–1436.

[147] G. Åkerlöf and O. A. Short, "The Dielectric Constant of Dioxane-Water Mixtures between 0 and 80°," *Journal of the American Chemical Society* **58** no. 7, (1936) 1241–1243.

[148] S. Sze, *Physics of Semiconductor Devices.* John Wiley & Sons, New York, 1986.

[149] D. D. Perrin, *Covalent Hydration in Nitrogen Heteroaromatic Compounds: II. Quantitative Aspects*, vol. Volume 4, pp. 43–73. Academic Press, 1965.

[150] C. C. Lynch and V. K. L. Mer, "Acid Dissociation Constants in Dioxane-Water Mixtures by Potentiometric Titration," *Journal of the American Chemical Society* **60** no. 5, (1938) 1252–1259.

[151] J. P. Shukla and S. G. Tandon, "Corrections to pH Measurements for Titrations in Dioxane-Water mixtures," *Journal of Electroanalytical Chemistry and Interfacial Electrochemistry* **35** no. 1, (1972) 423–427.

[152] J. P. Shukla and M. S. Subramanian, "Thermodynamics of Proton Dissociation of Acetylacetone and 3-Methylacetylacetone in Dioxane-Water Mixtures," *Thermochimica Acta* **35** no. 3, (1980) 293–305.

[153] E. J. R. Sudhölter, P. D. van der Wal, M. Skowronska-Ptasinska, A. van den Berg, P. Bergveld, and D. N. Reinhoudt, "Modification of ISFETs by Covalent Anchoring of Poly(hyroxyethyl methacrylate) Hydrogel. Introduction of a Thermodynamically Defined Semiconductor-Sensing Membrane Interface," *Analytica Chimica Acta* **230** (1990) 59 – 65.

[154] P. D. van der Wal, E. J. R. Sudhölter, B. A. Boukamp, H. J. M. Bouwmeester, and D. N. Reinhoudt, "Impedance Spectroscopy and Surface Study of Potassium-Selective Silicone Rubber Membranes," *Journal of Electroanalytical Chemistry and Interfacial Electrochemistry* **317** no. 1-2, (1991) 153–168.

SUMMARY

Nanowire Field-Effect Transistors: Sensing Simplicity?

Silicon nanowires are structures made from silicon with at least one spatial dimension in the nanometer regime (1-100 nm). From these nanowires, silicon nanowire field-effect transistors can be constructed. Since their introduction in 2001 silicon nanowire field-effect transistors have been studied because of their promising application as selective sensors for biological and chemical species. Their large surface-to-volume ratio promises an increased sensitivity compared to conventional, planar field-effect transistors. Selectivity can be added by smart modification of the surface of the nanowire.

The application of nanowire field-effect transistors as chemical sensors for ions is studied in this thesis. After briefly discussing the working principle of field-effect transistors, an extensive review on reported state-of-the-art surface modification techniques is presented. By far, most of this work covers the covalent attachment of molecules to the silicon oxide layer that is typically present on as-prepared silicon nanowires. In addition, some examples on non-covalent approaches have been reviewed. Alternatively, the oxide layer can be removed to attach molecules directly onto silicon.

Nanowire field-effect transistors are prepared using top-down fabrication techniques. Nanowires with a width of 20 to 2000 nanometer, a length of 3 to 5 micrometer and a height of 50 to 100 nanometer are etched from silicon-on-insulator wafers. Using a newly developed complementary metal-oxide-semiconductor compatible process, nanowire field-effect transistors are obtained. This process allows for the use of a broad variety of front oxides, which enables selective surface modification of the nanowires and the implementation of materials with different dielectric constants. Furthermore, the presence of a silicon nitride passivation layer on the area around the nanowire provides the possibility to modify only the nanowire surface. Chips typically consist of 28 individual nanowire field-effect transistors. The devices are characterized in air and the variation of the threshold voltage over the wafer is mapped. It is shown that the electrical characteristics make the devices suitable for sensing experiments.

The nanowire field-effect transistors are electrically characterized while exposed to water using a newly developed flow cell. A pulsed gate potential is

applied as method for stable characterization. While most methods reported in literature use a reference electrode, the pulsed method can be applied without it. Using the sensitivity towards protons of the Si-OH groups at the SiO_2 surface, the pH of aqueous solutions is determined using this pulsed gate potential method. It is found that upon increasing pH the threshold voltage increases, which is as expected.

The nanowire field-effect transistors are studied using two types of gating: back gating and front gating through the liquid via an Ag/AgCl electrode. It is found that both methods can be used to gate the device, and that in general smaller potentials are needed for front gating compared to back gating. Using this front-gate method, the influence of the non-aqueous solvent 1,4-dioxane on the device characteristics is studied by exposing the devices to different water-1,4-dioxane mixtures. The dependency of the threshold voltage on the mixture composition is found to be related to the decreased dissociation of the surface silanol groups and the electrical conductivity of the mixture used.

In the final experiments, the nanowire field-effect transistors are covered with an ionophore-containing polymer membrane via drop casting. This membrane consists of a silicon rubber polymer (Siloprene), embedding the ionophore valinomycin, which has a K^+/Na^+ selectivity of $\sim 10^5$. Using a setup with liquid gating and an Ag/AgCl reference electrode, accurate potassium ion concentrations are determined. Upon exposure of the membrane modified device to sodium ions at a fixed potassium ion concentration, the potential of the device only changes at very high sodium ion concentrations. This confirms the high ion selectivity of the membrane modified device. These results are comparable in line with those obtained using a conventional ion-selective electrode setup.

In conclusion, the experiments presented in this PhD thesis lead to an increased understanding of the electrical behavior of nanowire field-effect transistors under different circumstances. This will support the construction and operation of nanowire field-effect sensors, facilitating the further development of advanced sensors.

SAMENVATTING

Nanodraad Veldeffecttransistors: *"Sensing Simplicity"*?

Silicium nanodraden zijn structuurtjes van silicium waarvan tenminste één dimensie in het nanometergebied (tussen 1 en 100 nm) valt. Deze nanodraden kunnen gebruikt worden om silicium nanodraad veldeffecttransistors te maken. Sinds hun introductie in 2001, zijn dergelijke transistors veel onderzocht vanwege de veelbelovende toepassing als sensor voor biologische en chemische analieten. Omdat ze relatief veel oppervlakte hebben ten opzichte van hun volume wordt verwacht dat ze gevoeliger zullen zijn dan de conventionele, vlakke veldeffecttransistors. Door het oppervlak van de nanodraad slim te modificeren, kan selectiviteit worden toegevoegd.

In dit proefschrift is de toepassing van nanodraad veldeffecttransistors als sensors onderzocht. Allereerst wordt het principe achter de nanodraad veldeffecttransistor besproken. Vervolgens is er een literatuuroverzicht gemaakt, met daarin een uitgebreid overzicht van de beste methodes voor oppervlaktemodificatie van dit moment. Verreweg de meeste methodes gebruiken de covalente binding van moleculen op de oxidelaag die standaard aanwezig is op de nanodraden. Ook is een aantal methoden gerapporteerd die gebruiken maken van niet-covalente interacties. Een alternatief is het verwijderen van de oxidelaag, waarna moleculen direct aan het silicium gebonden kunnen worden.

Vervolgens worden nanodraad veldeffecttransistors gemaakt die typisch een breedte van 20 tot 2000 nanometer, een lengte van 3 tot 5 micrometer en een hoogte van 50 tot 100 nanometer hebben. Dit wordt gedaan door silicium *wafers* te etsen volgens een nieuw ontwikkelde methode, die bestaande *complementary metal-oxide-semiconductor* -technieken gebruikt. Deze methode maakt het mogelijk om verschillende oxides op de buitenkant van de nanodraad neer te leggen, wat selectieve modificatie van het oppervlak van de nanodraad makkelijker maakt. Ook wordt het de omgeving van de nanodraad gepassiveerd met behulp van een silicium-nitridelaag, wat het ook mogelijk maakt om selectief alleen het oppervlakte van de nanodraad te modificeren. Een chip bestaat typisch uit 28 individuele nanodraad veldeffecttransistors. De transistors worden gekarakteriseerd in lucht en de variatie in de drempelspanning van transistors over de hele *wafer* wordt in kaart gebracht. Uit de elektrische karakteristieken van deze transistors blijkt dat ze geschikt zijn om als sensor te gebruiken.

De nanodraad veldeffecttransistors worden ook in water elektrisch gekarakteriseerd met behulp van een nieuwe meetcel. Hiervoor wordt een methode ontwikkeld, waarbij de potentiaal op de gate gepulseerd wordt. De methode maakt, in tegenstelling tot wat in de literatuur wordt gerapporteerd, geen gebruik van een referentie-elektrode. Met behulp van deze methode wordt, gebruikmakend van de pH-gevoelige silanolgroepen op het oppervlak van de nanodraad, de pH van waterige oplossingen gemeten. De drempelspanning van de transistors blijkt toe te nemen met toenemende pH, wat overeenkomt met de verwachting.

De nanodraad veldeffecttransistors worden bestudeerd met behulp van twee soorten *gating*: via de achterkant en via een zilver-zilverchloride-elektrode door de vloeistof aan de voorkant. Beide methodes kunnen gebruikt worden om de transistor te *gaten*, hoewel in het algemeen kleinere potentialen nodig zijn via de voorkant dan via de acherkant. De invloed van het niet-waterige oplosmiddel 1,4-dioxaan op de elektrische eigenschappen van de transistor is bestudeerd met behulp van de methode waarbij de transistor via voorkant wordt aangestuurd. Hierbij is de transistor blootgesteld aan mengsels van water en 1,4-dioxaan. De drempelspanning van de transistors blijkt af te hangen van de samenstelling van het mengsel, en wel door de afgenomen dissociatie van de silanolgroepen aan het nanodraad oppervlak en de elektrische geleiding van de vloeistof.

In de laatste serie experimenten is de nanodraad veldeffecttransistor bedekt met een membraan dat een ionofoor bevat. Dit membraan wordt aangebracht via een druppeltje en bestaat uit een rubber van een siliconenpolymeer (Silopreen) dat het ionofoor valinomycin bevat. Valinomycin heeft een K^+/Na^+ selectiviteit van $\sim 10^5$. Met behulp van een opstelling met *gating* via de voorkant en een zilver-zilverchloridereferentie-elektrode kunnen verschillen in kaliumionconcentratie in waterige oplossingen worden waargenomen. Als de gemodificeerde nanodraad veldeffecttransistors aan oplossing met natriumionen worden blootgesteld, wordt alleen bij hele hoge concentraties een respons gevonden. Dit bevestigt de selectiviteit van het membraan. De resultaten zijn vergelijkbaar met resultaten die via een conventionele ion-selectieve elektrode worden behaald.

De experimenten in dit proefschrift leiden tot een beter begrip van het gedrag van de nanodraad veldeffecttransistors onder verschillende omstandigheden. Dit zal helpen met het verder maken en gebruiken van nanodraad veldeffectsensoren, wat de verdere ontwikkeling van geavanceerde sensoren mede mogelijk maakt.

CURRICULUM VITÆ

Marleen Mescher was born on September 20th in Eindhoven, the Netherlands. After finishing her pre-university education at Pleincollege van Maerlant in Eindhoven, she started her study of Chemistry at Utrecht University in 2002. During the Masters program Chemistry & Physics she conducted her master research on down conversion using the rare earth elements praseodymium and ytterbium. She did an internship at Philips Research in Eindhoven on "NW-FETs as sensor in a liquid environment" and graduated as Master of Science in 2009.

In the summer of 2009 she started working on her PhD project in the Organic Materials and Interfaces group at Delft University of Technology, under supervision of dr. ir. Louis de Smet and prof. dr. Ernst Sudhölter. A substantial part of the experimental work was carried out at the Micro Systems and Devices group at Philips Research in Eindhoven under supervision of dr. ir. Johan Klootwijk. The results of her PhD research are presented in this dissertation.

Marleen is coauthor of a book chapter, three patent applications and three journal articles. She was a member and chairwoman of the Philips PhD and Postdoc Committee and organized a study tour to Switzerland together with colleagues from Delft.

Since January this year she has been working as R&D Engineer at Blue Medical Devices in Helmond.

LIST OF PUBLICATIONS

WRITTEN PUBLICATIONS

- Pulsed Method for Characterizing Aqueous Media Using Nanowire Field Effect Transistors, M. Mescher, B. Marcelis, L. C. P. M. de Smet, E. J. R. Sudhölter and J. H. Klootwijk, *IEEE Transactions on Electron Devices*, Vol. 58, No. 7, (2011)

- Organic Surface Modification of Silicon Nanowire-Based Sensor Devices, L. C. P. M. de Smet, D. Ullien, M. Mescher and E. J. R. Sudhölter, *Nanowires - Implementations and Applications*, Abbass Hashim (Ed.), InTech, Rijeka, Croatia (2011)

- Robust Fabrication Method for Silicon Nanowire Field Effect Transistors for Sensing Applications, M. Mescher, L. C. P. M. de Smet, E. J. R. Sudhölter and J. H. Klootwijk, *Journal of Nanoscience and Nanotechnology*, Vol. 13, No. 8, (2013)

- Influence of Conductivity and Dielectric Constant of Water-Dioxane Mixtures on the Electrical Response of SiNW-Based FETs, M. Mescher, A. G. M. Brinkman, D. Bosma, J. H. Klootwijk, E. J. R. Sudhölter and L. C. P. M. de Smet,*Sensors*, Vol. 14 , No. 2, (2014)

INTERNATIONAL CONFERENCE PRESENTATION

- Pulsed Method for Characterizing Aqueous Media Using Nanowire Field Effect Transistors, M. Mescher, B. Marcelis, L. C. P. M. de Smet, E. J. R. Sudhölter and J. H. Klootwijk, *IEEE International Conference on Microelectronic Test Structures (ICMTS)*, Hiroshima, Japan, March 22–25 (2010)

ACKNOWLEDGEMENTS

Viereneenhalf jaar geleden begon ik aan dit promotieproject omdat ik op die manier bij Philips kon blijven en tegelijkertijd ook nog eens kon promoveren. Dat het wat anders zou lopen dan ik toen voor me zag, realiseerde ik me niet echt, maar dat ik dit dankwoord schrijf is wel het bewijs dat er meerdere wegen naar Rome leiden. Onderweg heb ik gelukkig hulp gehad van veel mensen, die ik hier graag wil bedanken.

Het begon dus met die stage bij Philips, in de praktijk voornamelijk met Johan als begeleider. De beginselen van elektrische karakterisatie had ik al snel van je geleerd, maar door de jaren heen kon ik altijd weer nieuwe dingen van je leren. Ik hoop dat er na deze eerste promovenda nog veel promovendi mogen volgen. Ernst, we waren er zo'n vijf jaar geleden toen ik met Johan naar Delft kwam al snel uit dat jij mijn promotor zou worden. Je zit altijd vol met nieuwe ideeën en ik had het idee dat ik na iedere afspraak vertrok met honderd nieuwe mogelijkheden, waar altijd wel iets bijzat dat me weer verder hielp. Louis, jij was daar steeds bij. Ook al gingen mijn experimenten niet zoals ik wilde, als ik er met jou over had gepraat zag het er ineens weer een stuk positiever uit. Alle tijd die je (zeker in de laatste maanden) hebt geïnvesteerd, heeft voor mij het verschil gemaakt. Ik vond het erg fijn om met je samen te werken.

Het werken op twee verschillende plekken zorgt voor twee groepen collega's: extra veel mogelijkheden voor gezellige koffiepauzes, inhoudelijke discussies, lunches en borrels en praktische tips. Bij Philips waren vanaf het begin Marcel&Pascal (nog steeds als eenheid) erg behulpzaam, maar de rest uit het originele team wil ik zeker niet vergeten: Erik, Bout, Marco, Wim en Rogier: jullie hebben allemaal op de een of andere manier bijgedragen aan het succes. My roomies Angel, Saeed, Marcus (and Ronald of course, although he only had a seat and no desk) were always there to listen to my stories and complaints. I'll let you know when the money, cars and the other things have arrived, as they are expected any time now. Ronald, treingezelschap, erg leuk dat je deel uit wilt maken van mijn commissie. Ook ben ik Derk en Hans dank verschuldigd dat ik ongestoord mijn gang kon gaan.

Behalve in de Micro Systems and Devices groep had ik bij Philips ook nog het 'lotgenotencontact' bij de PPC. Marjolein, Marian, Aaron, Emile, Tim, Popi, Tommi en Mieke: bedankt voor alle gezellige lunches en koffie. Tommi, those additional

c-breaks were an excellent distraction when I needed it most. Mieke, je was er voor me toen het nodig was en dat je als paranimf bij mijn verdediging bent, is alleen maar een logisch vervolg daarop.

In Delft begonnen we met een heel klein groepje, dat in de loop der tijd steeds groter werd. Daniela, Venkatesh, Aldo, Sumit, Anping, Aernout, Cristian, Stefan, Judith and Will: thanks for all discussions, and the fun we had in the lab and at coffee breaks. Duco, Louw, Lars, Piet en natuurlijk Marian en Astrid: bedankt voor de hulp bij allerlei praktische zaken waar ik niet zonder zou hebben gekund. I got help with some experiments from Anping as well, which was much appreciated. Aldo, ook jij bedankt voor je hulp met de experimenten, de interpretatie, je B&B en dat je mijn paranimf wilt zijn. Of course I want to thank all the other people at OMI and ASM for their support.

Of het werken bij Philips en de TUDelft nog niet genoeg was, was daar ook nog mijn 'echte' werkgever: M2i. Bij M2i kwam ik terecht in het beste cluster dat ik me kon wensen: Cluster 3 (leuker is d'r nie). Vanaf het eerste moment heb ik me daar erg welkom gevoeld. Merijn, Gilbère en Harm, ik heb erg veel lol gehad tijdens de roadtrips naar de clustermeetings en tijdens de conferenties, maar waardeer ook de inhoudelijke bijdragen van jullie kant. Derk, Pia, Monika, Oscar en Alice, Jonathan en de rest van het M2i-kantoor: jullie hebben het samen allemaal een beetje makkelijker voor mij gemaakt.

My visit to Yale is another thing I will always remember: Mark, it was a pleasure to be in your lab for a few weeks and I am honored that you are a part of my committee. Alek, Monika and Nitin: Thank you for your open way of sharing ideas and experiences. I will not forget your dedication and the evenings in the lab (nor the SEM donuts we found), but will also remember the evenings at GPSCY, the beach and NY and Philadelphia.

In de afgelopen jaren hebben ook een aantal studenten bijgedragen aan het project. Anke, jij begon toen ik nog net niet helemaal begonnen was en het is uiteindelijk helaas niet gelukt met het DNA, maar dat heeft mijn onderzoek zeker wel richting gegeven. Joost, dat ik je verslag doorlas terwijl ik naast het zwembad in Phoenix zat, maakte helemaal niet uit, want het was gewoon goed, zoals verwacht. Frank, ik ben je een hoop dank verschuldigd. Je begon bij Philips terwijl ik mijn onderzoek wilde afronden en je ging zelfstandig aan de gang met je eigen project terwijl ik in Delft aan het meten was. Dit is uiteindelijk de aanleiding geweest voor hoofdstuk vijf, maar wellicht nog belangrijker ook voor een boost van mijn motivatie tijdens het project. Dat je data uiteindelijk niet in het artikel terecht kwam, ligt absoluut niet aan jouw kwaliteiten als onderzoeker. Ik wens je veel succes met je eigen promotie.

Ik kan hier niet iedereen noemen, maar mensen die ik ook zeker niet wil vergeten zijn Veronique en Ramon, Johan, Erik, AnnA, Niels, de VML-dames en mijn loopmaatjes. Bedankt voor alles.

Mijn schoonfamilie heeft mij ook altijd gesteund in de afgelopen jaren. Ook al was het misschien niet altijd duidelijk waar ik nou mee bezig was, geïnteresseerd waren jullie altijd. Evelien, Jaap, en papa en mama waren er ook altijd. Ik heb wel eens gegrapt dat jullie toch wel trots zouden zijn, wat ik ook zou doen, maar de gedachte dat jullie steeds onvoorwaardelijk achter mij stonden was een hele grote steun voor me.

Vanzelfsprekend zijn mijn laatste woorden voor jou, Koen. Twee proefschriften afronden in twee jaar tijd was nog niet zo makkelijk, zeker niet toen het mijn beurt was, maar we hebben het samen gedaan. Jouw steun heeft me er doorheen geholpen en ik kijk uit naar onze toekomst samen. Ik hou van je.

Marleen
Eindhoven, februari 2014